THE UNIVERSITY OF MICHIGAN

INDUSTRY PROGRAM OF THE COLLEGE OF ENGINEERING

AN INVESTIGATION OF THE VISCOSITIES OF TITANIUM DIOXIDE-SOY BEAN OIL SUSPENSIONS

Mau-Tong Kuo

A dissertation submitted in partial fulfillment
of the requirements for the degree of
Doctor of Philosophy in the
University of Michigan
1958

April, 1958

IP-282

ACKNOWLEDGMENTS

The writer wishes to express his sincere gratitude to the following:

Professor L. L. Carrick, Chairman, and other members of the doctoral committee, Professors J. T. Banchero, K. F. Gordon, L. L. Kempe, R. A. Wolfe, for their guidance, timely aid, and interest in this research.

Messrs. G. Grieger and A. J. Amy fcr assistance with the electron miscroscopic studies.

The secretarial, library and shop staffs of the Chemical and Metallurgical Engineering Department for their ready cooperation.

The Michigan Memorial Phoenix Project, Nash-Kelvinator gift, for financial assistance.

The National Lead Company, Titanium Division, for supplying materials gratis.

TABLE OF CONTENTS

TABLE OF CONTENTS (Cont'd)

LIST OF TABLES

LIST OF TABLES (Cont'd)

LIST OF FIGURES

LIST OF FIGURES (Cont'd)

NOMENCLATURE

Symbol	Description	Author First Using Symbol	Equation Number
α	Vand shape factor	Vand	8
β	a constant	Robinson	10
γ	a collision time constant	Vand	9
$\overline{\delta}$	mean distance between structures	Kuo	24,25,27,28
ϵ	dielectric constant of a suspension	Bruggeman	20,21
ϵ_m	dielectric constant of a suspending medium	Bruggeman	20,21
ϵ_p	dielectric constant of solid particles	Bruggeman	21
η	viscosity of suspension	Arrhenius	3,4,5,6,7,8, 12,13,14,19, 24,27,28,29, 30,32
η_o	viscosity of liquid (distinguished from suspension)	Newton	1,3,4,5,6,7, 8,13,24,27, 28,29,30,32
η_r	relative viscosity of suspension	Vand	9,11
η_{sp}	specific viscosity of suspension	Robinson	10,32,33,35, 36,37
θ	hydrodynamic interaction constant	Vand	9
λ_i	a factor depending upon crowding action of spheres of size j on those of size i	Mooney	11
μ	fluidity or $\frac{1}{\eta_o}$	Bingham	2
ρ	density of test fluid	Van der Walt	14
σ	a characteristic constant of material	Arrhenius	3,7
τ	shear stress	Newton	1,18,19,24, 27
τ_o	yield value	Weltmann	22,23

NOMENCLATURE (Cont'd)

Symbol	Description	Author First Using Symbol	Equation Number
ϕ	volume fraction of solid particles in suspension	Einstein	4,5,6,10,11, 20,21,22,23, 30,31,33,35, 36,37
ψ	characteristic constant of material	Orr, Jr.	13
ω	angular velocity	Hatschek	15,16
a	characteristic constant of material	Hess	5
b	characteristic constant of material	Weltmann	7
f	friction factor	Bingham	2
h	characteristic constant of material	Maron	12
k_1	Einstein shape factor	Vand	9
k_2	a shape factor of collision doublets	Vand	9
k_3	a proportionality constant	Kuo	23
n	a characteristic constant of material	Kuo	23
q	a characteristic constant	Vand	8
r	distance between planes	Newton	1,2
t	time in seconds required for 100 revolutions of a rotor	Van der Walt	14,19
u	velocity of fluid flow	Kuo	26,27
u_1	velocity of flow of structure 1	Kuo	24,26
u_2	velocity of flow of structure 2	Kuo	24,26
u_1'	velocity of fluid flow near the surface of structure 1	Kuo	--
u_2'	velocity of fluid flow near the surface of structure 2	Kuo	--
v	velocity of fluid flow in the direction of shear stress	Newton	1,2
y	a characteristic constant of liquid	Maron	12

NOMENCLATURE (Cont'd)

Symbol	Description	Author First Using Symbol	Equation Number
A	characteristic constant for particular rotor, cup, etc.	Geddes	14
B	constant for particular rotor, cup, etc.	Van der Walt	--
C	weight of particles in unit volume of liquid medium	Arrhenius	3,7,13
$\overline{D}$	average diameter of structure	Kuo	24,27,28,29, 30,34,35
E	ratio of solid particle volume to liquid volume	Vand	8,9
F	form factor	Voet	20
H	characteristic constant for particular rotor, cup, etc.	Geddes	14
J	characteristic constant of material	Orr, Jr.	13
K	defined as $K = S_o\overline{D}/2V_s$	Kuo	30,33
K'	calibration coefficient	Kuo	19
K_s	a proportionality constant	Kuo	17,19
K_w	a proportionality constant	Kuo	18,19
M	a characteristic constant	Weltmann	22
N	a characteristic constant	Weltmann	22
N_a	total number of (fictitious) spherical structures	Kuo	34,35
Q	defined as $Q = Wt^2/B^2\rho$	Van der Walt	--
R_b	radius of bob	Hatschek	15,16,17
R_c	radius of cup	Hatschek	15,16,17
S	rate of shear	Hatschek	15,16
$\overline{S}$	mean rate of shear	Hatschek	16,17,19
S_o	surface area of all the individual structures	Kuo	25,29,30,34

NOMENCLATURE (Cont'd)

Symbol	Description	Author First Using Symbol	Equation Number
S'	relative sediment volume	Robinson	10
T	absolute temperature in °K	Kuo	--
V_c	total dead volume	Kuo	25,29,30, 33,35,36
V_m	volume of liquid medium	Kuo	25,29,30,21
V_p	volume of structures	Kuo	36
V_s	volume of solid particles	Kuo	30,31,33, 35,36
W	effective driving weight	Van der Walt	14,18,19
W_o	weight of oil in suspension	Kuo	--
W_p	weight of pigment in suspension	Kuo	--
W_s	weight of surface active agent added in a suspension	Kuo	--
ΔW	defined as $\Delta W = W - \tau_o$, i.e., driving weight - yield value	Kuo	--
X	distance from the axis of rotation	Hatschek	15,16,17
Z	defined as $Z = \alpha'/(1 - \alpha'\phi)$ where α' is a constant	Maron	12

ABSTRACT

In order to better understand the anomalous rheological behavior[24,25] (time-stress-strain relationship) of some industrial solid-liquid suspensions, the effects of the following properties of titanium dioxide-soy bean oil suspensions were investigated: (a) volume concentration, (b) particle size, (c) temperature, (d) milling time, (e) milling methods, (f) addition of a surface active agent.

These investigations revealed that the structures were formed after a dispersion operation. The speed of "structure formation" depended upon the strength of the flocculation forces. The shear stress applied to break the formed structures was called "yield value." When the shear stress exceeded the "yield value," the structures were broken down into smaller sizes because of the irregularity in structure shape. If the volume concentration was comparatively low, the broken structures would remain a constant size and almost the same shape - a Bingham type of flow. However, if the volume concentration was comparatively high, the structures were continually broken up and the viscosity decreased as the higher shear stress was applied - a Plastic type of flow.

The yield value varied inversely with respect to particle size, i.e., the yield value increased as the particle size decreased. The yield value was also affected by the volume concentration of the pigment as shown in the following equation:

$$\tau_o = K_3 \phi^n \qquad (23)$$

In order to explain the effect of particle size and volume concentration on suspension viscosities, the following equation was

derived utilizing the concept of "structure formation" in suspensions.

$$\eta_{sp} = \frac{K}{\frac{1}{\phi} - (1 + \frac{V_c}{V_s})} \tag{33}$$

Equation (33) has as its variables relative size of the structures, arrangement of the particles in the structures and the relative amount of dead volume contained in the structures. These variables are functions of the particle size, the temperature, and possibly the physical properties of the liquid medium.

Experimental and published data showed excellent correlation when used in Equation (33). These results indicated that once the yield value was exceeded, the nature of Bingham type of flow would be analogous to that of Newtonian type of flow.

Particle size affected the suspension viscosities. The smaller the particle size the higher the suspension viscosities at a constant temperature in volume concentrations ranging from 0 to 5% if the particle size was larger than 0.05 microns. However, at a higher volume concentration range, where Plastic type of flow was observed, the critical particle size was not observed.

The effect of temperature on the viscosity of the Bingham type of flow was well expressed by Arrhenius type equation. Addition of 1-amino-2-naphthol-4-sulfonic acid as a surface active agent reduced both the yield value and suspension viscosities at 25 $\pm$ 0.1°C.

INTRODUCTION

Rheology, being concerned with the flow and deformation of matter covers a very wide field. In practice, the term has generally been referred to a somewhat narrower field, namely the study of the rheological properties of those materials, mainly of industrial importance, which show a behavior intermediate between that of solids and liquids.

The greater part of what is generally called rheology is concerned with stress-strain-time relations in materials and the influence on them of temperature variation. The rheological problem of a system in which two phases are involved, such as in a gas-liquid system, a solid-liquid system or a solid-gas system, is much more complex.

In Figure 1 is shown the Newtonian model of flow. It consists of two parallel planes A and B, the intervening space being filled with the fluid under examination. A tangential shearing stress τ is applied uniformly at surface A. The plane A then moves with respect to plane B carrying with it the innumerable parallel planes of fluid existing between planes A and B. Each plane, however, is carried to a different distance. The top plane A goes the farthest with respect to the plane B. When the point b reached c, the straight line ac marks the distance traveled in one second, its length gives the velocity of plane A with respect to plane B. Then bc divided by ab becomes the rate of shear or velocity gradient. This is customarily written as dv/dr where v is the velocity in the direction of shearing stress τ and r is the

distance between the planes. In this type of model, for a given stress, τ, dv/dr is constant throughout the mass of material.

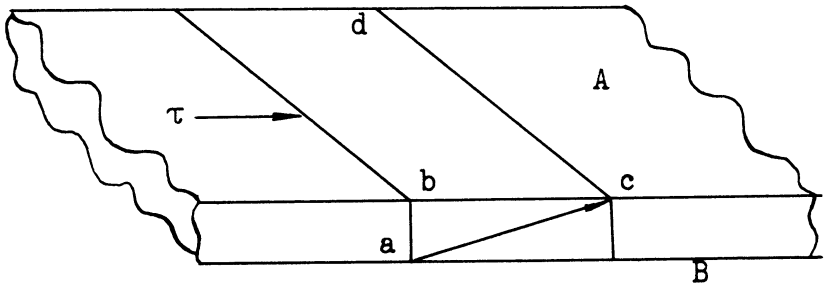

Figure 1. The Newtonian Model of Flow

Newton assumed that the rate of shear is directly proportional to the tangential shearing stress. His idea is expressed mathematically in the equation

$$\tau = \eta_o \, dv/dr \qquad (1)$$

The proportionality constant η_o is the viscosity and is defined as the tangential shearing force per unit area that will produce a unit rate of shear. Equation (1) is applicable only to those liquids whose molecules are not hampered in their motion by the formation of structure or by molecular alignment under high rates of shear.

For plastic clay suspensions in water, Bingham in 1916 [4] introduced a modification of the Newton concept. Bingham reasoned that a plastic flow could not start until the applied shearing stress exceeded the stress arising from frictional resistance between the clay particles.

He expressed his hypothesis by introducing into the Newtonian equation a friction factor f, thus,

$$\mu(\tau - f) = dv/dr \qquad (2)$$

where f is the tangential force per unit area just required to start the flow. Bingham replaced $1/\eta_0$ with μ, which he called the fluidity.

The letter f has been retained by many rheologists, even though the name "friction" is no longer employed. It seemed highly probable that friction might not be the only factor involved in producing the intercept which Bingham[4] first recognized on the stress axis in deriving his consistency curve for clay and water mixtures. The term "yield value" was suggested as a temporary expedient until something more appropriate could be found. The term "yield value" appeared for the first time in a joint publication by Bingham and Green in 1919[5].

Breyer[37] believed that the yield value is due to orientation forces which exist between particles so that the particles are held in a fixed position.

Green[17] showed experimentally that the force of flocculation arising, presumably from interfacial tension, plays an important part in explaining structure formation.

De Wael and Lewis[10] found that there is a field of force giving cross-linked flocculates which immobilize some of the fluid phase, thus creating resistance to flow.

Harvey[22] measured the viscosity of ferromagnetic dispersions with and without a magnetic field imposed and found that the yield value is a measure of the flocculating forces between the particles. The plastic viscosity is but little affected by the presence of the magnetic field whereas the yield value is greatly increased.

Voet[54], in order to investigate the behavior of suspended particles during shear, measured the dielectric constant of quiescent and sheared suspensions. By means of these measurements it is possible to measure, to some extent, the build-up of structure upon cessation of the application of the shearing stress, because the changes of the dielectric constant on application of a shearing stress are related to particle agglomeration and orientation.

Since Arrhenius[2] in 1887 proposed an equation expressing the relationship between the viscosity of a suspension and the concentration of particles and since Einstein[14] theoretically derived a viscosity equation in 1906, hundreds of equations have been published in the literature.

The Arrhenius viscosity Equation (3)[2] was not theoretically derived, however, it has been applied, quite often because of its simplicity, to the correlation of experimental data.

The Einstein viscosity Equation (4)[14] is rather simple and is useful for a first approximation of the viscosities of suspensions at an extremely low volume concentration, however, as the concentration increases it has been observed to deviate from the experimental results in most cases[1]. Even though the Einstein viscosity Equation (4) does not adequately explain the viscosity of a suspension, it opened the door for rheologists to investigate this subject.

A number of viscosity measurements in colloidal suspension, as well as in suspension consisting of particles very much larger than those which occur in colloidal suspensions, were conducted to verify the Einstein Equation (4) and the Arrhenius Equation (3).

Both the Einstein Equation (4) and the Arrhenius Equation (3) have been modified to some extent so as to describe the viscosity of more concentrated suspensions.

Among the published viscosity equations the more significant equations correlating the viscosity of the suspension and the volume concentration are summarized in Table I, pages 12 and 13.

Oden[40] in 1912 observed two important variations from the theoretical result when measuring the viscosities of sulfur solutions having particles of uniform size and of concentrations up to 25% by volume. He stated that the viscosity above a certain concentration increased more rapidly than the linear ratio, and also that the viscosity of solutions containing smaller particles was, for equal weights, higher than that of solutions with larger particles.

To explain the higher viscosity of highly dispersed systems, Hatschek[24] assumed that the effective volume was not constant for different dispersions. He assumed that the particles were surrounded with an adsorbed envelope of vehicle. If the thickness of the absorbed envelope is constant for a given system, it follows that the effective volume of the disperse phase increases with the increasing dispersion as found by Oden[40]

Hess[27] mentioned that the "dead space" existing between the suspended solid particles must be considered.

Humphrey and Hatschek[24] first demonstrated a decrease of viscosity with increasing rate of shear for suspensions of rigid and approximately spherical particles. This phenomenon was commonly observed in lyophilic solutions.

Hatschek and Jane[25] extended the study of Humphrey and

Hatschek and reported that a marked reduction in viscosity with increasing rate of shear was observed in suspension of 2 to 8 volume per cent of starch. To explain this anomaly, they assumed either a thick layer of adsorbed liquid around the particles or Hess's[27] "dead space" concept.

McDowell and Ueber[38] also tried to explain the anomaly from a different angle. They found that the electrically neutral particles, like those of starch or carbon black in an organic liquid did not distribute themselves uniformly in the medium, but instead formed clusters or "ramifying aggregates." They concluded that the liquid, which was no longer free, formed a network with demonstrable rigidity, thus causing a high viscosity at a low rate of shear; with the progressive destruction of these structures at increasing rate of shear the viscosity decreased.

By the addition of protective colloids, McDowell and Ueber[38] found that the formation of clusters or "ramifying aggregates" could be eliminated, and showed that suspensions thus protected did not exhibit any anomaly and behaved like normal liquids.

Lawrence[29] attacked the anomalous phenomenon by measuring the velocity distribution of flow in a number of anomalous system across a tube in which a stream of colored liquid was drawn into the liquid in flow. The profile of the colored liquid was photographed so as to show any deviation from Newtonian flow. He found that an anomaly appeared in systems of isodimensional particles only at high concentration.

Mardles[31] found that anomalous viscosity was less pronounced with suspensions in viscous liquids than in those of low viscosities. These anomalies were attributed to the disturbance of dispersed primary particles, alone or as aggregates of primary particles. This difference

between high and low viscosity liquids was attributed to a more sluggish rotational movement of the particles. He also found that the relative viscosity decreased with a rise in temperature.

In 1942, Mardles[34] mentioned that when the flocculation of solid particles was considerable there was a tendency for (a) anomalous and high viscosity with thixotropic behavior because of the three-dimensional bridgework in the settled solid, and (b) high settling rates and high sediment volumes.

Critical pigment volume concentration was defined as the volume concentration of pigment in the suspension under which the stress-rate of shear relation was linear and no yield value was observed. Mardles[33] found that the critical pigment volume concentration was a characteristic of each vehicle-pigment combination. However, there was no simple relation between the specific viscosity and yield value. Sedimentation experiments showed that the yield value decreased as the viscosity of the vehicle increased. It was also shown that pigments which have high sedimentation volumes tended to give higher yield values.

In 1949, Robinson[46] found that the "packed-sediment volume" appeared to be the effective volume of the particles at any concentration.

In 1951, Robinson[47] studied the effect of particle size by measuring the viscosities of suspensions of glass spheres in sugar solutions and found that small spheres in a viscous medium had a greater effective volume than their effective volume in water, and the increase in effective volume was greater as the size of spheres decreased.

The validity of the Einstein viscosity Equation (4) was again tested in 1951 by Donnet[11]. He found that the relative viscosity did not vary with temperature or with velocity gradient, and that the Einstein

shape factor was constant as the volume concentration of the suspension approached zero. However, contrary to theory, the Einstein shape factor was 7.8 instead of 2.5. Among the explanation discussed, Donnet considered the most likely to be the presence of aggregates of primary particles.

Williams[57] in 1953 studied the flow properties of concentrated suspensions by measuring the viscosities of suspensions of glass spheres in volume concentrations greater than 30 per cent. He found that the more nearly the particle sizes were equal to each other the lower was the concentration of spheres required for a given viscosity. It was also found that for particle sizes less than 1 micron in diameter, the smaller the size the greater the thixotropy.

Orr, Jr.[41] qualitatively studied the effect of particle size distribution on the suspension viscosities. By analysis of previously reported data, he reported that the viscosities of suspensions of spheres from the lowest to the highest concentration employed were described in terms of the viscosity of the pure liquid, the volume fraction of the solids, the packed-sediment volume of the solids, and the shape of the suspended solids.

Zettlemoyer[58] measured the viscosity of suspensions of calcium carbonate in polybutene. He found that the particle size of the pigment affected the viscosity of the suspension, i.e., the smaller the particle size, the greater the viscosity at a given loading. This effect was attributed to an envelope of "immobilized vehicle" on the surface of each pigment particle and in the narrow portions of the interstices of agglomerates. This "immobilized vehicle" increased the effective pigment volume to an extent proportional to the amount of pigment surface present.

A review of the literature revealed that the viscosity equations for suspensions are either the extension of Equation (3) of Einstein or the modification of Equation (4) of Arrhenius. The resultant equations take into consideration either the concept of particle population or the adherence of an immobilized liquid layer on the surface of the primary solid particles. These equations are not applicable to all suspensions of the Newtonian type (viscosity - rate of shear relationship is linear). Furthermore, the equations failed to explain the Bingham type and the Plastic type of flow which occur in suspensions of identical components but at different concentrations. Consequently an equation was derived which explained the anomalous rheological behavior of suspensions in general.

Many theoretical studies have been made to evaluate the effect of temperature on the viscosities of pure liquids, however, the exact effect of temperature on the suspension viscosities has not been definitely determined.

The effects of milling methods and milling time, although seldom studied, play an important role in the explanation of anomalous rheological behavior, particularly the formation of structions in suspensions.

Based on the concept of structure formation in suspensions a viscosity equation was derived. In order to explain the anomalous rheological behavior of suspensions observed in titanium dioxide-soy bean oil suspensions, a study was made of the effect of milling methods, milling time, volume concentration, particle size and additions of a surface active agent. The anomalous rheological behavior of suspensions in question has to do with the rate of shear. Thus, for low volume concentrations

in suspensions the viscosity is independent of rate of shear, while for high volume concentrations in suspensions the viscosity depends upon the rate of shear.

TABLE I

PUBLISHED VISCOSITY EQUATIONS

Author	Year	Viscosity Equation	Equation Number	Literature Reference Number
Arrhenius	1887	$\eta = \eta_o e^{\sigma C}$	3	2
Einstein	1906	$\eta = \eta_o (1 + 2.5 \phi)$	4	14
Hess	1911	$\eta = \frac{\eta_o}{1 - a \phi}$	5	27
Guth & Simha	1936	$\eta = \eta_o (1 + 2.5\phi + 14.1 \phi^2)$	6	18
Weltmann & Green	1943	$\eta = (\eta_o + b) e^{\sigma C}$	7	55

TABLE I(cont)

PUBLISHED VISCOSITY EQUATIONS

Vand	1945	$\eta = \frac{\eta_o}{(1 - E - E^2 q)^{\alpha}}$	8	50
Vand	1948	$\ln \eta_r = \frac{k_1 E + \gamma (k_2 - k_1) E^2}{1 - \theta E}$	9	51
Robinson	1949	$\eta_{sp} = \frac{\beta \phi}{1 - S' \phi}$	10	46
Mooney	1951	$\ln \eta_r = \frac{2.5 \phi}{1 - \lambda_i \phi}$	11	39
Maron	1951	$\ln \frac{\nu}{\eta} = h Z$	12	35
Orr, Jr.	1955	$\frac{\eta - \eta_o}{\eta} = J C^{\psi}$	13	41

DESCRIPTION OF APPARATUS

Commonly used viscometers are classified as follows:

1. Capillary type viscometer.

   Example: Ostwald viscometer, Ubbelohde viscometer, Redwood viscometer.

2. Falling ball viscometer.

   Example: Lawazeck viscometer, Hoppler viscometer.

3. Rotary viscometer.

   Example: Macmichael viscometer, Brookfield viscometer, Stormer viscometer.

4. Vibration viscometer.

   Example: Bendix Ultra-viscoson.

For plastic, pseudo-plastic and dilatant flows, the viscosity is dependent on the rate of shear, and consequently cannot be measured by a one-point method. A multiple-point method is necessary to obtain a viscosity curve for a non-Newtonian fluid.

The rotational type of viscometer in which shear stress is applied to the fluid by the rotation of a cup or of a rotor is useful for most of the measurements on Newtonian and non-Newtonian fluids. For certain materials, as clear non-thixotropic liquids of low viscosity, capillary-tube viscometers are preferable; for others, parallel-plate instruments are the only kind that give satisfactory results. A vibration viscometer is often used in the measurement of high viscosities.

In the present research, a commercial model Stormer viscometer was employed, as it was readily available and met the necessary requirements. That is, with the Stormer viscometer, the rotational speed of the rotor could be varied by changing the driving weights allowing a

multipoint determination of stress and rate of shear. The types of rotors and the containers were modified depending upon the volume concentration of particles in the suspensions. The assembled Stormer viscometer is shown in Figure 2, while paddle and bob-type rotors are shown in Figures 3 and 4, respectively. The selection of the suspension container depended upon the paddle-type rotor and the bob-type rotor employed. A pyrex-glass beaker (250 ml capacity) was used as the container of the fluid with the paddle-type rotor. The writer designed the brass container, shown in Figure 5, which was used with the bob-type rotor after calibration. To insure equal volumes of suspension samples, the viscometer container was filled each time to a line marked on the container wall.

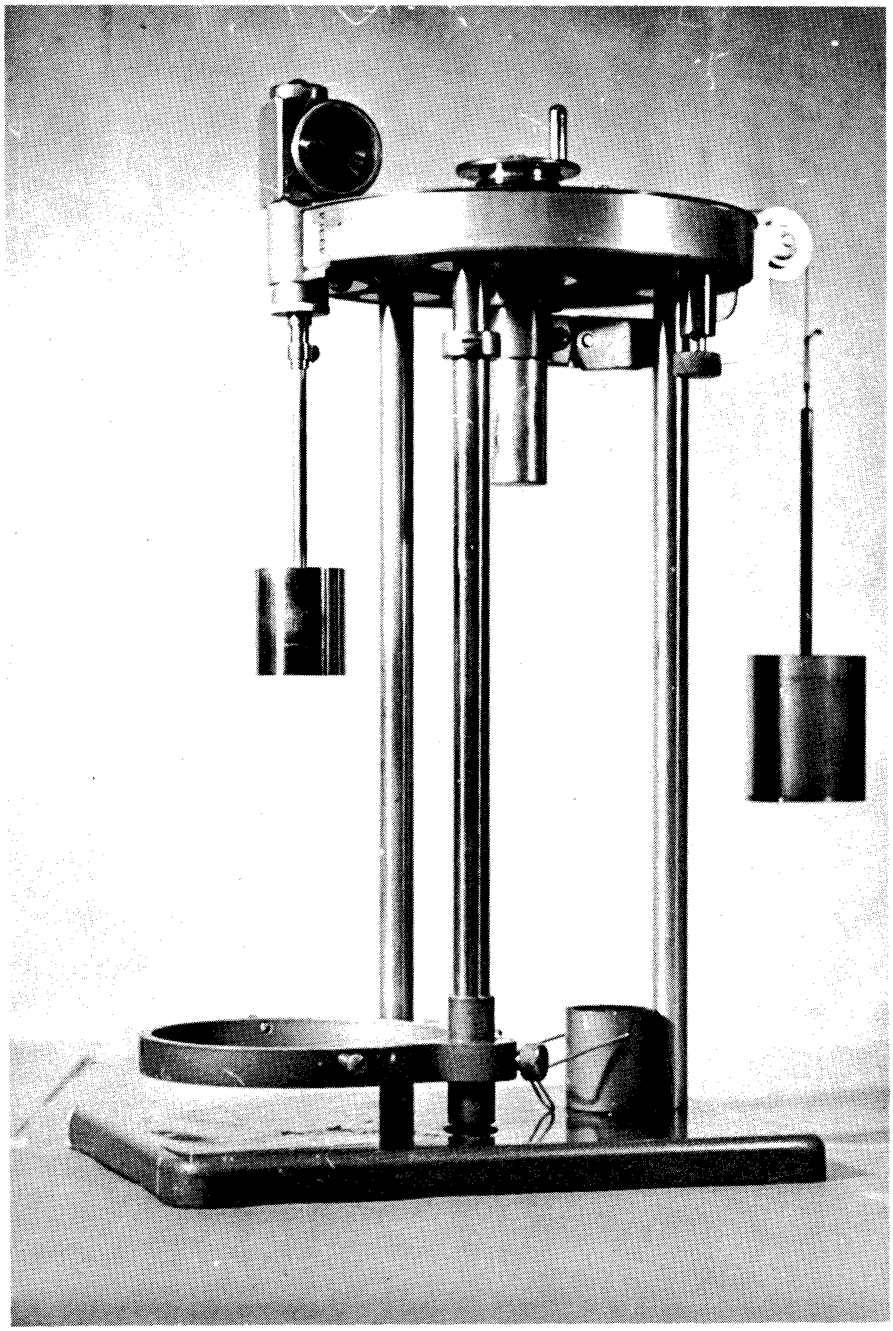

Figure 2. Assembly of Stormer Viscometer

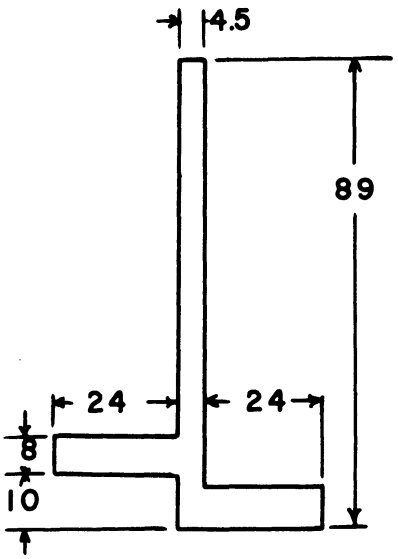

(Blades 15 mm thick)

FIGURE 3
DIMMENSION (in mm) OF
PADDLE-TYPE ROTOR

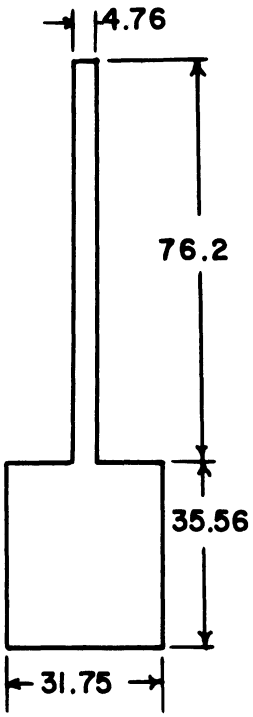

FIGURE 4
DIMMENSION (in mm) OF
BOB-TYPE ROTOR

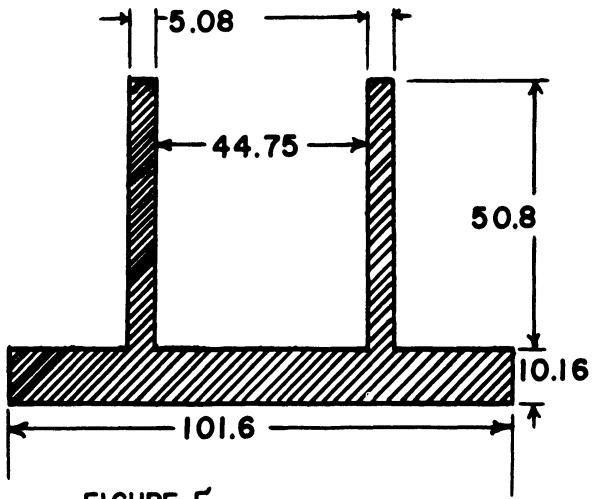

FIGURE 5
DIMMENSIONS (in mm) OF CUP

CALIBRATION OF THE APPARATUS

Stormer Viscometer with Paddle-Type Rotor

A paddle-type rotor was used in the low concentration range, i.e., 0-5% of solids (by volume) where the fluid flow was typified as the Bingham type.

Generally speaking, when the paddle-type rotor was used, the relation between driving weight and rotational speed of the rotor was not linear. Furthermore, because the theoretical equation showing the relation between the driving weight and the rate of shear for a paddle-type rotor was not well established, the calibration of the Stormer viscometer (with a paddle-type rotor) was experimentally determined.

Van der Walt[53] calibrated the Stormer viscometer with either paddle-type or bob-type rotor by correlating Q against a modified Reynold's number Re'.

Here Q was defined as $Wt^2/B^2\rho$ and the modified Reynold's number Re' was defined as $B\rho/\eta t$, where

ρ = density of test fluid

η = viscosity of the fluid

t = time in seconds required for 100 revolutions of a rotor in the test fluid

W = effective driving weight applied to the viscometer (actual driving weight minus frictional resistance)

B = a constant for a particular rotor, test cup, etc.

Geddes[16] derived an equation from the energy balance with respect to the fluid system, thus

$$\eta = \frac{[t\ (W - \frac{Ho}{t^2})]}{A} \qquad (14)$$

where t,ρ,W and η have the same meaning as in Van der Walt's correlation[53]. H and A in Equation (14) are the characteristic constants for a particular rotor and test cup, etc., which are determined from experimental data.

Many other published papers contributed to the calibration of the Stormer viscometer. However, none of them gave a convenient and satisfactory method of calibration for the Stormer viscometer with a paddle-type rotor because of the complex characteristics of fluid flow under observation.

Instead of deriving a theoretical equation or finding an experimental equation for the calibration of the Stormer viscometer with a paddle-type rotor, the writer correlated viscosity against the time required for the rotor to make a fixed number of revolutions with driving weights as the parameters. This method is not only very simple but is relatively more accurate than most other methods.

Standard liquids were obtained from the Bureau of Standards for the present calibration. The calibration curve is shown in Figure 44.

With this paddle-type rotor the accuracy was in a range of $\pm$ 3% for an ordinary liquid while it was estimated to be within $\pm$ 5% for a suspension fluid.

For 0-5% volume concentration of particles in suspension, the suspension viscosities were measured by reading the time required for 100 revolutions of the paddle rotor at a constant driving weight of 50, 75, 100, 125 and 150 grams; and the viscosities were read from the prepared calibration curve. This method not only indicated whether viscosity depended upon rate of shear, but also eliminated the erroneous results which could be introduced by a single-point method.

Stormer Viscometer with Bob-Type Rotor

When a Stormer viscometer with bob-type rotor was used, an instrument constant was determined by measuring the driving weight and rate of shear relationship on standard liquids obtained from the Bureau of Standards.

Some discussion regarding the rate of shear and its calculation for a rotational viscometer was necessary. (See Hatschek, E., "The Viscosity of Liquids," p. 32, 1928). The rate of shear (or velocity gradient) S is determined from the rate of rotation, radius of the bob, and the clearance between cup and the bob. For any angular velocity ω, S is not uniform throughout the annular space between the cup and bob, but depends upon the distance X from the axis of rotation:

$$S = \frac{2\ R^2_c\ X\ R^2_b}{R^2_c - R^2_b} \times \frac{1}{X^2} \times \omega \qquad (15)$$

where R_c and R_b are the radii of the cup and the bob. The mean value of $\overline{S}$ throughout the annular space may be found as follows:

$$\overline{S} = \frac{\int_{R_b}^{R_c} S\ dX}{\int_{R_b}^{R_a} d\ X} = \frac{2R_bR_c}{R^2_c - R^2_b} \times \omega \qquad (16)$$

When the clearance between cup and bob is small, the rate of shear at any point will not differ significantly from the mean value, within the limits of experimental error. It may, therefore, be calculated for the angular velocity ω by multiplying by a factor involving only the radii of the cup and the bob. Since ω is more conveniently found in r.p.m. than in radians per second, Equation (16) may be written:

$$\overline{S} = \frac{4X}{60} \times \frac{R_cR_b}{R^2_c - R^2_b} \times (\text{r.p.m.}) = K_s(\text{r.p.m.}) \qquad (17)$$

For Newtonian fluids the variation in rate of shear at different rates is not important, since the viscosity is independent of this variable. For non-Newtonian fluids, such as were examined, the effect may be of considerable importance, because the apparent viscosity, which, as shown above, may be taken as a reasonable representation of the behavior of the material being studied.

There is a second effect that may become significant for materials showing highly anomalous behavior. In the derivation of Equation (15) it was assumed that the viscosity is constant throughout the liquid being sheared. If the apparent viscosity varies rapidly with rate of shear, then the effect of varying the last quantity from point to point may be great enough to make the above assumption invalid. Ordinarily this is a second order effect, however, and would not introduce a significant error in the interpretation of the experimental data.

It is evident that at constant driving weight, the following relation is established between driving weight W and shear stress τ:

$$\tau = K_w W \tag{18}$$

From the above discussion, for the calibration of Stormer viscometer with bob-type rotor, the calibration coefficient K' of the particular rotor and cup combination must be determined. K' is defined by the following equation:

$$\eta = \frac{\tau}{\bar{S}} = \frac{K_w W}{K_s (\text{r.p.m.})} = K' \frac{W}{(1/t)} \tag{19}$$

where W is the driving weight in grams, t is the time in seconds required for 100 revolutions of the bob-type rotor and η is the viscosity in centipoise. The unit in which K' is expressed, is dependent upon the units selected to express η, t and W, thus $K' = \frac{\text{centipoise}}{\text{gram seconds}}$.

The constant K' (calibration coefficient) was determined by measuring the viscosities of standard liquids which were obtained from the Bureau of Standards. The calibration curve is shown in Figure 45. ($K' = 6.94 \times 10^{-2}$)

With the bob-type rotor, the accuracy was estimated to be within $\pm$ 5% for suspensions.

PIGMENTS AND VEHICLE

Throughout the present experiments, titanium dioxide pigments and commercial soy bean oil were used.

Especially prepared titanium dioxide (anatase) pigments were supplied from the National Lead Company, Titanium Division, New Jersey.

The particle size and shape of each pigment are listed in Table II. The mean particle size and shape of the pigments were obtained by electron microscopic studies.

TABLE II

SIZE AND SHAPE OF TITANIUM DIOXIDE PIGMENTS

Pigments Batch Identification No.	Mean Diameter (micron)	Shape
TiO_2-MP-776-1	0.061	round
TiO_2-MP-776-3	0.171	round
TiO_2-MP-776-4	0.04	round
TiO_2-MP-776-5	0.05	round
TiO_2-MP-776-6	0.25	irregular
TiO_2-MP-1250	0.30	irregular

A commercial soy bean oil was used as the liquid medium.

The viscosities of the soy bean oil at various temperatures as measured by the Stormer viscometer are tabulated in Table III.

TABLE III

VISCOSITY OF COMMERCIAL SOY BEAN OIL

Temperature (°C)	Viscosity (cps.)
20 ± 0.1	70.1
25 ± 0.1	52.2
30 ± 0.1	40.9
35 ± 0.1	33.2

The pigments employed in this investigation were dried by heating at 220°F for two hours in a forced draft constant temperature electric oven.

EXPERIMENTAL PROCEDURE

Plastic Flow

It was known from preliminary experiments that with a volume concentration of pigment in the range of 5 - 30% the titanium dioxide-soybean oil suspensions belonged to the class of plastic flow which showed a yield value and the viscosities of the dispersed systems depended on the rate of shear.

Preparation of Suspension Systems

Suspensions were prepared from soy bean oil and the various titanium dioxide pigments, TiO_2-MP-776-3, TiO_2-MP-776-4, TiO_2-MP-776-5 and TiO_2-MP-1250. The pigments bear the batch identification numbers of National Lead Company. These pigments were pretreated as mentioned.

The paste was prepared for each pigment-soy bean oil combination with a definite amount (392.6 g) of pigment and a definite amount of soy bean oil (132.3 g) by dispersion on a three-roller mill. Lower volume concentrations of suspensions were prepared by diluting the above prepared paste with soy bean oil. The ball milling process was not too adequate for the preparation of paste at such high volume concentration because the balls in the jar stuck to the paste and did not create the necessary shear stress to disperse the pigment in the liquid medium.

Measurement of Viscosity

There are two ways in which apparent viscosity may be determined. The data may be plotted as accurately as possible, and then the ratio of shear stress/rate of shear at the rate of shear in question is calculated. The second method is to fit the experimental data to some empirical equation expressing stress in terms of rate of shear and then

to calculate the ratio of shear stress/rate of shear at any point. This method does not require such accurate draftsmanship as does the first and, once the empirical equation has been determined, permits immediate calculation of the apparent viscosity at any rate of shear.

In the present investigation, the first method was employed to evaluate the apparent viscosities of suspensions.

Rheological measurements for suspensions in the volume concentration range of 5 - 30% were made on a modified commercial model Stormer viscometer. The cup and paddle assembly supplied with the instrument were replaced by a cylindrical bob and cup machined from brass, with the dimensions shown in Figures 4 and 5.

The procedure in making these measurements follows. The cup and bob were aligned carefully by means of adjusting screws on the support for the bath. The cup was filled with the material to be measured, and, to hasten the attainment of thermal equilibrium, both bob and material were heated to the desired temperature beforehand. A series of readings was taken with different loads at different times. Most of the data were obtained in random order of loads; some readings were taken also at decreasing loads to afford an indication of any change in structure, while some readings were taken in an increasing load order so as to check the accuracy of the experiments and note any thixotropic tendency. The measurements were conducted at a constant temperature ($25 \pm 0.1°C$), since the effect of temperature on the viscosity was not the main purpose in this study.

Experimental results were plotted on ordinary graph paper with driving weight as the ordinate and rotational speed $1/t$, where t is the time in seconds required for 100 revolutions of a rotor, as the abscissa. The

experimental data are shown in Table IX and are plotted in Figures 11 - 15. The curves are convex to the stress (the driving weight) axis, and intersect the stress axis at $1/t = 0$. This fact implies the existence of yield values in these suspensions. Viscosities were obtained by multiplying the ratio of $\Delta W/(1/t)$ at certain value of $1/t$ by a calibration coefficient of the viscometer. Viscosity, $1/t$ and volume concentration data are shown in Table X.

Yield values were determined by the method mentioned above. Readings of yield values are tabulated in Table XI. They are plotted as ordinate on rectangular graph paper with particle size as parameters and volume concentrations as abscissa in Figure 24.

Bingham Flow

Bingham flow is one which shows a linear relation between stress and rate of shear and possesses a yield value. Bingham did not deduce by any mathematical process an equation, but introduced the yield value directly into the Poiseuille equation and obtained, naturally, a linear equation of flow.

The effects of particle size, volume concentration of pigment in the suspension, temperature change and ball milling time, were studied. It was known from the preliminary studies that, in the titanium dioxide-soy bean oil system, the flow was classifiable as Bingham type when the volume concentration of the pigment in the suspension was lower than 5%.

Preparation of Suspension Systems

Titanium dioxide pigments labeled by National Lead Company as TiO_2-MP-776-1, TiO_2-MP-776-3, TiO_2-MP-776-4, TiO_2-MP-776-5 and TiO_2-MP-776-6 and soy bean oil were used throughout the experiments. These pigments were pretreated as previously described.

Instead of using a three-roller milling process, the suspension with desired volume concentration was prepared by the ball milling process. During the ball milling process, variables involved were kept constant as possible so as to prevent errors in the interpretation of the experimental data which might be caused by those variables. The variables considered were: size of the jar, number of the balls, rotational speed of the mill, milling time, etc. In the present experiments these variables were fixed as follows:

Volume of glass jar . . . 750 cc

Number of balls . . . 25 (they were so selected that each set of 25 balls had the same weight)

Shape of balls . . . spherical

Rotational speed of mill . . . 200 revolutions per minute

Milling time . . . 96 hours (determination of milling time will be discussed later)

Measurement of Viscosity

Rheological measurements of viscosity of suspensions in the volume concentration range of 0 - 5% were made on a commercial model Stormer viscometer with paddle-type rotor. The dimensions of the paddle are shown in Figure 3. A cup used with the paddle-type rotor was an ordinary 250 ml pyrex beaker. The calibration curve for the paddle-type rotor and cup combination was prepared as previously described. (See Figure 44 and Appendix F).

The procedure for viscosity measurement was the same as previously mentioned.

The driving weights were 50, 75, 100, 125, 150 and 200 grams. From the driving weight and corresponding readings of the time in seconds required for 100 revolutions of the paddle rotor, the viscosity was read from the calibration chart, Figure 44. If the viscosity was variable with respect to driving weight (or rate of shear), the viscosity thus obtained would not be constant. The viscosities of suspensions of definite volume concentration and particle size at a definite temperature were constant in the low volume concentration range of 0 - 5%.

Temperature of the suspensions during the measurements was varied by 5°C intervals, between the limits of 20°C to 35°C so as to afford information about the effect of temperature on the viscosity.

The main reason for using this type of paddle rotor was to reduce the sedimentation effect when the above-mentioned bob-type rotor was employed for measurement of viscosity at lower volume concentrations[53].

Plastic Flow

The experimental data which show the relationship between the shear stress and the rate of shear are plotted in Figures 11 - 15. Viscosities of the suspensions, in a volume concentration range of 5 - 30%, were calculated from these figures. Results are tabulated in Table X and are shown in Figures 16 - 23.

In the volume concentration range of 5 - 30%, it was evident from Table X that the viscosities of the suspensions of titanium dioxide pigments in soy bean oil depended on both rate of shear and volume concentration of particles in the suspensions. Furthermore, the suspensions possessed yield value.

According to the classification suggested by Pryce-Jones[42], see Appendix A, the Plastic flow was dominant in titanium dioxide-soy bean oil systems in the volume concentration range of 5 - 30%.

When Bingham[4] first confirmed the existence of an intercept on the pressure axis while working with clay-water suspensions, he called it "friction." He thought the intercept gave a measure of the force necessary to overcome the frictional resistance of the particles before the flow started. Later, Green[17] found that flocculation played an important part in the formation of structures and the production of the intercept. Green[5] considered the term "friction" not broad enough to include all the causes for the production of the intercept, and so the term "friction" was discarded and "yield value" was used in its place.

De Wael and Lewis[10] and Harvey[22] also mentioned in their papers that "flocculation force" plays an important part in the formation of structures.

The forces of flocculation probably depend upon (a) the force of electrical origin between particles or (b) the force of the London - Van der Waals type. The existence of the electrical origin force seems to be well established. The principles on which they have been treated are clear. However, the quantitative side of the treatment in the case of high charge densities still leaves much to be desired. Adequate experimental data are still lacking in all but the most simple cases. The London - Van der Waals force, in general, causes attraction and promotes coagulation. Although they have been incorporated into the present theories of colloid stability, their actual role is still open to discussion. Quantitative data are scarce and conflicting.

However, Breyer[37] believed that the force of orientation existing between particles caused the yield value.

Vand[50], Robinson[47] and other investigators confirmed the principle that the particles were capable of absorbing and swelling in the liquid, and that the particles were appreciable solvated and would be surrounded by an envelope of the liquid medium. Zettlemoyer[58] designated this envelope of the liquid medium as the "immobilized liquid."

In ideal cases where the particle is rigid and non-attractive, the envelope of the liquid medium could be very thin and the particles could exist independently in very dilute concentrations. However, when the particles are slightly attracted or the concentration of the suspension is rather high, the boundaries of one particle would merge with boundaries of adjacent particles. Thus a structure is formed instead of a suspension of many independent particles. The thickness of the immobilized liquid envelope and the size of the structure would be a function of characteristics of the particles and the liquid medium.

Generally the mass of particles is dispersed in a liquid medium by the application of shear stress, produced by a ball mill or a three roller mill. The mass of particles is broken into small groups of particles or into individual particles and the liquid medium penetrates into the void space between the particles. Thus the solid particles are dispersed in the liquid. When the application of shear stress ceases, the formation of "structure" starts. However, the rate of formation of structure and the compactness of the structure should be dependent upon the characteristics of the particles and the liquid medium.

In suspensions of non-attractive particles, the structure could not be formed in concentrated suspensions where the mass of the particles is simply piled up. There is not sufficient force acting between the particles to bind them tightly to form structures.

Street[48] suggested "that all bodies possessing a yield value are also thixotropic; however, if their time of rebuilding structure is extremely short, then they are not recognized as such. In other words, those suspensions that have been called thixotropic are those whose time effect is of medium value; those with very fast or those with very slow effects have not been recognized as thixotropic."

According to this statement Plastic type of flow could be thixotropic because the structure is broken down or is rebuilt.

The anomalous phenomenon was explained by the writer as follows:

As the suspension was sheared in a viscometer container, the structure was pulled in the direction of the shear stress while the shear stress was lower than the yield value. When the shear stress was sufficiently high, the structure was broken down into smaller size structures; hence, causing the dispersed system to flow. This critical shear stress was called yield value.

As the shear stress was increased, the structures were further broken down into smaller sizes, and, as a consequence, the apparent viscosity decreased. This was a Plastic type of flow. If a point was reached at which no further change in the size of the structures occurred, then the relationship between stress and rate of shear would become linear. In other words, the viscosity of the suspension would be independent of the rate of shear. This was a Bingham type of flow.

A Plastic type of flow was observed when the volume concentration of titanium dioxide pigment in soy bean oil was between 5 - 30%. Flow curves are shown in Figures 11 - 15 in which the driving weights were plotted against 1/t. The time in seconds required for 100 revolutions of a rotor is t. These plots were the same as the ordinary shear stress vs. rate of shear plot, and they indicate a typical Plastic type of flow at the volume concentration range of 5 - 30%. In other words, the structures were still continuously broken down into smaller sizes as the rate of shear was gradually increased.

Since the dielectric constant of suspensions of spherical particles is appreciably less than that of non-spherical particles when the volume of the suspended phase is constant, Voet[54] measured the dielectric constant of suspensions. He derived the equation

$$\epsilon = \epsilon_m(1 + 3F\phi) \tag{20}$$

from Bruggeman's[9] equation for the suspension of spherical particles:

$$1 - \phi = \frac{\epsilon_p - \epsilon}{\epsilon_p - \epsilon_m} (\epsilon_m/\epsilon)^{1/3} \tag{21}$$

where ϕ is the volume fraction of the dispersed phase, ϵ is the dielectric constant of the suspension, ϵ_p is the dielectric constant of the solid particles, and ϵ_m is the dielectric constant of the suspending medium. The "form factor" F was introduced by Voet[54] for non-spherical

particles in dispersions where the dielectric constant of the dispersed phase is much larger than the dielectric constant of the medium. For spherical particles, F = 1, for non-spherical particles F > 1.

Voet[54] mentioned "it has not been found possible, however, to relate form factor directly to specific ratios of particle dimensions. Our knowledge at present is limited to the qualification that the larger the form factor, the more deviation there is from the spherical shape... it must be emphasized that, in order to cause an increased dielectric constant of the dispersion, the particles must touch one another directly, forming conductive chains. Particles connected by forces having minima of potential energy at a distance are dielectrically equivalent to totally independent particles. Thus, the experimental evidence indicates that the particle structures are composed of directly connected particles." He said furthermore, that "when particle agglomerates are subjected to shear, they are partly broken up, but in the presence of strong agglomeration particle chains will still exist at moderate shearing stress.....It was observed that strong forces between particles will cause an immediate agglomeration after discontinuation of the applied shearing forces, leading to a rheologically hardly perceptible thixotropy, while weak forces will only slowly rebuild a structure, making thixotropy more apparent."

From Figures 11 - 15, the viscosities of the Plastic type suspensions were observed to be depending upon both the rate of shear and the volume fraction of the solid particle in the suspensions.

The qualitative relations between the viscosities of the suspensions and the rate of shear are shown in Figures 16 - 19.

The viscosities of the suspensions decreased as the rate of shear increased as shown in the Figures 16 - 19. In other words, the viscosities of the suspensions decreased as the size of the structure in the suspensions became smaller compared to the original structure. Thixotropy was not observed in the present experiments, possibly because the rate of reformation of structures was so fast that the original structure was rebuilt immediately after the application of the shear stress.

In Figure 24, the yield values possessed by each suspension are shown.

As described before, the yield value is the critical shear stress which is required to pull the structure to some extent in the direction of flow before the original structure is broken down into smaller structures and the fluid begins to flow.

Weltmann and Green[55], in 1943, correlated yield values and volume fraction of pigments on semi-log paper and deduced the following equation

$$\tau_o = M\, e^{N\phi} \qquad (22)$$

where τ_o is the yield value, ϕ is the volume fraction of the pigment in the suspension, M and N are two constants depending on the material. They also found that N depends on the particle size.

However, they failed to correlate the data at lower concentrations, i.e., straight lines were not obtained at lower concentrations on semi-log paper.

From Equation (22), at zero volume concentration ($\phi = 0$), τ_o is equal to M. In reality, τ_o should be equal to zero. In other words, the liquid medium should not possess yield values unless the liquid

medium were either of the Bingham or Plastic type. Consequently, Equation (22) is invalid at very low pigment volume concentrations.

The writer correlated the yield value data by the following equation

$$\tau_o = k_3 \phi^n \qquad (23)$$

where τ_o is the yield value in grams which was found by the method previously described, ϕ the volume fraction of solid particles in suspension, and k_3 is the proportionality constant depending on particle size in Equation (23), and n is the characteristic constant of suspended solids.

The numerical values of n and k_3 were calculated from the data given in Table XI and Figure 24, and are tabulated in Table IV.

TABLE IV

CALCULATED NUMERICAL VALUES OF k_3
AND n EMPLOYED IN EQUATION (23)

Pigment	TiO_2-MP-776-3	TiO_2-MP-776-4	TiO_2-MP-776-5
k_3	2.26×10^4	6.06×10^4	3.81×10^4
n	2.54×10^4	2.62×10^4	2.61×10^4

As shown in Table IV, the numerical values of n for different particles sizes of titanium dioxide are almost equal, while the numerical values of k_3 are larger as the particle size becomes smaller. The conclusion is reached immediately that the magnitude of the yield value of a suspension depends largely upon the particle size and less upon the volume concentration of the suspended solids.

Bingham Flow

Effect of Volume Concentration on the Viscosity of the Suspension

The Bingham type of flow (one type of Plastic flow) possesses yield values, but the viscosity of the fluid is independent of rate of shear.

In 1954, Harper[20] found that "in the case of Plastic flow (according to present definition of flow, this is Bingham type of flow) once the yield stress is exceeded, the excess dissipation of energy due to the presence of the solute is entirely analogous to the case of Newtonian solution (suspension).....After the shearing stress has exceeded the yield stress, the interference offered by the solute particles to the flow of the medium appears completely similar to the case of Newtonian flow. It would be difficult to explain why this should not be so unless a change in the applied shear stress is associated with a change in the extent of agglomeration or particle size."

Green[17] explained the structure in his paper as follows, "the flocculated pigment is the Structure which holds the mass together, giving it a plastic nature; when this structure is destroyed plasticity tends to vanish.....Flocculation is a condition of aggregation; it is that condition or state of affairs which has arisen when the dispersed phase ceases to be uniformly dispersed and exists in groups or clusters, the individual units (particles) which are closely held together. When the word Flocculation is used, it implies three things: (a) a previous state having existed in which the discontinuous phase was dispersed in a continuous phase, (b) the unit of the discontinuous phase brought into contact with each other forming groups (flocculates), and (b) adherence of the touching units."

He illustrated "undispersed lump," "particle dispersed" and "flocculate" as follows:

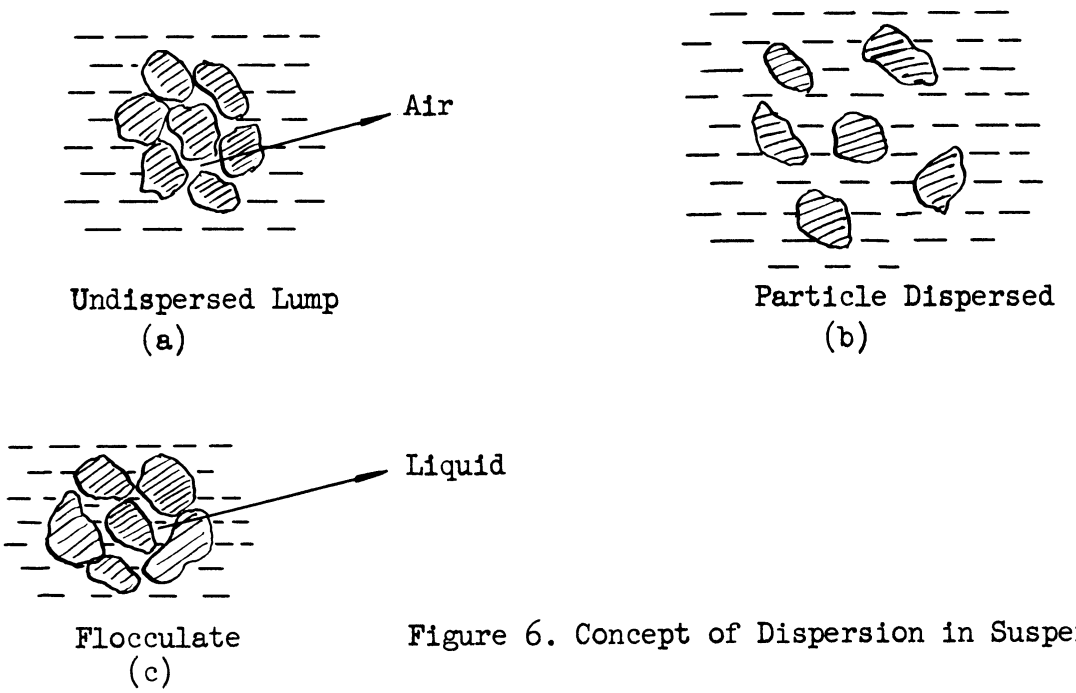

Figure 6. Concept of Dispersion in Suspension

The writer has derived from Newton's definition of viscosity a more general equation for the viscosities of suspensions.

In most cases, particles which are dispersed in the vehicle do not exist in an isolated form. In other words, they form structures with other neighboring particles and small portions of vehicle. More precisely speaking, the structures are formed from a number of particles, dead volume of vehicle or immobilized vehicle which are contained in the space between each particle and the thin layer of vehicle on the structure surface (see Appendix B). An ideal structure is a primary particle which is isolated from other particles and exists alone and is enveloped by a thin layer of vehicle.

The velocity gradient and the model of structures are shown in Figures 7 and 10 respectively (see Appendix B).

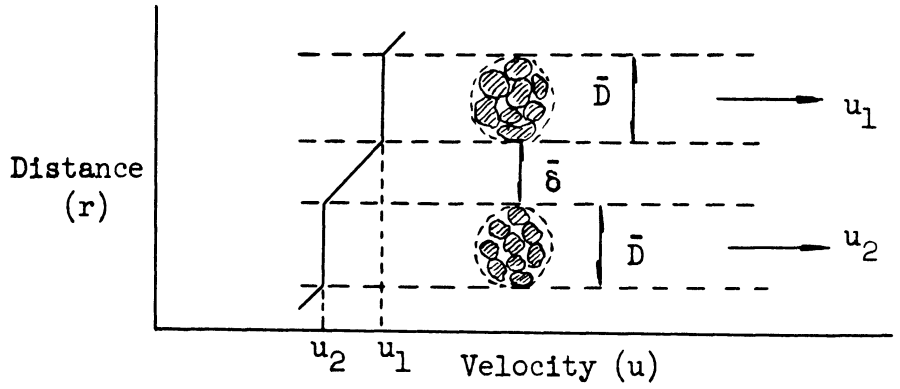

Figure 7. Velocity Gradient in a Suspension

The assumptions made for the derivation of an equation were:

(a) Each structure moves in the fluid with a uniform velocity u. In other words, the velocity function across the structure is discontinuous as shown in Figure 7. This assumption is reasonable because, as was described in the explanation of Plastic flow, no more breakdown of structure is expected if the viscosity of the fluid is independent of rate of shear. If there were a velocity gradient across the structure body, the structure would be broken up into smaller structures which would cause a decrease in the viscosity, i.e., the viscosity should be dependent upon the rate of shear.

(b) Liquid medium which is near the surface of the structure flows at the same velocity as the structure.

(c) Liquid medium is in Newtonian flow.

(d) Flow of the suspension is analogous to Newtonian flow when the shear stress is in excess of the yield value.

From Newton's definition of viscosity, the following equation can be formed:

$$\tau = \eta_o \frac{\Delta u_1}{\bar{\delta}} = \eta \frac{\Delta u_2}{\bar{\delta} + \bar{D}} \tag{24}$$

u_1 is the velocity of flow of structure 1 under shear

u_2 is the velocity of flow of structure 2 under shear

$$\Delta u_1 = u_1 - u_2$$

u_1' is the velocity of fluid flow near the surface of structure 1 under shear

u_2' is the velocity of fluid flow near the surface of structure 2 under shear

$$\Delta u_2 = u_1' - u_2'$$

where τ is the shear stress, η_o is the viscosity of liquid medium, η is the viscosity of suspension, $\bar{D}$ is the average diameter of the structure as shown in Figure 7, $\bar{\delta}$ is the mean distance between each structure shown in Figure 7, and is defined as follows:

$$\bar{\delta}/2 = \frac{V_m - V_c}{S_o} \tag{25}$$

S_o is the total surface area of the whole structures, V_c is the total dead volume which is involved in the structures and does not play any role in the fluid flow and V_m is the volume of the liquid medium.

From the assumption (a)

$$\Delta u_1 - \Delta u_2 = \Delta u \tag{26}$$

Substituting Equation (26) into Equation (24) gives

$$\tau = \eta_o \frac{\Delta u}{\bar{\delta}} = \eta \frac{\Delta u}{\bar{\delta} + \bar{D}} \tag{27}$$

Equation (27) can then be simplified by dividing by Δu and rearranging

$$\eta = \eta_o(1 + \bar{D}/\bar{\delta}) \tag{28}$$

Substituting Equation (25) in Equation (28) gives,

$$\eta = \eta_o(1 + \frac{S_o\bar{D}}{2(V_m - V_c)} \tag{29}$$

Substituting $K = S_o\bar{D}/2V_s$ in Equation (29) gives,

$$\eta = \eta_o(1 + \frac{S_o\bar{D}/2V_s}{\frac{V_m+V_s}{V_s} - \frac{V_s+V_c}{V_s}}) = \eta_o(1 + \frac{K}{1/\phi - (1 + V_c/V_s)}) \tag{30}$$

where ϕ is the volume fraction of particles in the suspension defined as

$$\phi = \frac{V_s}{V_m + V_s} \tag{31}$$

V_s is the total volume of solid particles and V_m is the volume of liquid medium.

According to the definition of specific viscosity[14]

$$\eta_{sp} = (\frac{\eta}{\eta_o} - 1) \tag{32}$$

the Equation (30) may be written in dimensionless terms

$$\eta_{sp} = \frac{K}{\frac{1}{\phi} - (1 + \frac{V_c}{V_s})} \tag{33}$$

Equation (33) has the same form as the Robinson Equation (10) which states

$$\eta_{sp} = \frac{\beta\phi}{1 - S'\phi} \tag{10}$$

where S' is the relative sediment volume expressed as volume of sediment per volume of solid particles. The volume fraction of particles in suspension is ϕ, and β is a constant determined by experiment.

Hess[27] also showed

$$\eta = \frac{\eta_o}{1 - a\phi} \tag{5}$$

where "a" is a factor greater than 1, ϕ is the volume fraction of suspended particles.

When the structure is spherical, then

$$S_o = N_a \pi \bar{D}^2 \tag{34}$$

where N_a is the total number of spherical structures and $\bar{D}$ is the average diameter of each spherical structure.

Substituting Equation (34) in Equation (29) gives,

$$\eta_{sp} = \frac{N_a \pi \bar{D}^3 / 2V_s}{\frac{1}{\phi} - (1 + \frac{V_c}{V_s})} \tag{35}$$

or on simplification we have

$$\eta_{sp} = \frac{3V_p/V_s}{\frac{1}{\phi} - (1 + V_c/V_s)} \tag{36}$$

where V_p is the total volume of the structures $V_p = \frac{N_a \pi \bar{D}^3}{6}$

and η_{sp} is the specific viscosity.

Equation (36) shows that the Einstein Equation (4) can be applied only to the super-ideal case where each particle is completely isolated from neighboring particles and the particles are not enveloped by a thin layer of liquid which is assumed in most rheological papers. Under this condition, Equation (36) becomes

$$\eta_{sp} = 3 \phi \tag{37}$$

which is very close to the Einstein equation for the viscosity of a suspension:

$$\eta_{sp} = 2.5 \phi \tag{4}$$

The only difference is the coefficient of 3.0 instead of 2.5 in Einstein's equation.

From Equation (33), a linear relation should be obtained when $1/\eta_{sp}$ is plotted against $1/\phi$. Furthermore, numerical values of K and

V_c/V_s can be obtained from the slope of the line and the intersection of the line with the $1/\phi$ axis, respectively.

Numerical values of K and V_c/V_s afford qualitative information about the relative size and shape of the structure when the shear stress is being applied in the viscometer.

Three different types of $\frac{1}{\eta_{sp}}$ vs. $1/\phi$ curves are expected. These three types are shown in Figures 8(a), 8(b) and 8(c).

In Figure 8(a), there is no break in the $1/\eta_{sp}$ vs. $1/\phi$ curve. This implies that the size of the final structure is unchangeable with respect to volume fraction of solid particles in the suspension because the numerical value of K is constant, Equation (33).

In Figure 8(b), there is a break in the $1/\eta_{sp}$ vs. $1/\phi$ curve at the point B. The slope of the line AB is larger than the slope of the line BC. In other words, the numerical value of K for the suspension in the volume concentration range represented by line AB is lower than that of the suspension in the concentration range represented by line BC. This implies that the size of the final structure is smaller as the volume fraction of the solid particles in the suspension increases.

In Figure 8(c), there is also a break in $1/\eta_{sp}$ vs. $1/\phi$ curve at the point E. However, the slope of the line DE is smaller than the slope of the line EF. In other words, the numerical value of K for the suspension in the concentration range represented by line DE is higher than that of the suspension in the concentration range represented by line EF. This implies that the size of the final structure is larger as the volume fraction of the solid particles in the suspension increases.

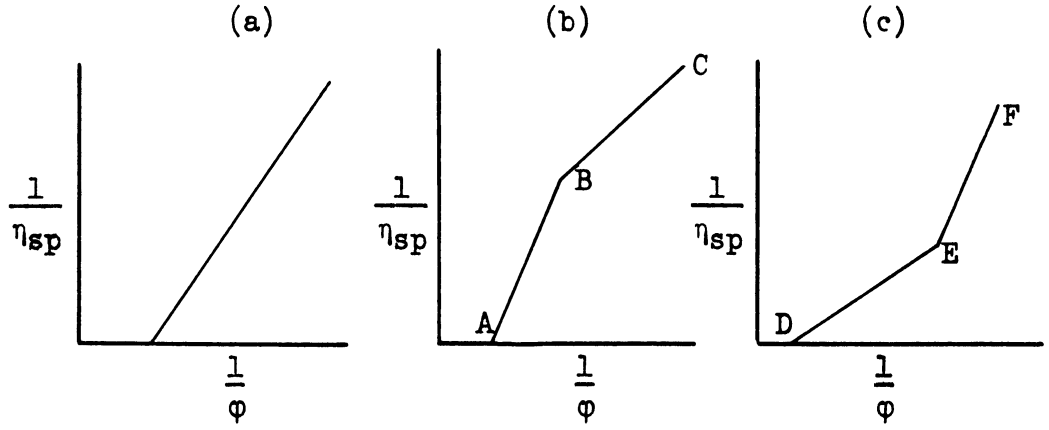

Figure 8. Three Considerable Types of $1/\eta_{sp}$ - $1/\varphi$ Relations.

The experimentally measured viscosities of suspensions in the volume concentration range of 0 - 5% at temperatures of 20°, 25°, 30° and 35°C are shown in Table XII and are plotted in Figures 25 - 28 with $1/\eta_{sp}$ as ordinates and $1/\phi$ as abscissa.

Straight lines were obtained in this range of volume fractions. In other words, the size of the final structures did not change with respect to the volume fraction of the solid particles in this volume fraction range.

Numerical values of K and V_c/V_s were obtained from the slope and the intersection of the line with $1/\phi$ axis in Figures 25 - 28 and are tabulated in Table V.

TABLE V

NUMERICAL VALUES OF K AND V_c/V_s AS DEFINED BY EQUATION (33)

Temp. (°C)	Pigments	V_c/V_s	K
20 ± 0.1	TiO_2-MP-776-1	8.2	28.5
20 ± 0.1	TiO_2-MP-776-3	7.4	25.8
20 ± 0.1	TiO_2-MP-776-4	9.0	31.5
20 ± 0.1	TiO_2-MP-776-5	9.0	31.5
20 ± 0.1	TiO_2-MP-776-6	7.3	25.2
25 ± 0.1	TiO_2-MP-776-1	5.5	52.0
25 ± 0.1	TiO_2-MP-776-3	4.9	41.4
25 ± 0.1	TiO_2-MP-776-4	6.0	50.4
25 ± 0.1	TiO_2-MP-776-5	6.0	50.4
25 ± 0.1	TiO_2-MP-776-6	4.5	38.4
30 ± 0.1	TiO_2-MP-776-1	3.0	60.9
30 ± 0.1	TiO_2-MP-776-3	2.5	57.3
30 ± 0.1	TiO_2-MP-776-4	3.0	68.7
30 ± 0.1	TiO_2-MP-776-5	3.0	68.7
30 ± 0.1	TiO_2-MP-776-6	2.5	51.3
35 ± 0.1	TiO_2-MP-776-1	1.7	72.6
35 ± 0.1	TiO_2-MP-776-3	1.0	68.4
35 ± 0.1	TiO_2-MP-776-4	2.0	81.6
35 ± 0.1	TiO_2-MP-776-5	2.0	81.6
35 ± 0.1	TiO_2-MP-776-6	1.0	60.0

From Table V, the following facts were deduced:

(a) If the size of the solid particles was the same, the dead volume was smaller as the temperature increased.

(b) If the size of the solid particle was the same, the numerical value of K, i.e., the relative size of the structure was larger as the temperature increased.

(c) At the same temperature, the size of the structures was larger as the size of the individual particles became smaller.

Equation (33) implied that the viscosity of the suspension was not only a function of the volume fraction of the solid particles in the suspension but also was a function of the size of the structures which was represented by the numerical values of K. Furthermore, the size of the structures was a function of the temperature, the size of the particles, and possibly the physical characteristics of the liquid medium and the solid particles.

Equation (33) was also applied to the correlation of the published data of Eilers[13], Broughton[8], Robinson[46], Traxler[49], Zettlemoyer[58] and Maron[36]. The correlations are shown in Figures 29 - 34.

These figures indicate that in suspensions of glass spheres - water, diatomaceous earth - asphalt, gray-green mica - asphalt, and calcium carbonate - polybutene, the relations between $1/\eta_{sp}$ and $1/\phi$ were linear and the size of the final structures did not change with volume fraction of solid particles in suspension within the volume fraction range investigated by the various authors. However, in the suspensions of black slate - asphalt, the relation between $1/\eta_{sp}$ and $1/\phi$ was not linear, i.e., the size of the structures changed with respect to the volume fraction of solid particles in the suspensions.

From the above analysis of the experimental data, as Harper mentioned in 1954[20], once the yield stress was exceeded, the nature of the Bingham type of flow was analogous to that of Newtonian flow.

Effect of Particle Size on the Viscosity of the Suspension

In most of the classical work reviewed the effect of particle size on viscosities of suspensions was not mentioned.

In 1951 Robinson[47] studied the effect of particle size on viscosities of suspensions and found that the increase in effective volume was greater as the size of the sphere decreased. He defined the effective volume of the solid as the volume of the solid plus the volume of the liquid medium associated with the solid particle which does not play any role in the fluid flow. He measured the viscosity of three sizes of glass spheres, suspended in a sugar solution, the sphere diameters ranging from 3 to 4 microns, 4 to 10 microns and 10 to 30 microns, respectively.

Zettlemoyer[58] also found that the viscosity of suspensions of calcium carbonate in polybutene was affected by the particle size. According to Zettlemoyer, dispersed particles were covered with a shell of "immobilized vehicle" to an extent proportional to the amount of pigment surface present, which affects the particle size and viscosity of the suspensions.

As shown in Table V for titanium dioxide-soy bean oil suspensions, at a constant temperature the numerical values of V_c/V_s and K increased as the size of the particles decreased.

In other words, the size of the structures was larger as the size of the particles decreased.

Consequently the viscosities of the suspensions were affected by the size of the particles. The experimental data, Figures 25 - 28, indicated that viscosities of the suspensions were lower as the particle size increased, providing the particle size was larger than 0.05 microns. However, viscosities of suspensions which were prepared by milling with a ball mill were no longer affected by the size of particles if the particle size was smaller than 0.05 microns.

The Effect of Temperature On Viscosity

Many theoretical and experimental equations have been developed to indicate the relation between the viscosity of pure liquids and temperature. However, most of the investigators who studied viscosities of suspensions, measured the viscosity at constant temperature and paid less attention to a study of the effect of temperature on viscosity.

Mardles[33] measured viscosities of suspensions of kaolin, graphite, zinc oxide, silica, red oxide of iron, etc., at different temperatures and with different liquid media and concluded that the relative viscosity decreased with a rise in temperature.

However, in 1951, as a result of viscosity studies on water-carbon black suspensions with a Ubbelohde viscometer, Donnet[11] concluded that the relative viscosity did not vary with temperature.

In order to investigate the effect of temperature on viscosities of suspensions, the viscosities were measured at four different temperatures, i.e., 20, 25, 30, 35°C.

The experimental data, tabulated in Table XII, showed a straight line correlation in Figures 35 - 39 for plots of $\ln \eta$ vs. $1/T$, where T represents temperature in degrees Kelvin.

As shown in Table V, the temperature affected the size of the structures and consequently, the viscosities of the suspensions. For a constant particle size, the sizes of the structures were larger as the temperature increased.

Milling Time Effect

Milling time in a ball mill was studied to determine the effect on suspension viscosity as well as a suitable milling time for the experimental procedure.

The dispersion of pigments by a ball or jar mill operation bore some resemblance to pigment dispersion in a roller mill since the initial wetting of the pigment was followed by disintegration of the agglomerates.

The action in the jar mill was classified by Hoback[28], in the following four stages:

Stage I: Penetration of the vehicle into the pigment mass.

Stage II: Formation of a cluster.

Stage III: Breaking of the cluster.

Stage IV: Mixing to full mobility.

Stage I and Stage II generally proceeded very fast. However, Stage III took a long time before the fluid displayed full mobility.

Pigment TiO_2-MP-776-5 was used in this study. Volume concentrations were 3.48, 2.34 and 1.36% and were milled 5, 10, 20, 30, 40, 60, 80 and 96 hours (4 days) each. The viscosity of each sample was measured by a Stormer viscometer (with paddle-type rotor) at a constant temperature ($25 \pm 0.1°C$).

Experimental data are shown in Table XIV and are plotted in Figure 40 with the viscosity as ordinate and the milling time as abscissa.

From 0 to 15 hours of milling, the viscosities of the suspensions rapidly increased.....this was called an "initiation period" implying the beginning of the cluster breakdown.

From 15 to 60 hours of milling, the viscosities of the suspensions were comparatively stable but were still changing...this was called a "transition period," which implied an unstable viscosity change.

From 60 to 96 hours of milling, the viscosities of suspensions were relatively constant.....this was called a "stable period."

The viscosities of suspensions became stable after the transition period where suspension viscosities were changing with respect to length of milling time.

The primary particles were poorly dispersed in the liquid medium during the initiation and transition periods. In these stages the suspension viscosities depended upon the length of milling time because a number of air pockets were present in the clusters, causing irregular breakdown of the formed clusters while shear stress was applied in the viscometer. In the stable period the primary particles were adequately dispersed in the liquid medium and the suspension viscosities did not depend upon the length of milling time.

Figure 40 shows the interdependence between the suspension viscosities and length of milling time.

From the experimental results, a four-day milling time was selected for preparing suspensions to be employed in the study of volume concentration effect.

Addition of a Surface Active Agent

A surface active agent was added to the suspension to investigate the effect on structure formation in the pigment suspension system.

The pigment, liquid medium and surface active agent used in this experiment were TiO_2-MP-776-4, soy bean oil and 1-amino-2-naphthol-4-sulfonic acid, respectively.

Sample suspensions were prepared by diluting the TiO_2-MP-776-4 soy bean oil paste which was previously prepared (5.08% volume concentration) with soy bean oil. The surface active agent was mixed with the sample suspension and was shaken violently in a shaking machine for 20 minutes.

In order to determine the effect of the surface active agent on both viscosity and yield value of the suspension, the commercial model Stormer viscometer (with bob-type rotor) was used. During the measurements, the temperature was kept at 25 $\pm$ 0.1°C.

The experimental data are recorded in Table VI-A and VI-B and are plotted in Figure 41 with the driving weight as ordinate and 1/t as abscissa, where t is time in seconds required for 100 revolutions of a rotor.

As is shown in Tables VI-A and VI-B, and in Figure 41, the addition of the surface active agent reduced both the viscosity of the suspension and the yield values without affecting the viscosity of soy bean oil.

The surface active agent was assumed to be adsorbed on the surface of the dispersed cluster during the mixing process, and as a consequence, the flocculation forces which play an important part in structure formation were reduced. Therefore, the structure size, the yield values, and viscosity of the suspension were reduced as the amount of the surface active agent was increased.

Comparison of Milling Methods

When the suspensions were prepared by milling with a ball mill, the viscosities of the suspensions were independent of particle size if the particle size was smaller than 0.05 microns and in volume concentrations of 0 - 5 per cent.

The suspensions in this low volume concentration range were also prepared by diluting the paste prepared by milling on a three-roller mill and the viscosities were measured by using a commercial type Stormer

TABLE VI-A

EFFECT OF ADDITION OF A SURFACE ACTIVE AGENT ON THE VISCOSITY OF SOY BEAN OIL

W_p* (g)	W_o* (g)	W_s* (g)	Viscosity (cps.)
0	35.3	0	52.2
0	35.3	0.0767	51.8
0	35.3	0.4580	52.0
0	35.3	2.7742	52.1
0	35.3	5.3161	51.5

TABLE VI-B

EFFECT OF ADDITION OF A SURFACE ACTIVE AGENT ON THE VISCOSITY OF SUSPENSION

W_p* (g)	W_o* (g)	W_s* (g)	W_s/W_p	Driving Weight (g)	1/t (rev/sec)	Viscosity (cps.)	Yield Value (g)
7.87	35.03	0	0	125	0.055	118	35
				100	0.0394		
				75	0.025		
				50	0.0116		
7.87	35.03	.8255	.105	150	0.072	116	32
				100	0.0403		
				75	0.0252		
				50	0.0118		
7.87	35.03	2.0415	.26	150	0.074	114	28
				125	0.0578		
				100	0.0428		
				75	0.0277		
				50	0.0134		
7.87	35.03	3.3743	.43	150	0.0775	112.5	26
				125	0.0602		
				100	0.0459		
				75	0.030		
				50	0.0151		
7.87	35.03	4.9429	.63	150	0.0806	109.5	22
				125	0.0655		
				100	0.0492		
				75	0.0331		
				50	0.017		

*W_p = weight of pigment

*W_o = weight of oil

*W_s = weight of surface active agent

viscometer equipped with a paddle-type rotor, in order to investigate the dependence of the suspension viscosities on particle size when the particles are smaller than 0.05 microns.

The experimental data are recorded in Table VII and are plotted in Figure 42 with $1/\eta_{sp}$ as ordinate and $1/\phi$ as abscissa.

TABLE VII

COMPARISON OF MILLING METHODS, EXPERIMENTAL DATA.
TEMPERATURE 25 ± 0.1°C

Pigments	Volume Conc. (%)	Viscosity η(cps.)	$1/\eta_{sp}$	$1/\phi$
		Milling with Three-Roller Mill		
TiO_2-MP-776-5	5.15	108.3	0.93	19.4
	4.05	94.8	1.22	24.7
	3.18	84.4	1.61	31.4
	1.52	66.3	3.70	65.8
TiO_2-MP-776-4	5.08	118.0	0.79	19.7
	4.11	103.7	1.01	24.3
	2.68	83.9	1.64	37.3
	1.17	65.0	4.17	85.5
		Milling with Ball Mill		
TiO_2-MP-776-5	3.48	172.5	0.43	28.7
	2.34	125.9	0.71	42.7
	1.76	104.8	0.99	56.8
	1.18	86.1	1.54	84.7
TiO_2-MP-776-4	4.57	185.9	0.30	21.9
	4.02	197.2	0.36	24.9
	2.34	125.0	0.72	42.7
	1.18	86.1	1.54	84.7

Suspensions prepared by 96 hours milling with a ball mill showed higher viscosities than those prepared by milling with a three-roller mill.

Numerical values of V_c/V_s and K in Equation (33) are reported in Table VIII.

TABLE VIII

COMPARISON OF MILLING METHODS
CALCULATED VALUES OF K AND V_c/V_s IN EQUATION (33)

Pigments	V_c/V_s	K
	Milling with Three-Roller Mill	
TiO_2-MP-776-5	2	17.8
TiO_2-MP-776-4	3	21.2
	Milling with Ball Mill	
TiO_2-MP-776-5	6.0	50.4
TiO_2-MP-776-4	6.0	50.4

The data in Tables VII and VIII indicate that there are differences in milling processes in a three-roller mill and in a ball mill. The larger values of K for suspensions milled with a ball mill are indicative of larger structures. When suspensions were prepared by milling with a three-roller mill, their viscosities depended on particle size in the range below 0.05 microns. However, when suspensions were prepared by milling with a ball mill, 96 hours milling time, the viscosities were not affected by particle size in the range below 0.05 microns.

SUMMARY

The explanation of anomalous rheological behavior of titanium dioxide-soy bean oil suspensions has been confirmed through the studies of the effects of particle size, volumetric concentration, temperature, milling time, milling methods and addition of a surface active agent, which are summarized as follows:

A modified Stormer viscometer was used to measure suspension viscosities. Some of the data showed excellent correlation with other viscosity data obtained with a Brookfield viscometer.

The suspensions were prepared either by milling on a three-roller mill or in a ball mill.

The titanium dioxide pigments were either round or irregular and varied in size from 0.04 to 0.30 microns.

Volume concentrations of pigment varied from 0 to 30%. Bingham type of flow was observed in volume concentrations of 0 to 5%, while the Plastic type of flow was observed with volume concentrations of 5 to 30%. Higher than 30% volume concentrations produced zero fluidity.

The yield value varied inversely with respect to particle size, i.e., the yield value increased as the particle size decreased. The yield value was also affected by volume concentration of pigment as shown in the following equation:

$$\tau_o = k_3 \phi^n \qquad (23)$$

In order to explain the effect of particle size and volume concentration on suspension viscosities the following equation was derived utilizing the concept of "structure formation" in suspensions.

$$\eta_{sp} = \frac{K}{\frac{1}{\phi} - (1 + \frac{V_c}{V_s})} \qquad (33)$$

Equation (33) has as its variables relative size of the structures, arrangement of the particles in the structures and the relative amount of dead volume contained in the structures. These variables are functions of the particle size, the temperature, and possibly the physical properties of the liquid medium.

Experimental and published data showed excellent correlation when used in Equation (33). These results indicated that once the yield value was exceeded the nature of Bingham type of flow would be analogous to that of Newtonian type of flow.

Particle size affected the suspension viscosities. The smaller the particle size the higher the suspension viscosities at a constant temperature in volume concentrations ranging from 0 to 5% if the particle size was larger than 0.05 microns. However, at a higher volume concentration range, where Plastic type of flow was observed, the critical particle size was not observed.

The effect of temperature on the viscosity of the Bingham type of flow was well expressed by Arrhenius type equation.

The ball milling process was analyzed at a constant temperature. Three milling periods were observed: (a) 0 - 15 hours initiation period, (b) 15 - 60 hours transition period and (c) 60 - 96 hours steady period.

The surface active agent used was 1-amino-2-naphthol-4-sulfonic acid. Addition of this surface active agent reduced both the yield value and suspension viscosities at 25 $\pm$ 0.1°C.

The viscosities of suspensions prepared by milling with a ball mill were higher than those prepared by milling with a three-roller mill.

These investigations revealed that the structures were formed after a dispersion operation. The speed of "structure formation" depended

upon the strength of the flocculation forces. The shear stress applied to break the formed structures was called "yield value." When the shear stress exceeded the yield value, the structures were broken down into smaller sizes because of the irregularity in structure shape. If the volume concentration was comparatively low, the broken structures would remain constant size and almost the same shape ... a Bingham type of flow. However, if the volume concentration was comparatively high, the structures were continually broken down and the viscosity decreased as the higher shear stress was applied ... a Plastic type of flow.

APPENDIX A

CLASSIFICATION OF THE RHEOLOGICAL STATE OF DISPERSION

It is essential to define certain terms so that the reader understands precisely the meaning in which the terms are used in this thesis. It is not claimed they are acceptable to all rheologists, but the following scheme is offered by Pryce-Jones[42] and meets the needs of the present discussion.

Definition of rheological state:

1. Newtonian Liquids

   Systems with viscosities independent of time or rate of shear and do not possess yield value.

2. Non-Newtonian Fluids

   Systems with viscosities dependent on rate of shear but independent of time of shear and may or may not have yield value.

3. Plastic Dispersions

   Dispersions which possess a finite yield value, their viscosities depend on the rate of shear but are independent of time of shear.

4. Pseudo-Plastic Dispersions

   Dispersions which possess no yield value, but their viscosities depend on the rate of shear, and are independent of time.

5. Bingham Dispersions

   Dispersions which possess yield value, their viscosities are independent of the rate of shear and of time.

6. Dilatant Dispersions

Dispersions which are Newtonian liquids at low rate of shear but their viscosities increase with increasing rate of shear above a minimum critical value. The value of the viscosity is independent of time.

7. Shear-Hardening Dispersions

Dispersions which increase in viscosity at constant rate of shear which increasing time of shear, but revert to their original viscosity when left at rest.

8. Thixotropic Dispersions

Dispersions which show the isothermal reversible gel/sol/gel transformation. In a state of rest they are gels which possess a yield value and their viscosities are a function of the rate of shear, as well as the time of shear and the time of rest. At high rates of shear they are sols, their viscosities in the sol state are independent of the rate of shear or time of shearing.

9. False-Body Dispersions

Dispersions which are permanent gels, but the viscosity of the gel is a function of the rate of shear as well as the time of shear or of rest.

10. Sol

A colloidal system which possesses no yield value, but its viscosity is independent of the rate of shear or time of shear.

11. Gel

A colloidal system which possesses a yield value, but its viscosity is a function of the rate of shear. If the gel is thixotropic or false-bodied the viscosity is a function of the time of shear, or time of rest, as well as the rate of shear.

The following scheme was proposed also by Pryce-Jones[42]; each class forms a "rheological state" and this can be determined by measuring the viscosity of the system at different rates of shear at definite intervals of time after the system has been left at rest.

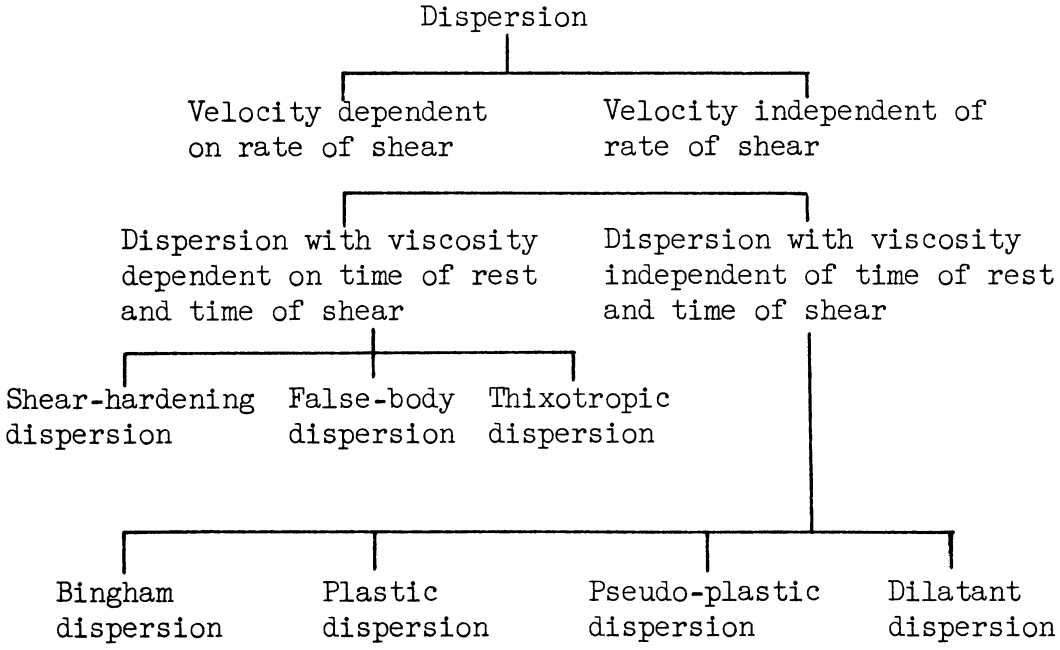

The following figure was prepared to show stress-rate of shear relationship of the rheological states of dispersions.

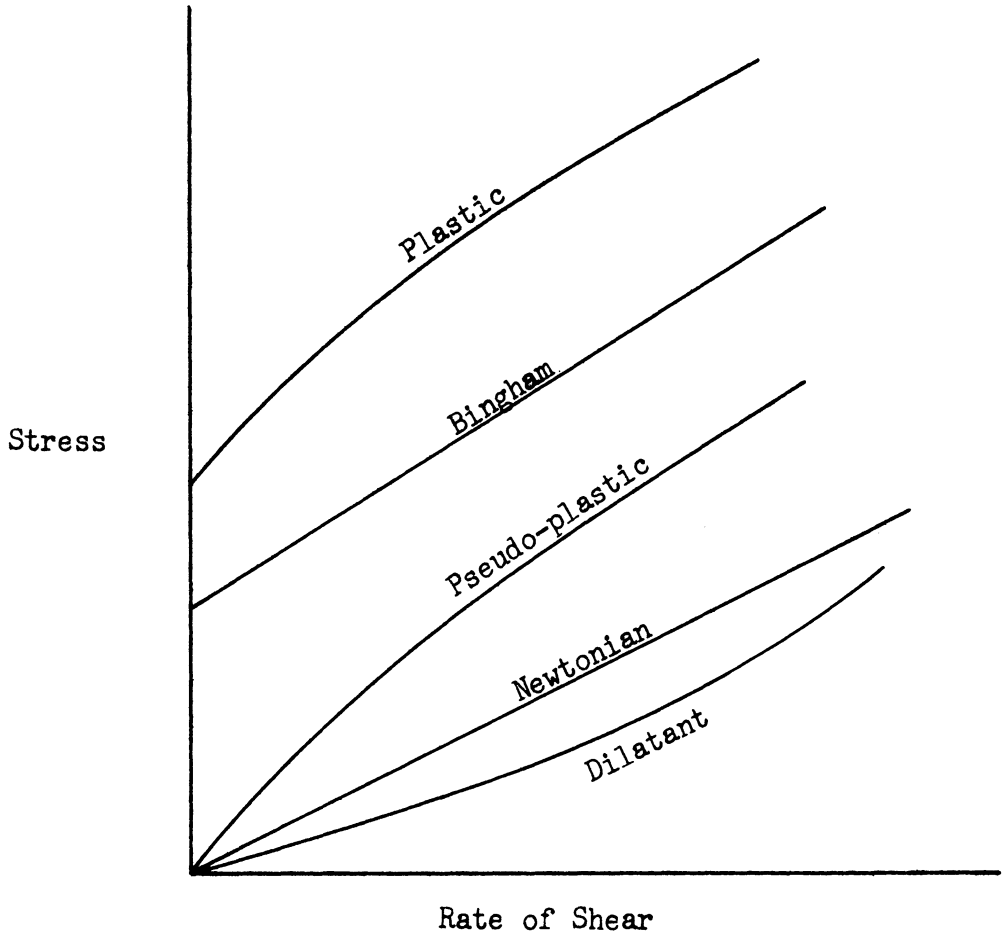

Figure 9. Diagramatic Sketch of Flow Curves

APPENDIX B

STRUCTURES IN AQUEOUS SUSPENSIONS

Figures 10(a) and 10(b) show the electron microscopic pictures (30,000 magnification) of the suspensions of TiO_2-MP-1250 pigment in water and portray the concept of the structures which are formed in the suspensions.

In the discussion, the writer assumed the formation of long chain type of structure shown in Figure 10(a) before the application of the shear stress in viscometer container.

As the shear stress is applied in the viscometer container, the original structure as shown in Figure 10(a), is gradually broken up to smaller substructures as shown in Figure 10(b).

The size and shape of the substructures and original structure should be dependent upon the physical properties of pigment, liquid medium, temperature and milling methods as previously described.

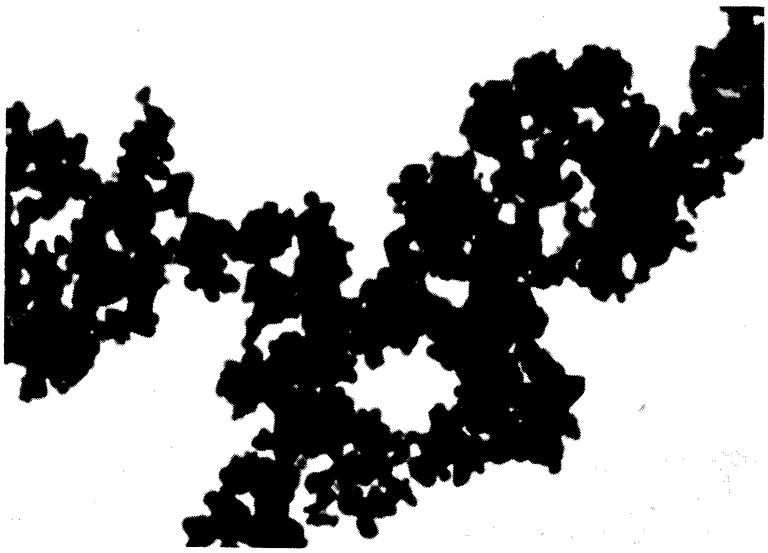

30,000X

(a)

Original Model Structure
Before Application of Shear Stress
in a Viscometer

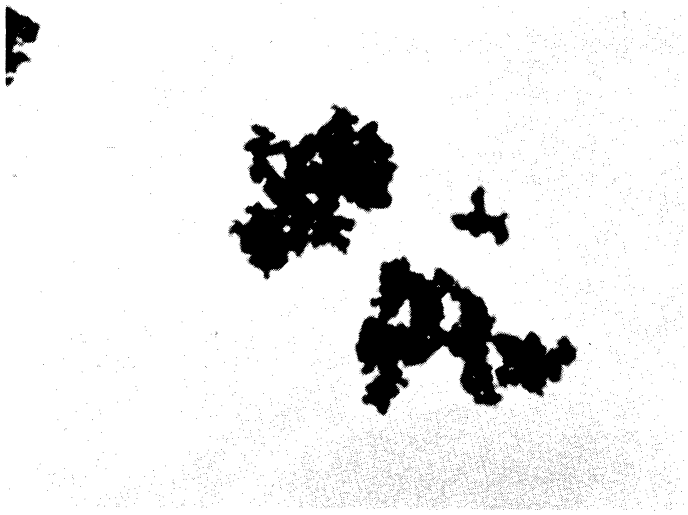

30,000X

(b)

Model Structures
After Application of Shear Stress
in Excess of Yield Value

Figure 10. Models of Structures in Suspension.

APPENDIX C

COMPILATION OF DATA - PLASTIC TYPE OF FLOW

The compilation of the data is presented in tables and graphs.

The volume concentrations covered are 5 - 30% where the rheological state was of the Plastic type.

The viscosity measurements were conducted at a temperature of 25 $\pm$ 0.1°C, employing a Stormer viscometer (bob-type rotor) unless otherwise specified.

The sample suspensions were prepared by diluting the pastes to the desired concentrations with soy bean oil. The pastes were prepared by milling definite amounts of pigment and soy bean oil with a three-roller mill.

The experimental data are reported in Table IX and are plotted in Figures 11 - 15.

The viscosities were calculated from Figures 11 - 15 by multiplying the ratio $\Delta W/(1/t)$, of the driving weight vs. $1/t$ curves at a certain value of $1/t$, by the calibration coefficient of the viscometer.

The calculated results are reported in Table X and are plotted in Figures 16 - 23.

The yield values reported in Table XI were obtained from the intersections of the curves on the stress axis (or driving weight axis) in Figures 11 - 15. They are plotted in Figure 24.

TABLE IX

EXPERIMENTAL RESULTS, USING STORMER VISCOMETER
(WITH BOB-TYPE ROTOR)
Volume concentration 5 - 30%, Temperature 25 ± 0.1°C

Exp. No.	Pigment	Vol. % (100φ)	Driving weight (g)	Sec./100 Rev. t	1/t
174	TiO_2-MP-776-3	26.2	750	828.0	.00121
175			800	431.0	.00232
173			850	322.0	.0031
172			900	234.5	.00426
178		23.1	600	984.5	.00102
176			650	678.5	.00148
177			700	344.5	.0029
179			750	221.5	.00452
181		19.7	400	630.0	.00159
180			450	310.0	.00322
183			475	190.1	.00526
182			500	153.0	.00654
344		16.29	300	145.0	.0069
187			350	74.90	.0134
186			400	46.95	.0213
184			450	32.90	.0304
185			500	24.50	.0408
356		15.2	250	182.0	.0055
188			300	74.65	.0134
357			325	53.25	.0188
189			350	42.20	.0237
358			375	34.65	.0288
190			400	29.0	.0345
191			425	24.70	.0405
359		14.3	200	200.0	.005
360			250	80.0	.0125
192			300	43.7	.0229
361			325	35.95	.0278
193			350	29.25	.0342
362			375	24.9	.0402
194			400	21.4	.0468
195			450	16.4	.061
196		11.8	150	103.8	.0096
363			175	59.70	.0168
197			200	40.95	.0244
364			225	31.0	.0322
198			250	24.45	.0409
199			275	19.95	.0501

TABLE IX (Cont'd)

Exp. No.	Pigment	Vol. % (100φ)	Driving weight (g)	Sec./100 Rev. t	1/t
203	TiO_2-MP-776-3	9.91	100	114.9	.0087
367			125	60.8	.0164
200			150	38.35	.0261
368			175	28.0	.0357
201			200	21.3	.0469
365			225	17.00	.0589
206	TiO_2-MP-776-4	20.6	1,455	637.0	.00157
207			1,614	250.0	.00400
205			1,714	207.0	.00484
204			1,914	91.5	.01092
210		18.7	1,005	814.0	.00123
209			1,055	577.5	.00173
208			1,155	360.0	.00278
211			1,205	217.5	.0046
213		16.9	700	833.0	.00120
215			750	412.5	.00242
212			800	317.0	.00316
214			850	205.0	.00488
218		14.9	450	913.0	.00109
216			500	504.5	.00198
217			550	215.0	.00466
219			600	145.0	.0069
221		12.8	300	481.0	.0021
220			350	203.0	.0049
223			400	108.4	.0092
222			500	44.70	.0229
341			600	24.85	.0402
225		11.2	200	688.0	.0014
224			300	91.40	.0109
319			350	51.15	.0196
226			400	35.3	.0284
343			450	24.8	.0404
320		10.1	150	514.0	.0019
228			200	135.1	.0074
230			250	60.55	.0165
229			300	35.90	.0279
231			350	24.20	.0414
350			400	17.65	.0566

TABLE IX (Cont'd)

Exp. No.	Pigments	Vol. % (100Φ)	Driving weight (g)	Sec./100 Rev. t	1/t
352	TiO_2-MP-776-4	9.14	150	167.0	.006
235			200	61.20	.0163
232			250	34.15	.0283
233			300	22.55	.0444
234			325	18.80	.0532
340		7.65	75	378.0	.0026
236			100	123.1	.0081
237			150	41.2	.0243
238			200	22.9	.0437
239			250	15.30	.0655
240		6.41	50	322	.0030
241			75	86.30	.0116
242			100	45.7	.0219
243			125	29.6	.0338
342			150	21.60	.0463
245		5.08	50	42.90	.0116
244			75	39.95	.025
246			100	25.4	.0394
247			125	18.20	.055
289	TiO_2-MP-776-5	20.13	800	32.0	.0031
292			850	19.9	.0050
290			900	16.25	.0062
370			950	11.65	.0086
291			1,000	9.20	.0109
371		16.72	450	220.0	.0045
372			500	108.0	.00975
294			550	78.3	.0128
293			650	42.9	.0233
295			750	27.3	.0366
296			800	11.4	.0439
300		13.91	250	238.0	.0042
299			300	90.9	.011
373			350	55.2	.0181
298			400	35.7	.0280
297			500	20.8	.0481
303		11.47	150	167.5	.0060
302			200	62.6	.016
374			250	33.9	.0295
375			300	24.0	.0417
301			350	16.95	.059

TABLE IX (Cont'd)

Exp. No.	Pigment	Vol. % (100Φ)	Driving weight (g)	Sec./100 Rev. t	1/t
307	TiO_2-MP-776-5	8.8	75	186.0	.00538
306			100	77.5	.0129
304			150	32.2	.0312
305			200	19.25	.052
311		5.15	30	127.5	.0078
309			50	49.5	.0202
308			75	27.9	.0358
376			100	19.10	.0524
159	TiO_2-MP-1250	24.8	800	729.0	.00137
160			850	455.5	.0022
161			900	262.0	.00382
162			950	171.0	.00586
166		22.7	600	745.0	.00134
163			650	435.5	.0023
164			700	254.5	.00392
165			750	162.0	.00617
170		21.1	450	1306.0	.00076
167			500	568.0	.00176
168			550	294.5	.00339
169			600	164.0	.0061
322		16.8	350	117.5	.0085
256			400	63.0	.0159
253			450	42.15	.0238
254			500	30.25	.033
255			550	22.90	.0437
314		15.51	250	209.3	.0048
257			300	90.75	.071
258			350	52.30	.0191
259			400	34.40	.0291
260			450	24.80	.0408
321		14.36	200	231.2	.00433
261			250	88.75	.0113
262			300	48.15	.0208
263			350	30.75	.0326
264			400	22.10	.0452
268		12.93	200	88.25	.0113
265			250	43.55	.023
266			300	27.10	.0369
316			325	22.70	.044
267			350	18.95	.0528

TABLE IX (Cont'd)

Exp. No.	Pigment	Vol. % (100Φ)	Driving weight (g)	Sec./100 Rev. t	1/t
318	TiO_2-MP-1250	11.26	150	86.20	.0116
271			175	54.80	.0183
270			200	38.35	.0261
272			225	29.35	.0341
269			250	23.10	.0433
273		8.24	75	104.6	.00956
274			100	49.95	.0200
275			125	31.5	.0318
276			150	22.65	.0441
323			175	17.20	.0581

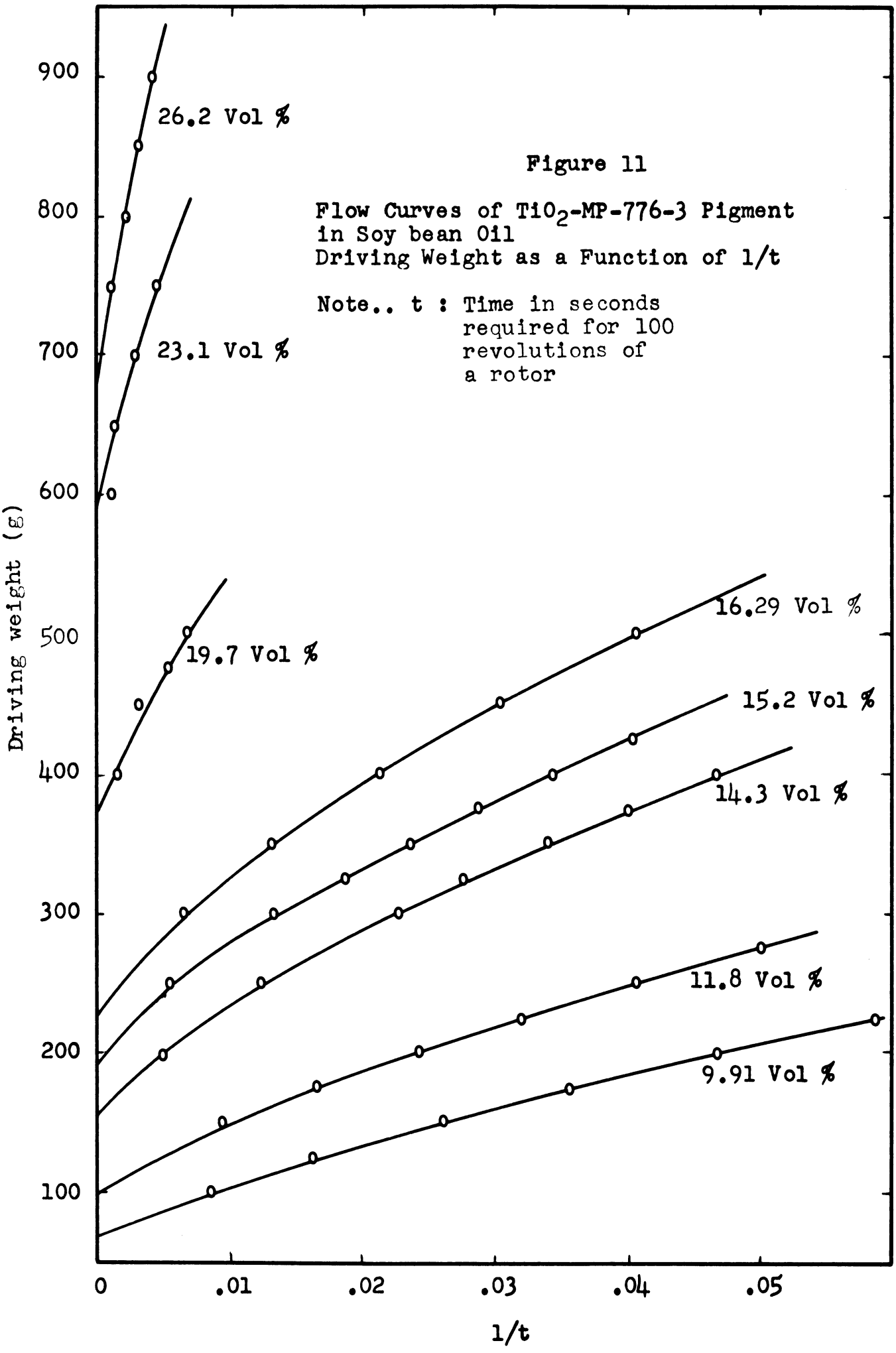

Figure 11

Flow Curves of TiO_2-MP-776-3 Pigment in Soy bean Oil Driving Weight as a Function of 1/t

Note.. t : Time in seconds required for 100 revolutions of a rotor

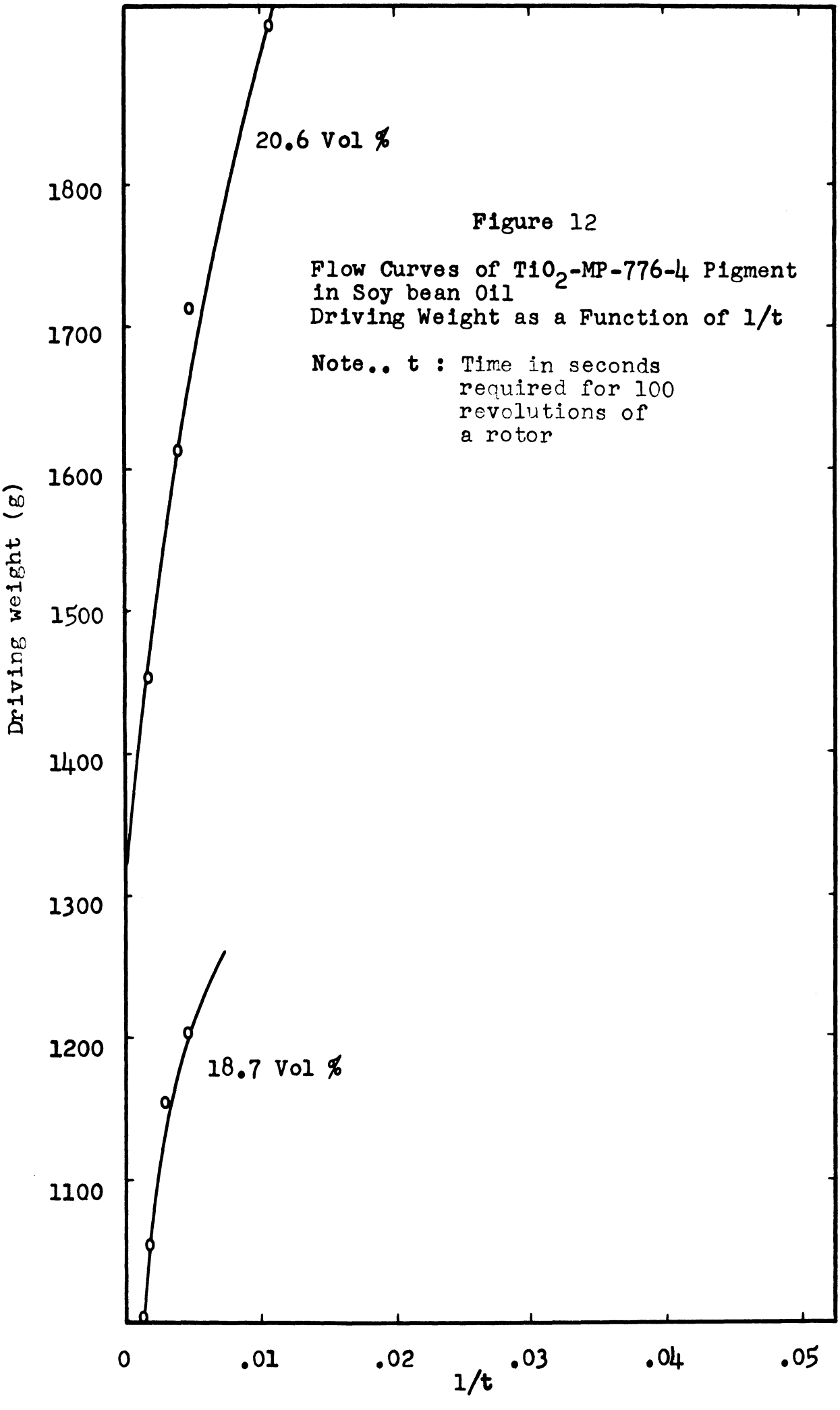

Figure 12

Flow Curves of TiO_2-MP-776-4 Pigment in Soy bean Oil
Driving Weight as a Function of 1/t

Note.. t : Time in seconds required for 100 revolutions of a rotor

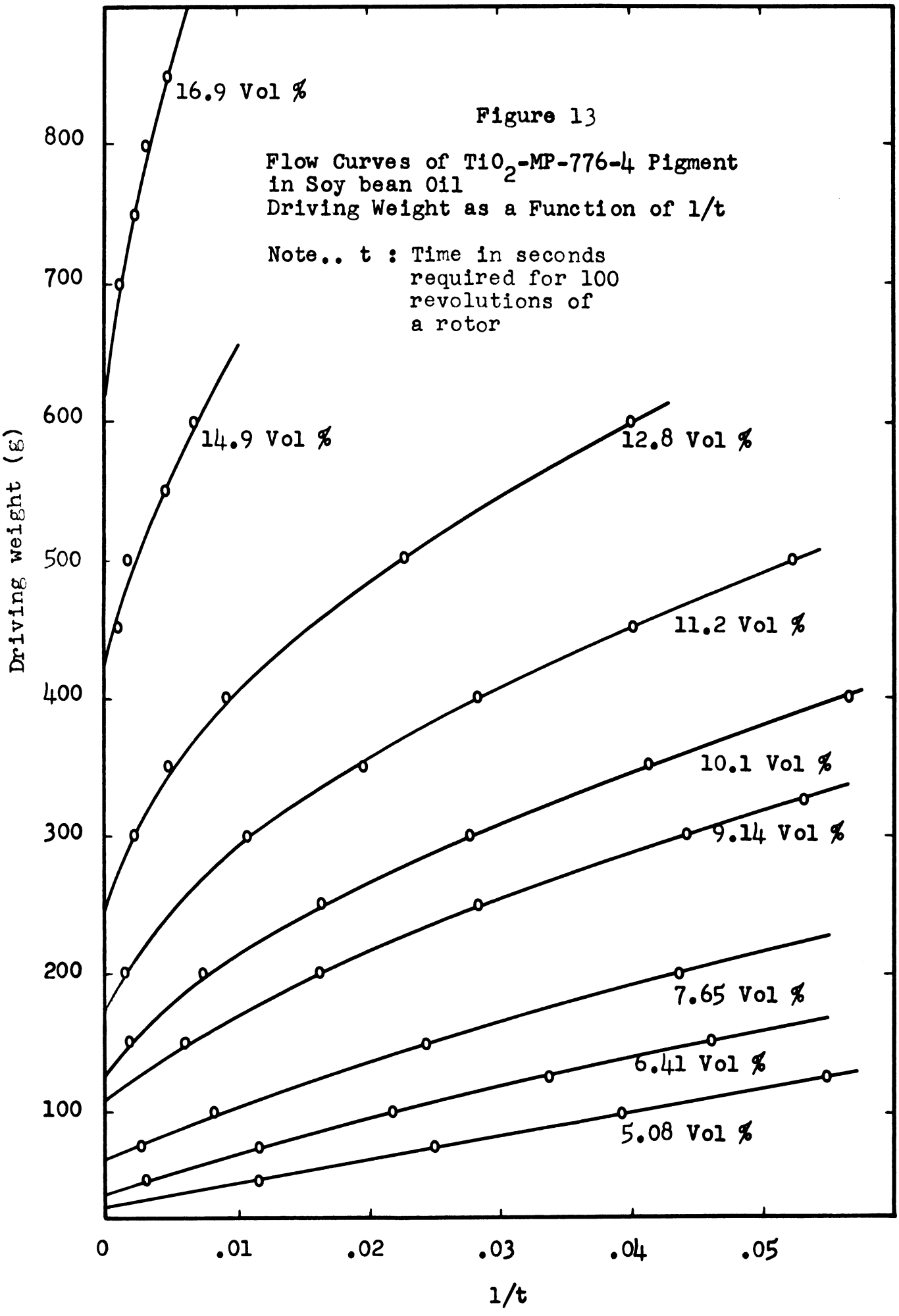

Figure 13

Flow Curves of TiO_2-MP-776-4 Pigment in Soy bean Oil
Driving Weight as a Function of 1/t

Note.. t : Time in seconds required for 100 revolutions of a rotor

Figure 14

Flow Curves of TiO_2-MP-776-5 Pigment in Soy bean Oil
Driving Weight as a Function of 1/t

Note.. t : Time in seconds required for 100 revolutions of a rotor

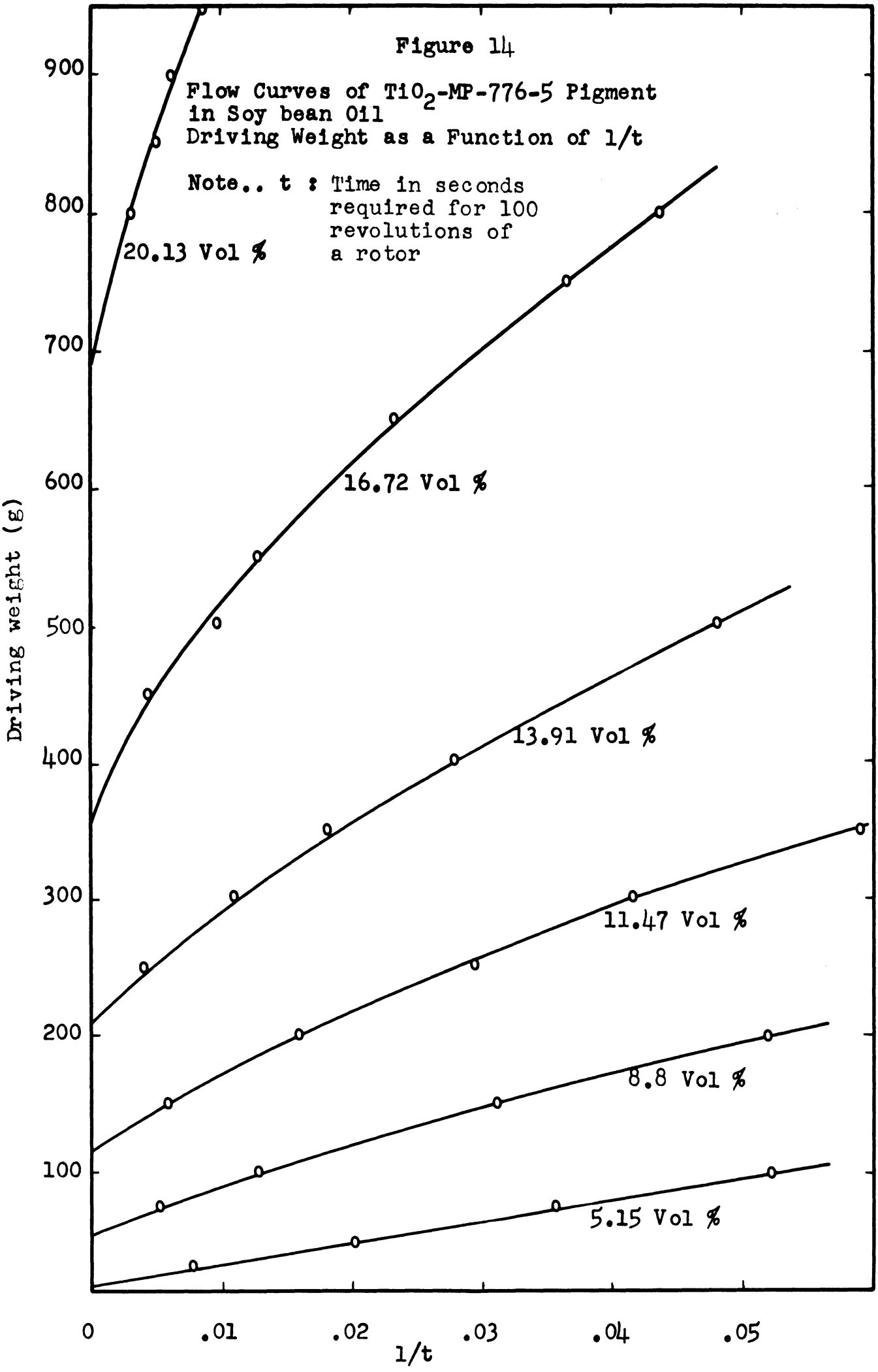

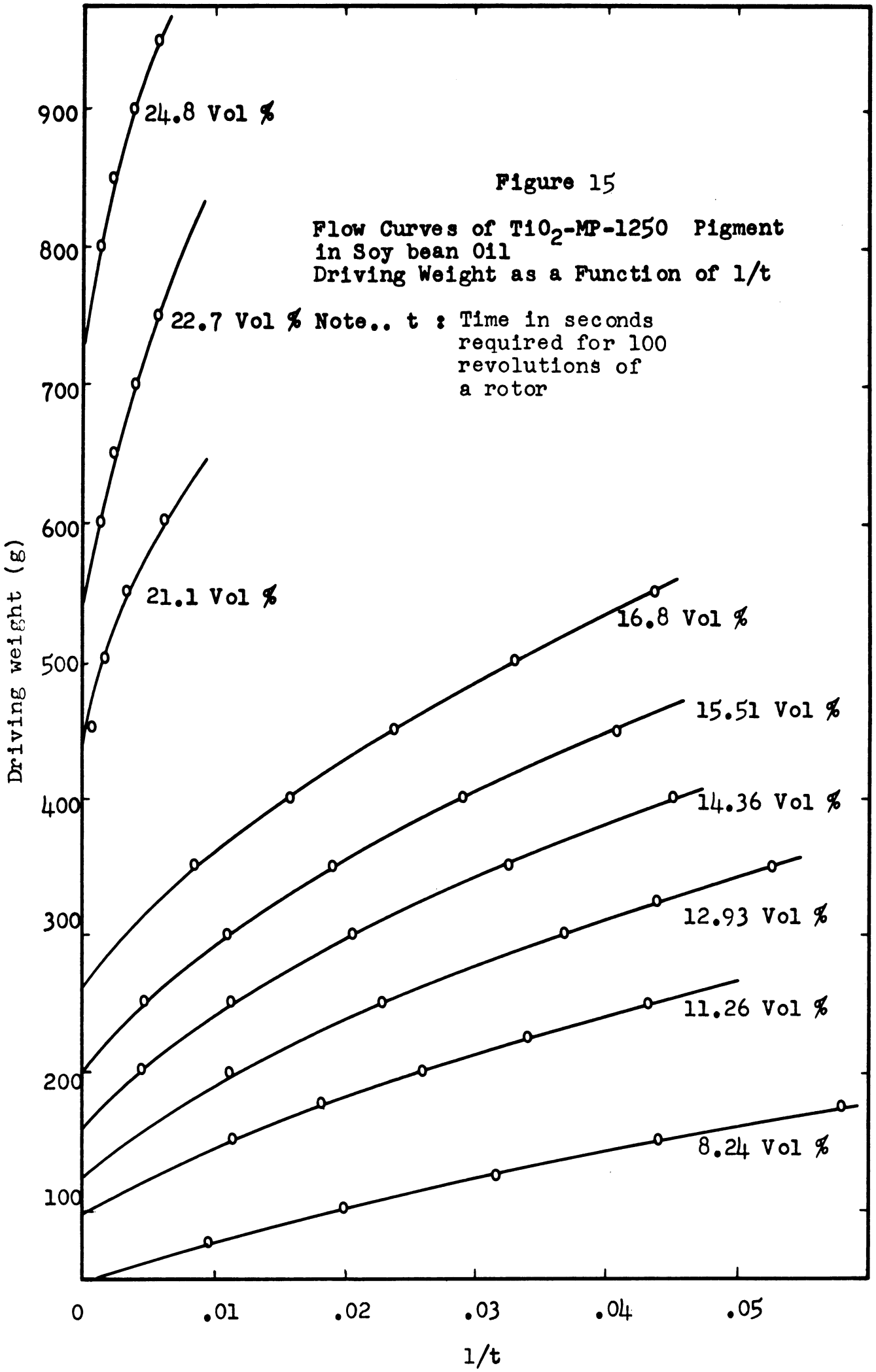

Figure 15

Flow Curves of TiO_2-MP-1250 Pigment in Soy bean Oil
Driving Weight as a Function of 1/t

Note.. t : Time in seconds required for 100 revolutions of a rotor

TABLE X

VISCOSITIES OF TITANIUM DIOXIDE PIGMENT - SOY BEAN OIL SUSPENSIONS

Volume concentration: 5 - 30% , Temperature: 25 ± 0.1°C

Note : t : Time in seconds required for 100 revolutions of a rotor.
η : Viscosity of suspension calculated from an equation

$$\eta = \frac{\Delta W \times 6.94 \times 10^{-2}}{(1/t)}$$

ΔW : Driving weight - yield value

Pigment	Vol%	ΔW(g)	1/t	Viscosity η(cps.)
TiO_2-MP-776-3	26.2	255	.005	3,539.4
	23.1	160	.005	2,220.8
	19.7	95	.005	1,318.6
		170	.01	1,179.8
	16.29	60	.005	832.8
		100	.01	694.0
		167.5	.02	581.2
		222.5	.03	514.6
		270	.04	468.4
	15.2	52.5	.005	728.3
		90	.01	624.6
		140	.02	485.8
		190	.03	439.5
		235	.04	407.7
	14.3	45	.005	624.6
		80	.01	555.2
		132.5	.02	459.8
		177.5	.03	410.6
		215	.04	373.0
		255	.05	353.9
	11.8	25	.005	347.0
		50	.01	347.0
		87.5	.02	303.6
		120	.03	277.6
		150	.04	260.2
		175	.05	242.9
	9.91	17.5	.005	242.9
		35	.01	242.9
		62.5	.02	216.9
		90	.03	208.2
		115	.04	199.5
		136	.05	188.8
TiO_2-MP-776-4	20.6	350	.005	4,858.0
	16.9	230	.005	3,192.4
	14.9	135	.005	1,873.8

TABLE X (Cont'd)

Pigment	Vol %	ΔW (g)	1/t	Viscosity η (cps.)
TiO_2-MP-776-4	12.8	100	.005	1388.0
		145	.01	1006.3
		232.5	.02	806.8
		295	.03	682.3
		350	.04	607.2
	11.2	70	.005	971.6
		117.5	.01	815.4
		180	.02	624.6
		232.5	.03	537.8
		275	.04	477.1
		315	.05	437.2
	10.1	55	.005	763.4
		90	.01	624.6
		140	.02	485.8
		185	.03	427.9
		220	.04	381.7
		255	.05	353.9
	9.14	35	.005	485.8
		60	.01	416.4
		107.5	.02	373.0
		145	.03	335.4
		180	.04	312.3
		210	.05	291.5
	7.65	17.5	.005	242.9
		34	.01	236.0
		65	.02	225.6
		95	.03	219.7
		122.5	.04	212.5
		145	.05	201.2
	5.08	----	---	118.0
TiO_2-MP-766-5	20.13	160	.005	2220.8
		280	.01	1943.2
	16.72	105	.005	1457.4
		167.5	.01	1162.4
		267.5	.02	928.2
		350	.03	809.6
		425	.04	737.4

TABLE X (Cont'd)

Pigment	Vol %	ΔW (g)	l/t	Viscosity η (cps.)
TiO_2-MP-776-5	13.91	45	.005	624.6
		80	.01	555.2
		140	.02	503.2
		200	.03	462.6
		252.5	.04	438.1
		300	.05	416.4
	11.47	27	.005	374.8
		52.5	.01	364.4
		97.5	.02	338.3
		137.5	.03	318.0
		175	.04	303.6
		205	.05	284.5
	8.8	20	.005	277.6
		35	.01	242.9
		65	.02	225.6
		95	.03	219.7
		117.5	.04	203.9
		140	.05	194.3
	5.15	----	----	108.3
TiO_2-MP-1250	24.8	205	.005	2845.4
	22.7	180	.005	2498.4
		300	.01	2082.0
	21.1	130	.005	1804.4
		205	.01	1422.7
	16.8	57.5	.005	798.1
		100	.01	694.0
		165	.02	572.6
		225	.03	520.4
		275	.04	477.1
	15.51	50	.005	694.0
		90	.01	624.6
		155	.02	537.8
		205	.03	474.2
		247.5	.04	429.4
	14.36	50	.005	694.0
		85	.01	589.9
		140	.02	485.8
		185	.03	427.9
		225	.04	390.4

TABLE X (Cont'd)

Pigment	Vol %	ΔW	l/t	Viscosity η (cps.)
TiO_2-MP-1250	12.93	35	.005	485.8
		65	.01	451.1
		112.5	.02	390.4
		150	.03	347.0
		185	.04	321.0
		217.5	.05	301.9
	11.26	22.5	.005	312.3
		45	.01	312.3
		80	.02	277.6
		112.5	.03	260.2
		140	.04	242.9
	8.24	12.5	.005	173.5
		25	.01	173.5
		50	.02	173.5
		72.5	.03	167.7
		92.5	.04	160.5
		110	.05	152.7

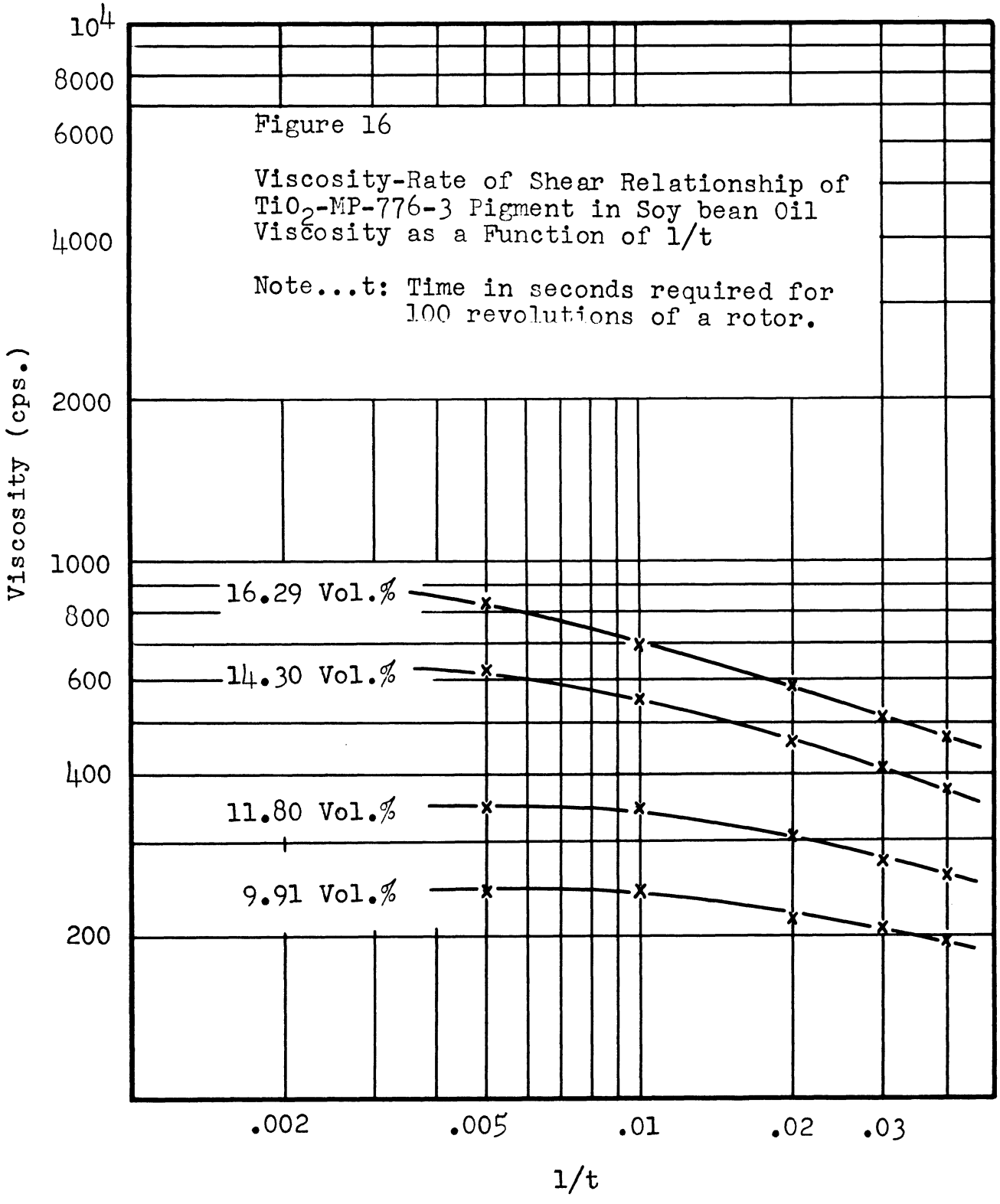
Figure 16
Viscosity-Rate of Shear Relationship of TiO_2-MP-776-3 Pigment in Soy bean Oil
Viscosity as a Function of 1/t
Note...t: Time in seconds required for 100 revolutions of a rotor.
Viscosity (cps.)
10^4
8000
6000
4000
2000
1000
800
600
400
200
16.29 Vol.%
14.30 Vol.%
11.80 Vol.%
9.91 Vol.%
.002
.005
.01
.02
.03
1/t

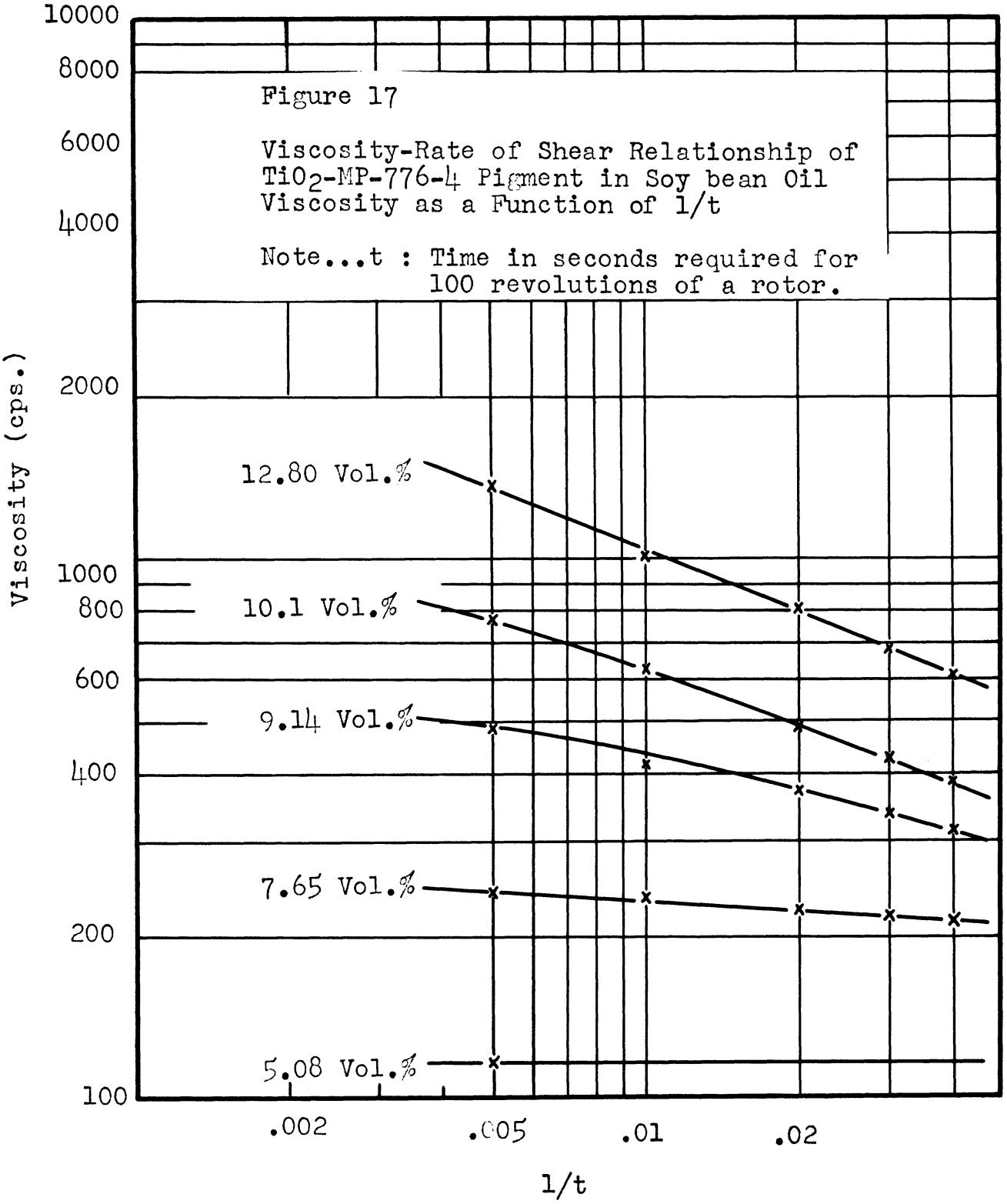
Figure 17
Viscosity-Rate of Shear Relationship of TiO2-MP-776-4 Pigment in Soy bean Oil
Viscosity as a Function of 1/t
Note...t : Time in seconds required for 100 revolutions of a rotor.
Viscosity (cps.)
10000
8000
6000
4000
2000
1000
800
600
400
200
100
12.80 Vol.%
10.1 Vol.%
9.14 Vol.%
7.65 Vol.%
5.08 Vol.%
.002
.005
.01
.02
1/t

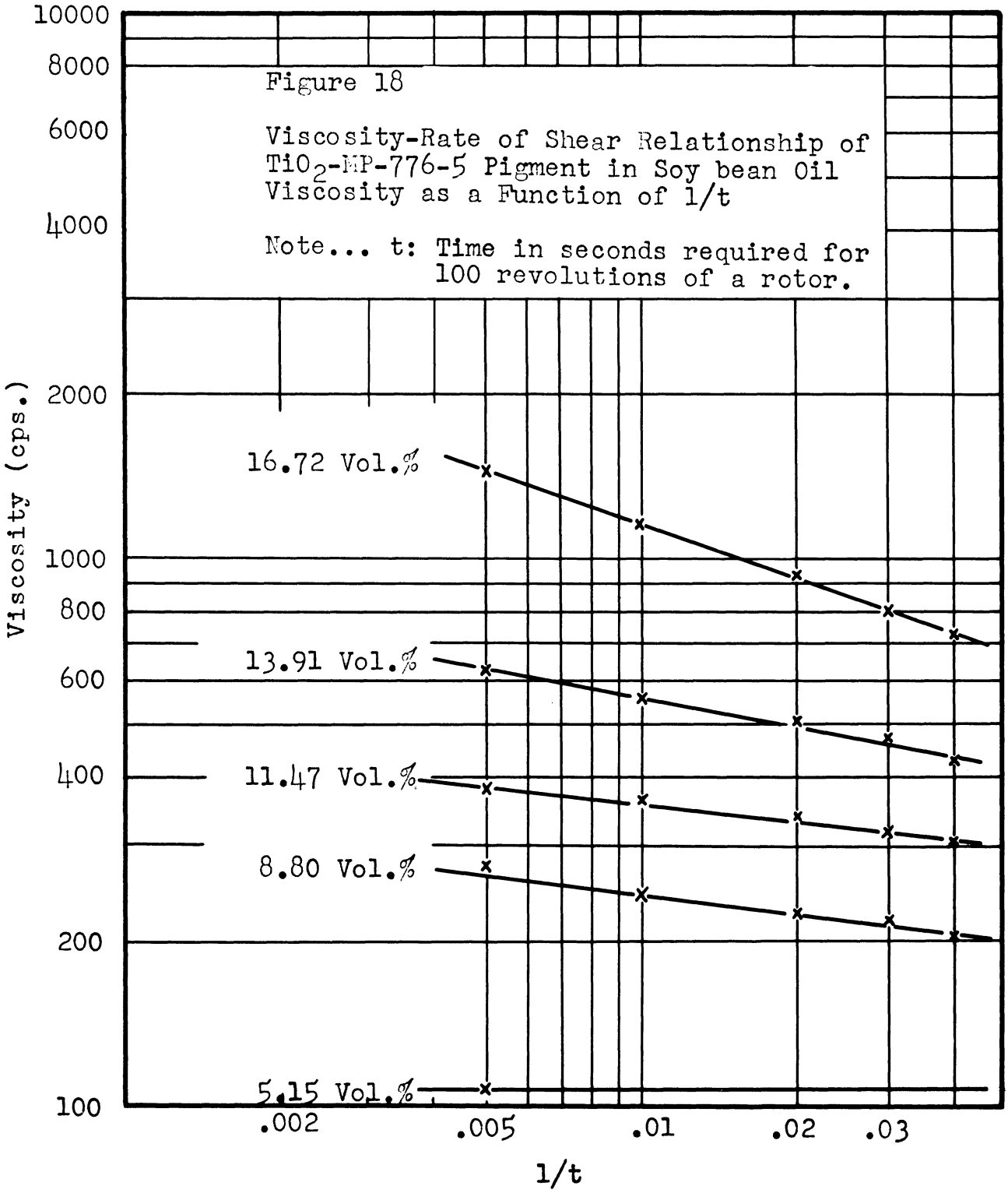
Figure 18
Viscosity-Rate of Shear Relationship of TiO_2-MP-776-5 Pigment in Soy bean Oil
Viscosity as a Function of 1/t
Note... t: Time in seconds required for 100 revolutions of a rotor.
16.72 Vol.%
13.91 Vol.%
11.47 Vol.%
8.80 Vol.%
5.15 Vol.%
Viscosity (cps.)
10000
8000
6000
4000
2000
1000
800
600
400
200
100
.002
.005
.01
.02
.03
1/t

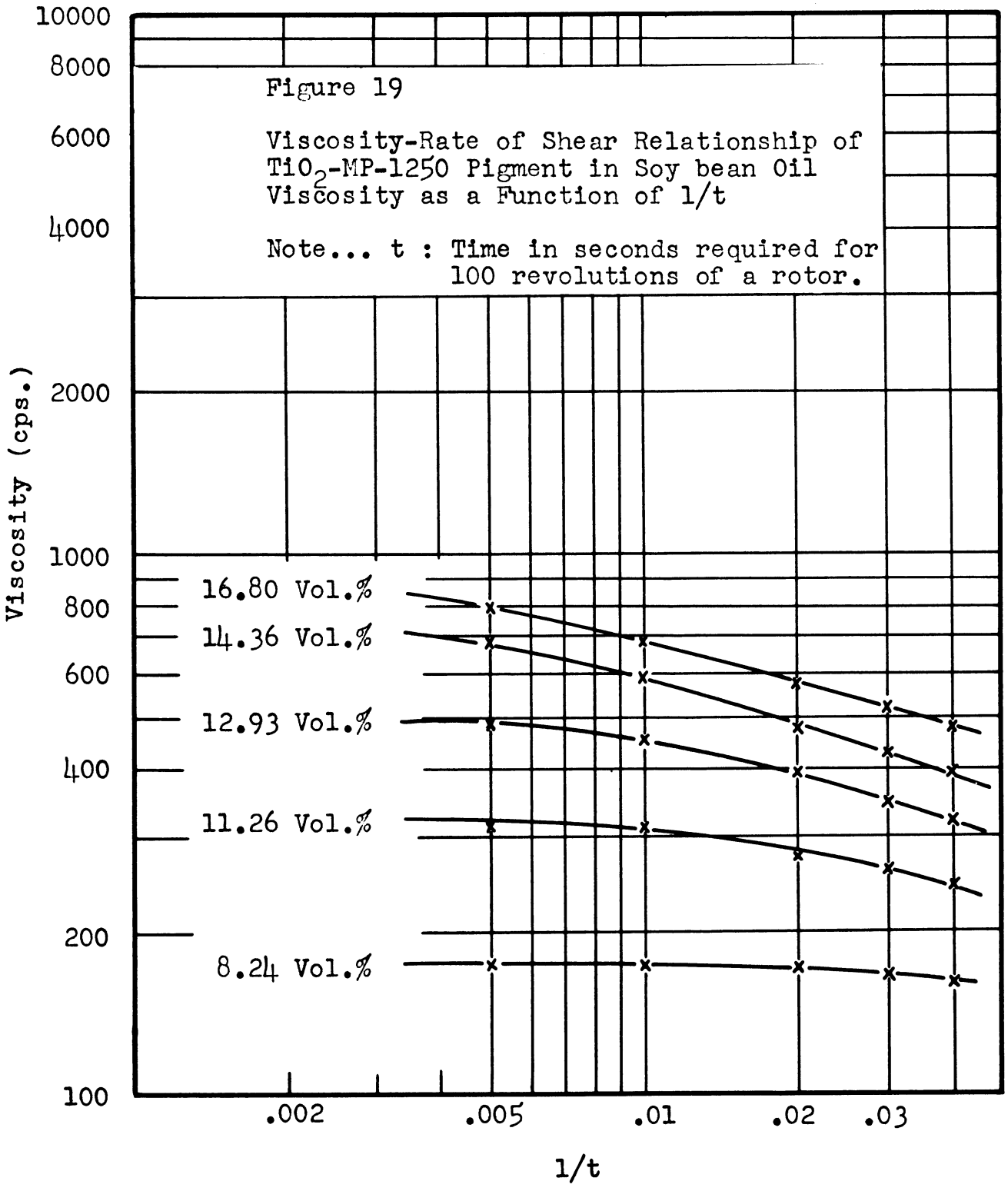
Figure 19
Viscosity-Rate of Shear Relationship of TiO_2-MP-1250 Pigment in Soy bean Oil
Viscosity as a Function of 1/t
Note... t : Time in seconds required for 100 revolutions of a rotor.
16.80 Vol.%
14.36 Vol.%
12.93 Vol.%
11.26 Vol.%
8.24 Vol.%
Viscosity (cps.)
10000
8000
6000
4000
2000
1000
800
600
400
200
100
.002
.005
.01
.02
.03
1/t

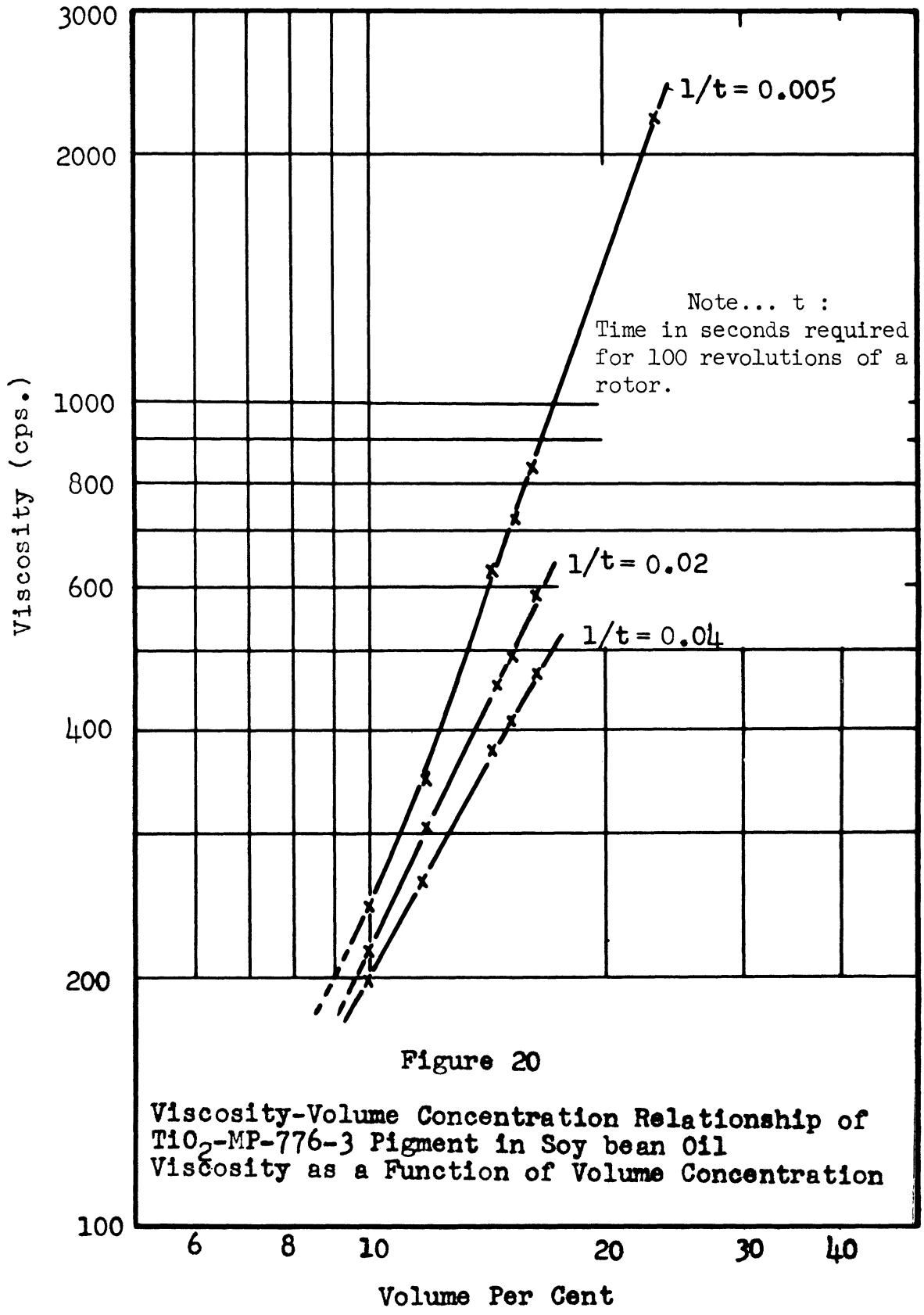

Figure 20

Viscosity-Volume Concentration Relationship of TiO_2-MP-776-3 Pigment in Soy bean Oil
Viscosity as a Function of Volume Concentration

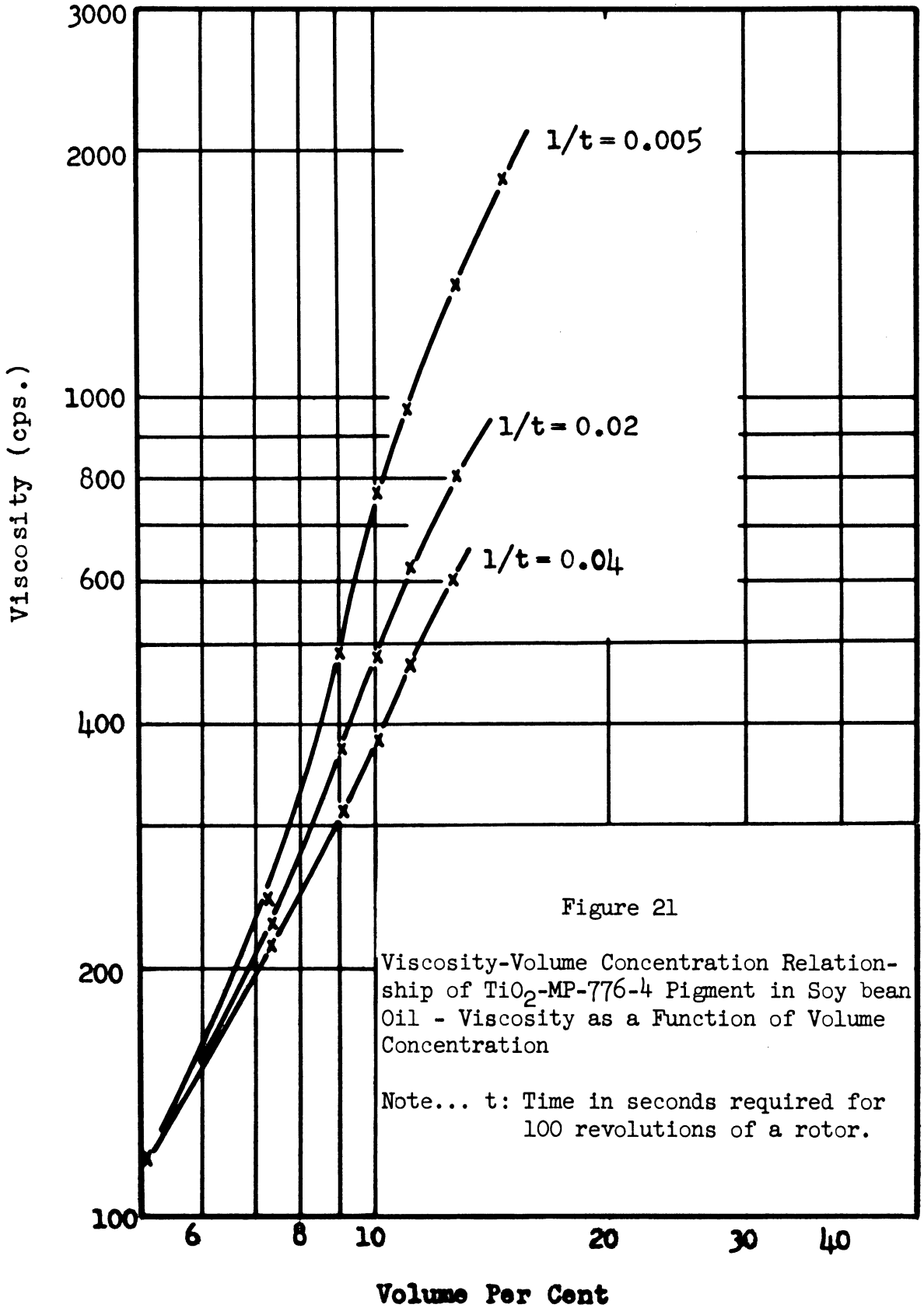

Figure 21

Viscosity-Volume Concentration Relationship of TiO_2-MP-776-4 Pigment in Soy bean Oil - Viscosity as a Function of Volume Concentration

Note... t: Time in seconds required for 100 revolutions of a rotor.

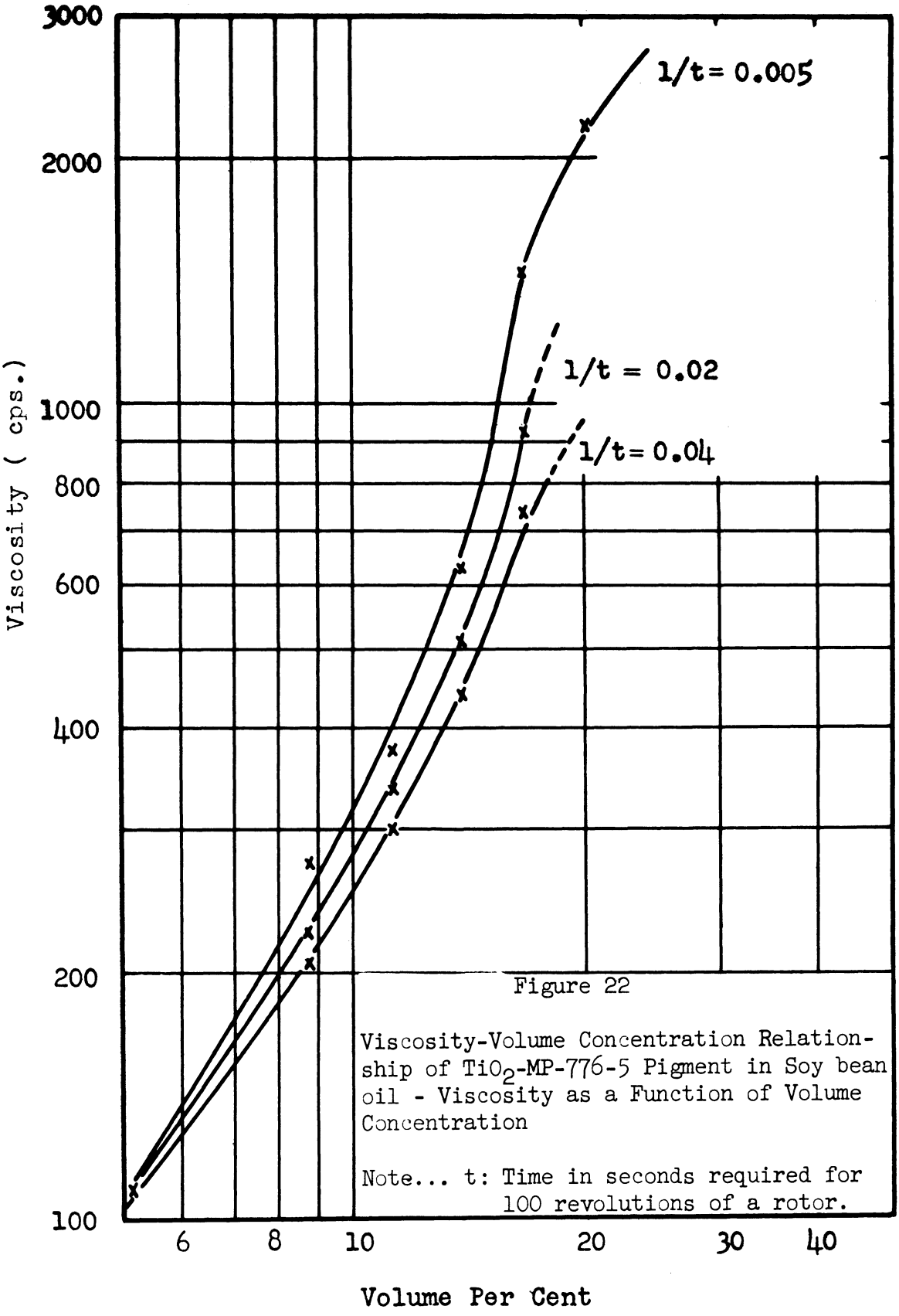

Figure 22

Viscosity-Volume Concentration Relationship of TiO_2-MP-776-5 Pigment in Soy bean oil - Viscosity as a Function of Volume Concentration

Note... t: Time in seconds required for 100 revolutions of a rotor.

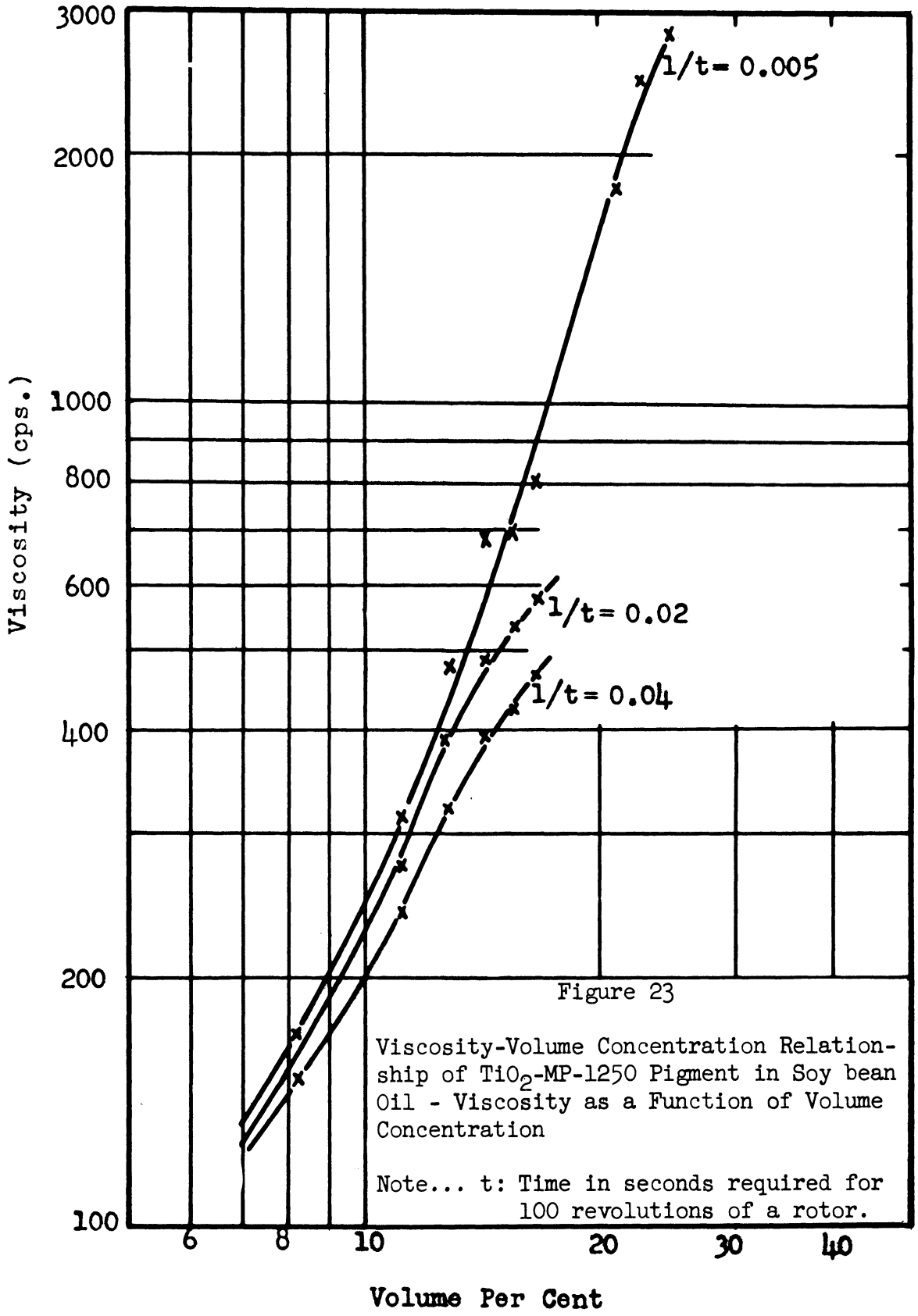

Figure 23

Viscosity-Volume Concentration Relationship of TiO_2-MP-1250 Pigment in Soy bean Oil - Viscosity as a Function of Volume Concentration

Note... t: Time in seconds required for 100 revolutions of a rotor.

TABLE XI

YIELD VALUES OF TITANIUM DIOXIDE PIGMENT - SOY BEAN OIL SUSPENSIONS

Obtained from Figure 11 - 15. Temperature 25 ± 0.1°C

Exp. No.	Pigment	Vol %	Yield Value (g)
175	TiO_2-MP-776-3	26.2	675
179		23.1	600
183		19.7	375
187		16.29	225
191		15.20	190
195		14.30	155
199		11.80	100
203		9.91	70
207	TiO_2-MP-776-4	20.6	1,325
211		18.7	625
215		16.9	625
219		14.9	425
223		12.8	250
227		11.2	175
231		10.1	125
235		9.14	110
239		7.65	70
243		6.41	40
248		5.08	35
292	TiO_2-MP-776-5	20.13	700
296		16.72	350
300		13.91	210
303		11.47	120
307		8.80	55
311		5.15	20
162	TiO_2-MP-1250	24.8	725
166		22.7	550
170		21.1	450
256		16.8	260
260		15.51	200
264		14.36	155
268		12.93	125
272		11.26	100
276		8.24	50

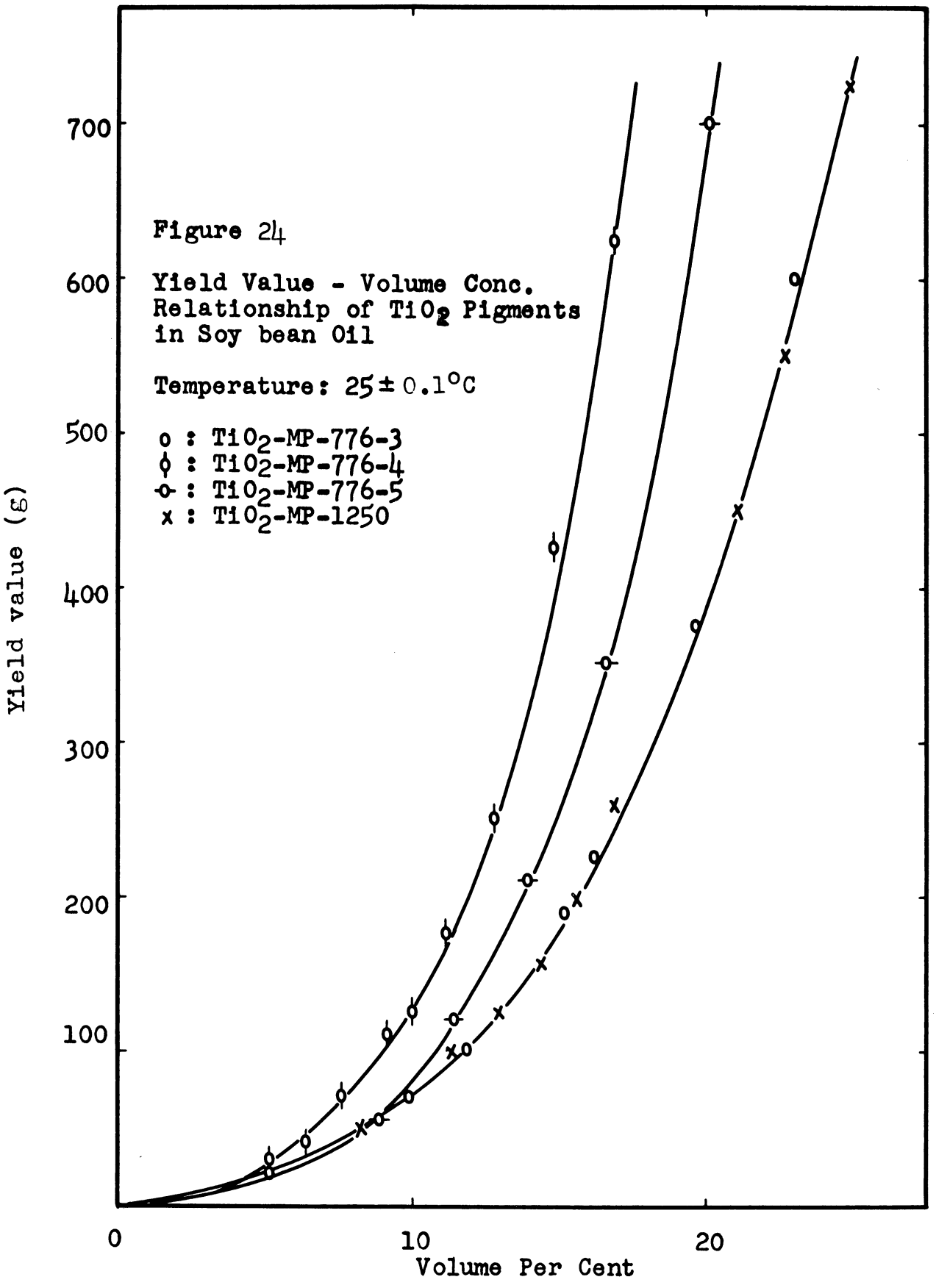
Figure 24
Yield Value - Volume Conc. Relationship of TiO_2 Pigments in Soy bean Oil
Temperature: 25 ± 0.1°C
o : TiO_2-MP-776-3
ϕ : TiO_2-MP-776-4
o : TiO_2-MP-776-5
x : TiO_2-MP-1250
Yield value (g)
700
600
500
400
300
200
100
0
10
20
Volume Per Cent

APPENDIX D

COMPILATION OF DATA - BINGHAM TYPE OF FLOW

The compilation of data is presented in tables and graphs.

The volume concentrations covered are 0 - 5% where the rheological state was of the Bingham type.

The viscosity measure ents were conducted at temperatures of 20°C, 25°C, 30°C and 35°C, employing a Stormer viscometer (paddle-type rotor) unless otherwise specified.

The sample suspensions were prepared by milling with a ball mill from the desired amount of pigment and soy bean oil for four days (96 hours).

The experimental data are reported in Table XII and are shown in Figures 25 - 28.

Generally speaking, the viscosity of the suspension was affected by the size of the primary particles.

Published data shown in Table XIII are correlated in Figures 29 - 34 according to Equation (33).

Effect of the temperature on viscosity is shown in Figures 35 - 39.

The milling time effect on the viscosity is shown in Table XIV and Figure 40, while the effect of the addition of a surface active agent is portrayed in Figure 41.

Milling methods are compared in Figure 42.

TABLE XII

EXPERIMENTAL RESULTS - USING STORMER VISCOMETER
(WITH PADDLE-TYPE ROTOR)

Volume concentration 0 - 5%

Pigment	Temp. (°C)	Vol.% (100Φ)	Viscosity η (cps.)	Specific Viscosity	$1/\eta_{sp}$	$1/\Phi$
TiO_2-MP-776-1	35 ± 0.1	2.34	93.8	1.83	0.55	42.7
		3.48	128.3	2.86	0.35	28.7
		4.57	160.5	3.83	0.26	21.9
		1.76	77.9	1.35	0.74	56.8
	30 ± 0.1	2.34	10.48	1.56	0.64	42.7
		3.48	140.1	2.46	0.40	28.7
		4.57	180.0	3.40	0.29	21.9
		1.76	87.9	1.15	0.87	56.8
	25 ± 0.1	2.34	116.0	1.22	0.82	42.7
		3.48	156.2	2.00	0.50	28.7
		4.57	205.0	2.93	0.34	21.9
		1.76	98.6	0.89	1.12	56.8
	20 ± 0.1	2.34	130.0	0.85	1.18	42.7
		3.48	171.9	1.45	0.69	28.7
		4.57	235.1	2.35	0.42	21.9
		1.76	112.2	0.60	1.67	56.8
TiO_2-MP-776-3	35 ± 0.1	4.57	147.0	3.43	0.29	21.9
		2.34	90.1	1.71	0.58	42.7
		3.48	117.3	2.53	0.40	28.7
		5.11	163.2	3.92	0.26	19.6
	30 ± 0.1	4.57	165.5	3.05	0.33	21.9
		2.34	100	1.44	0.69	42.7
		3.48	130.8	2.20	0.45	28.7
		5.11	183.2	3.48	0.29	19.6
	25 ± 0.1	4.57	185.9	2.56	0.39	21.9
		2.34	110.2	1.11	0.90	42.7
		3.48	146.6	1.81	0.55	28.7
		5.11	210.1	3.02	0.33	19.6
	20 ± 0.1	4.57	212.2	2.03	0.49	21.9
		2.34	123.0	0.75	1.33	42.7
		3.48	164.3	1.34	0.75	28.7
		5.11	235.8	2.36	0.42	19.6
TiO_2-MP-776-4	35 ± 0.1	4.57	175.2	4.28	0.23	21.9
		2.34	102.4	2.08	0.48	42.7
		4.02	154.8	3.66	0.27	24.9
		1.18	66.5	1.00	1.00	84.7

TABLE XII (Cont'd)

Pigment	Temp. (°C)	Vol.% (100φ)	Viscosity η (cps.)	Specific Viscosity	$1/\eta_{sp}$	$1/\phi$
TiO_2-MP-776-4	30 ± 0.1	4.57	192.5	3.71	0.27	21.9
		2.34	112.8	1.76	0.57	42.7
		4.02	171.4	3.19	0.31	24.9
		1.18	76.4	0.87	1.15	84.7
	25 ± 0.1	4.57	226.2	3.34	0.30	21.9
		2.34	125.0	1.39	0.72	42.7
		4.02	197.2	2.78	0.36	24.9
		1.18	86.1	0.65	1.54	84.7
	25 ± 0.1	4.57	245.4	2.50	0.36	21.9
		2.34	138.9	0.98	1.02	42.7
		4.02	213.3	2.04	0.45	24.9
		1.18	101.2	0.44	0.24	84.7
TiO_2-MP-776-5	35 ± 0.1	2.34	102.5	2.09	0.48	42.7
		3.48	134.1	3.04	0.33	28.7
		1.76	82.3	1.48	0.68	56.8
		1.18	66.1	0.99	1.01	84.7
	30 ± 0.1	2.34	112.6	1.75	0.57	42.7
		3.48	148.7	2.64	0.38	28.7
		1.76	92.8	1.27	0.79	56.8
		1.18	76.0	0.86	1.16	84.7
	25 + 0.1	2.34	125.9	1.41	0.71	42.7
		3.48	172.5	2.30	0.43	28.7
		1.76	104.8	1.01	0.99	56.8
		1.18	86.1	0.65	1.54	84.7
	20 ± 0.1	2.34	138.9	0.98	1.02	42.7
		3.48	186.8	1.66	0.60	28.7
		1.18	101.0	0.43	2.35	84.7
		1.76	118.5	0.69	1.46	56.8
TiO_2-MP-776-6	35 ± 0.1	2.34	82.1	1.47	0.68	42.7
		3.48	106.4	2.20	0.45	28.7
		4.57	133.3	3.16	0.32	21.9
		1.76	69.0	1.08	0.92	56.8
	30 ± 0.1	2.34	93.9	1.30	0.77	42.7
		3.48	123.1	2.01	0.50	28.7
		4.57	159.8	2.91	0.34	21.9
		1.76	79.8	0.95	1.05	56.8

TABLE XII (Cont'd)

Pigment	Temp. (°C)	Vol.% (100φ)	Viscosity η (cps.)	Specific Viscosity	$1/\eta_{sp}$	$1/\phi$
TiO_2-MP-776-5	25 ± 0.1	2.34	106.1	1.03	0.97	42.7
		3.48	135.6	1.60	0.62	28.7
		4.57	176.7	2.39	0.42	21.9
		1.76	91.4	0.75	1.34	56.8
	20 ± 0.1	2.34	120.6	0.72	1.39	42.7
		3.48	157.1	1.24	0.81	28.7
		4.57	201.8	1.88	0.53	21.9
		1.76	106.6	0.52	1.94	56.8

TABLE XIII

PUBLISHED VISCOSITY DATA

Zettlemoyer's Data (58):

Rotating cylinder viscometer was used.

Suspension: Calcium carbonate in polybutene No. 12

(A) Mean particle diameter: 0.13 ± 0.08 micron.

Vol. Frac. (ϕ)	$1/\phi$	η_{sp}	$1/\eta_{sp}$
.02	50	.169	5.9
.0304	32.9	.251	4.0
.0404	24.8	.339	2.9
.0508	19.7	.470	2.1
.0612	16.3	.595	1.7
.0652	15.3	.619	1.6
.0819	12.2	.882	1.1
.0911	11.0	1.027	.97

(B) Mean particle diameter: 0.18 ± 0.09 micron.

Vol. Frac. (ϕ)	$1/\phi$	η_{sp}	$1/\eta_{sp}$
.0196	51.0	.139	7.2
.0290	34.5	.222	4.5
.0498	20.1	.366	2.7
.0699	14.3	.563	1.8
.0896	11.2	.792	1.3

(C) Mean particle diameter: 0.23 ± 0.10 micron.

Vol. Frac. (ϕ)	$1/\phi$	η_{sp}	$1/\eta_{sp}$
.0303	33.0	.202	5.0
.0407	24.6	.284	3.5
.0499	20.0	.353	2.8
.0698	14.3	.525	1.9
.0913	11.0	.742	1.3
.121	8.3	1.172	.80

(D) Mean particle diameter: 0.39 ± 0.28 micron.

Vol. Frac. (ϕ)	$1/\phi$	η_{sp}	$1/\eta_{sp}$
.0196	51.0	.124	8.1
.0302	33.1	.193	5.2
.0414	24.2	.266	3.8
.0455	22.0	.274	3.6
.0706	14.2	.477	2.1
.0914	10.9	.673	1.5
.122	8.2	1.056	.9

TABLE XIII (Cont'd)

(E) Mixture of (A) and (D).

Vol. Frac.(ϕ)	$1/\phi$	η_{sp}	$1/\eta_{sp}$
.0200	50.0	.119	8.4
.0299	33.4	.195	5.1
.0402	24.9	.275	3.6
.0502	19.9	.359	2.8

Maron's Data (35):

Concentric cylinder viscometer was used.

(A) Suspension: Latex in water. Temperature 20.13°C.

Vol. Frac.(ϕ)	$1/\phi$	η_{sp}	$1/\eta_{sp}$
.0306	32.7	.09	11.1
.0515	19.4	.16	6.25
.1010	9.9	.36	2.78
.1795	5.57	.82	1.22
.2481	4.02	1.48	.68

(B) Suspension: Latex in water .Temperature 50.0°C.

Vol. Frac.(ϕ)	$1/\phi$	η_{sp}	$1/\eta_{sp}$
.0306	32.7	.10	10.0
.0515	19.4	.18	5.56
.1010	9.9	.38	2.63
.1795	5.57	.85	1.17
.2481	4.02	1.53	.65

Traxler's Data (49):

Falling coaxial cylinder viscometer was used.

(A) Suspension: Gray-green mica in Venezuelan asphalt.

Vol. Frac.(ϕ)	$1/\phi$	η_{sp}	$1/\eta_{sp}$
.05	20	.64	1.6
.10	10	1.58	.63
.15	6.7	2.96	.34
.20	5.0	5.82	.17

TABLE XIII (Cont'd)

(B) Suspension: Black slate in Venezuelan asphalt.

Vol. Frac.(ϕ)	$1/\phi$	η_{sp}	$1/\eta_{sp}$
.05	20	.46	2.2
.10	10	.92	1.1
.15	6.7	1.59	.63
.20	5.0	2.65	.38

(C) Suspension: Diatomaceous earth in Venezuelan asphalt.

Vol. Frac.(ϕ)	$1/\phi$	η_{sp}	$1/\eta_{sp}$
.024	41.7	.46	2.17
.048	20.8	1.03	.97
.072	13.9	1.58	.63
.096	10.4	2.87	.35

Vand's Data (51):

Ostwald capillary viscometer was used.
Suspension: Glass spheres 100-160 microns in aqueous solution of zinc iodide and glycol.

Vol. Frac.(ϕ)	$1/\phi$	η_{sp}	$1/\eta_{sp}$
.05	20	.145	6.90
.10	10	.34	2.94
.15	6.7	.62	1.61
.20	5.0	1.02	.98
.25	4.0	1.63	.61
.30	3.3	2.64	.38

Broughton's Data (8):

Macmichael rotating cylinder viscometer was used.
Suspension: Glass spheres 37-74,74-147, 147-295 microns in mixture of acetylene tetrachloride and monobromobenzene.

Vol. Frac.(ϕ)	$1/\phi$	η_{sp}	$1/\eta_{sp}$
.05	20	.15	6.67
.10	10	.35	2.86
.15	6.7	.61	1.64
.20	5.0	.94	1.06

TABLE XIII (Cont'd)

Robinson's Data (46):

Buchdahle rotating cylinder viscometer was used.
Suspension: Glass sphere 10-20 microns in S.A.E. oils No. 30 and 50 and in castor oil.

Vol. Frac. (ϕ)	$1/\phi$	η_{sp}	$1/\eta_{sp}$
.05	20	.16	6.25
.10	10	.36	2.78
.15	6.7	.62	1.61
.20	5.0	.98	1.02

Eilers's Data (13)

Vogel-Ossage capillary viscometer was used.
Emulsion: Bitumin-Tall oil emulsion.

Vol. Frac. (ϕ)	$1/\phi$	η_{sp}	$1/\eta_{sp}$
.1	10	.25	4
.2	5	.84	1.19
.3	3.3	1.55	.64
.5	2.0	6.6	.15
.6	1.67	17.0	.059
.7	1.43	89.0	.011

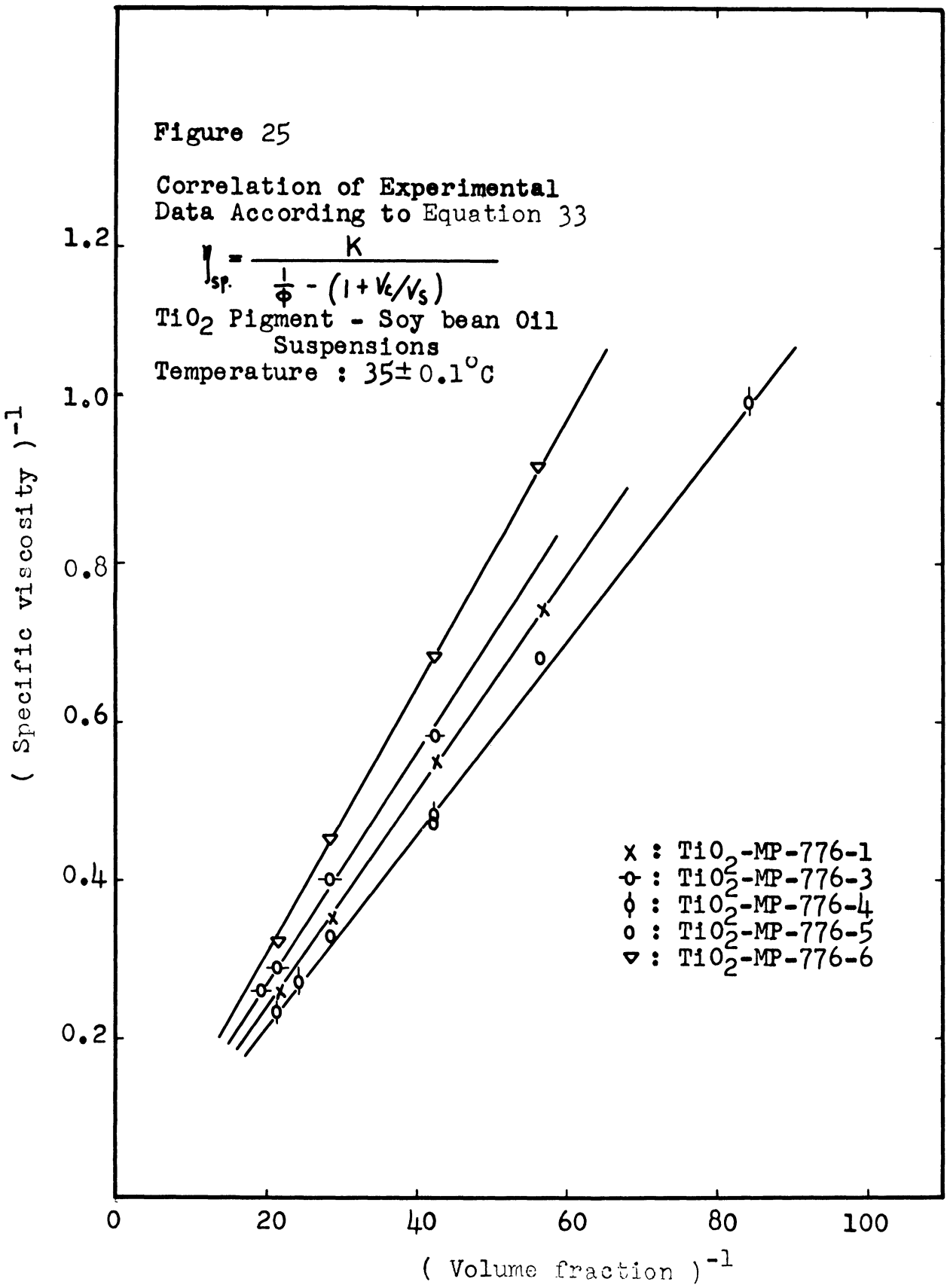
Figure 25
Correlation of Experimental Data According to Equation 33
$\eta_{sp.} = \frac{K}{\frac{1}{\Phi} - (1 + V_c/V_s)}$
TiO_2 Pigment - Soy bean Oil Suspensions
Temperature : 35± 0.1°C
(Specific viscosity)$^{-1}$
(Volume fraction)$^{-1}$
0
20
40
60
80
100
0.2
0.4
0.6
0.8
1.0
1.2
x : TiO_2-MP-776-1
o : TiO_2-MP-776-3
ϕ : TiO_2-MP-776-4
o : TiO_2-MP-776-5
▽ : TiO_2-MP-776-6

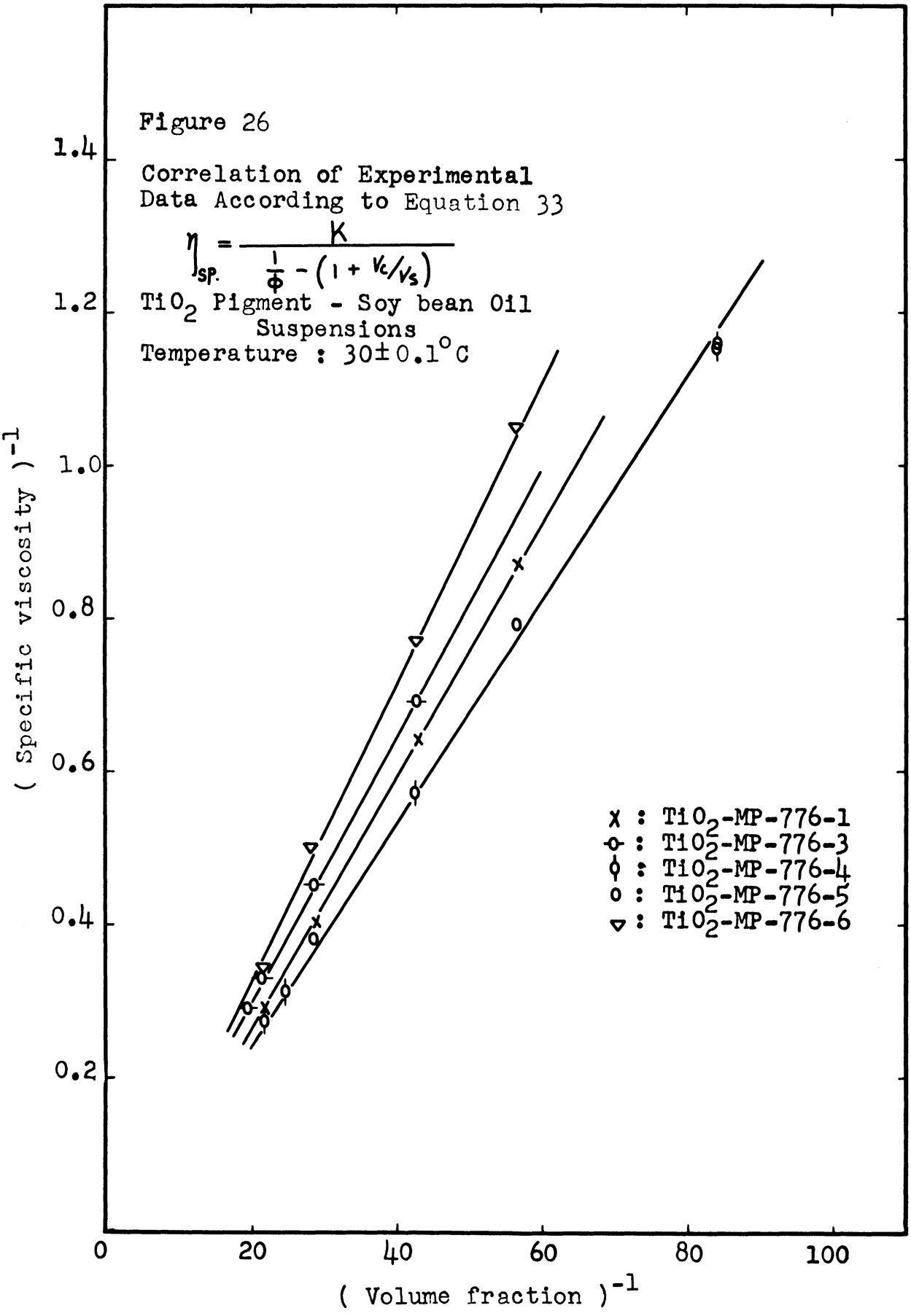
Figure 26
Correlation of Experimental Data According to Equation 33
$\eta_{sp.} = \frac{K}{\frac{1}{\Phi} - (1 + V_c/V_s)}$
TiO_2 Pigment - Soy bean Oil Suspensions
Temperature : 30±0.1°C
(Specific viscosity)$^{-1}$
(Volume fraction)$^{-1}$
0
20
40
60
80
100
0.2
0.4
0.6
0.8
1.0
1.2
1.4
x : TiO_2-MP-776-1
o : TiO_2-MP-776-3
◊ : TiO_2-MP-776-4
o : TiO_2-MP-776-5
▽ : TiO_2-MP-776-6

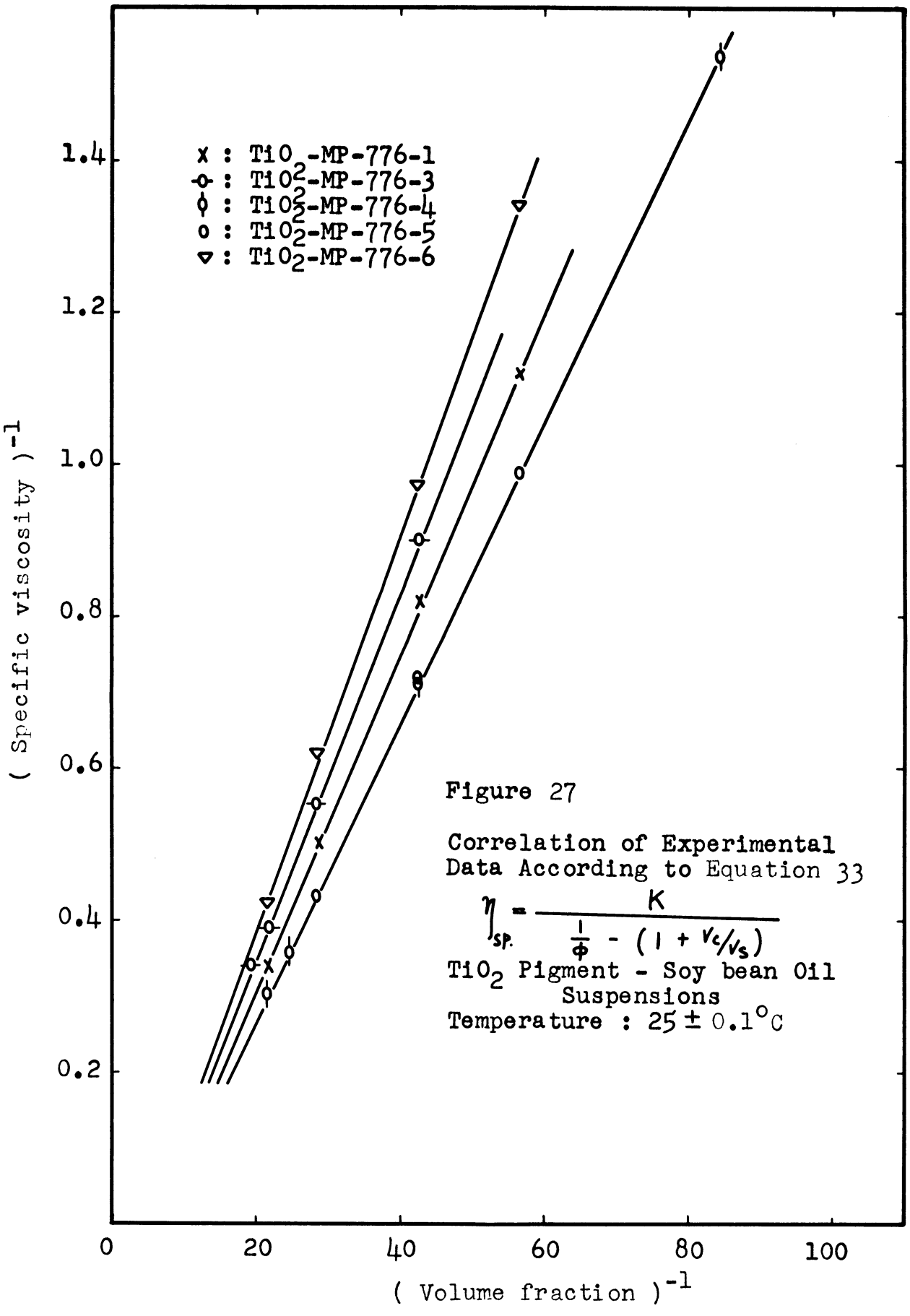

Figure 27

Correlation of Experimental Data According to Equation 33

$$\eta_{sp.} = \frac{K}{\frac{1}{\Phi} - (1 + V_c/V_s)}$$

TiO_2 Pigment - Soy bean Oil Suspensions

Temperature : $25 \pm 0.1^{\circ}C$

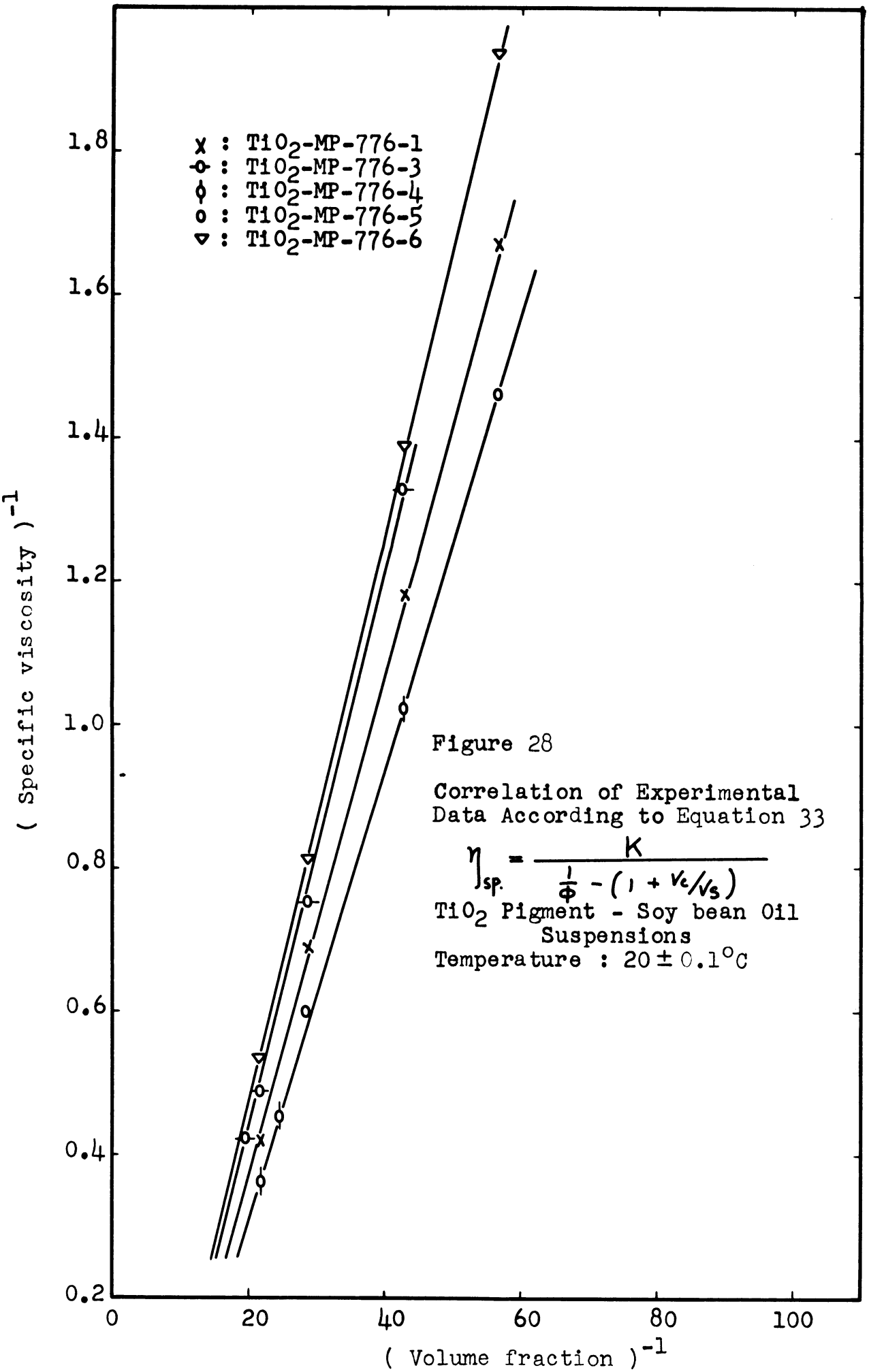

Figure 28

Correlation of Experimental Data According to Equation 33

$$\eta_{sp.} = \frac{K}{\frac{1}{\Phi} - (1 + V_c/V_s)}$$

TiO_2 Pigment - Soy bean Oil Suspensions

Temperature : $20 \pm 0.1^{\circ}C$

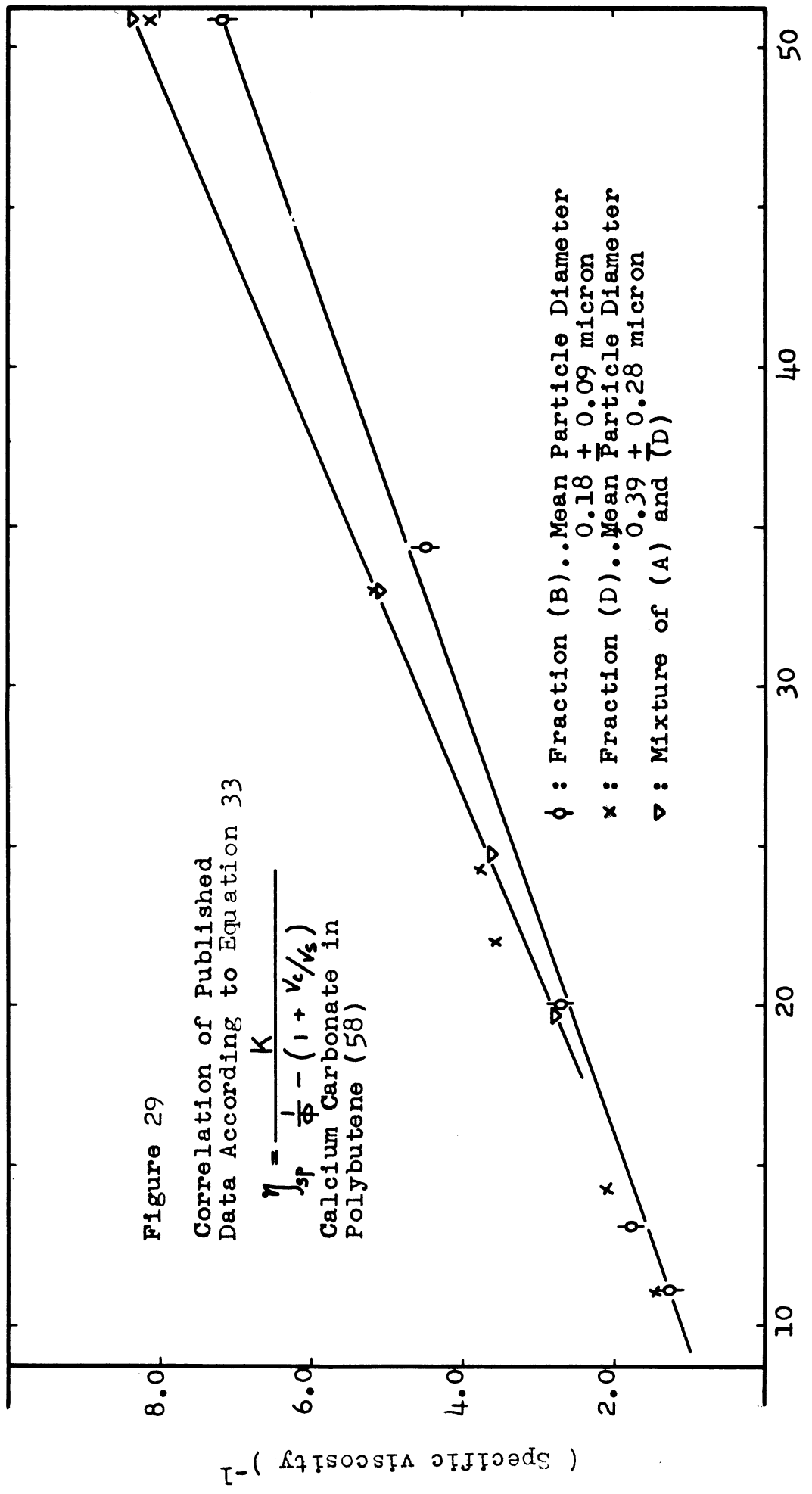

Figure 29

Correlation of Published Data According to Equation 33

$$\eta_{sp} = \frac{K}{\frac{1}{\phi} - \left(1 + V_c/V_s\right)}$$

Calcium Carbonate in Polybutene (58)

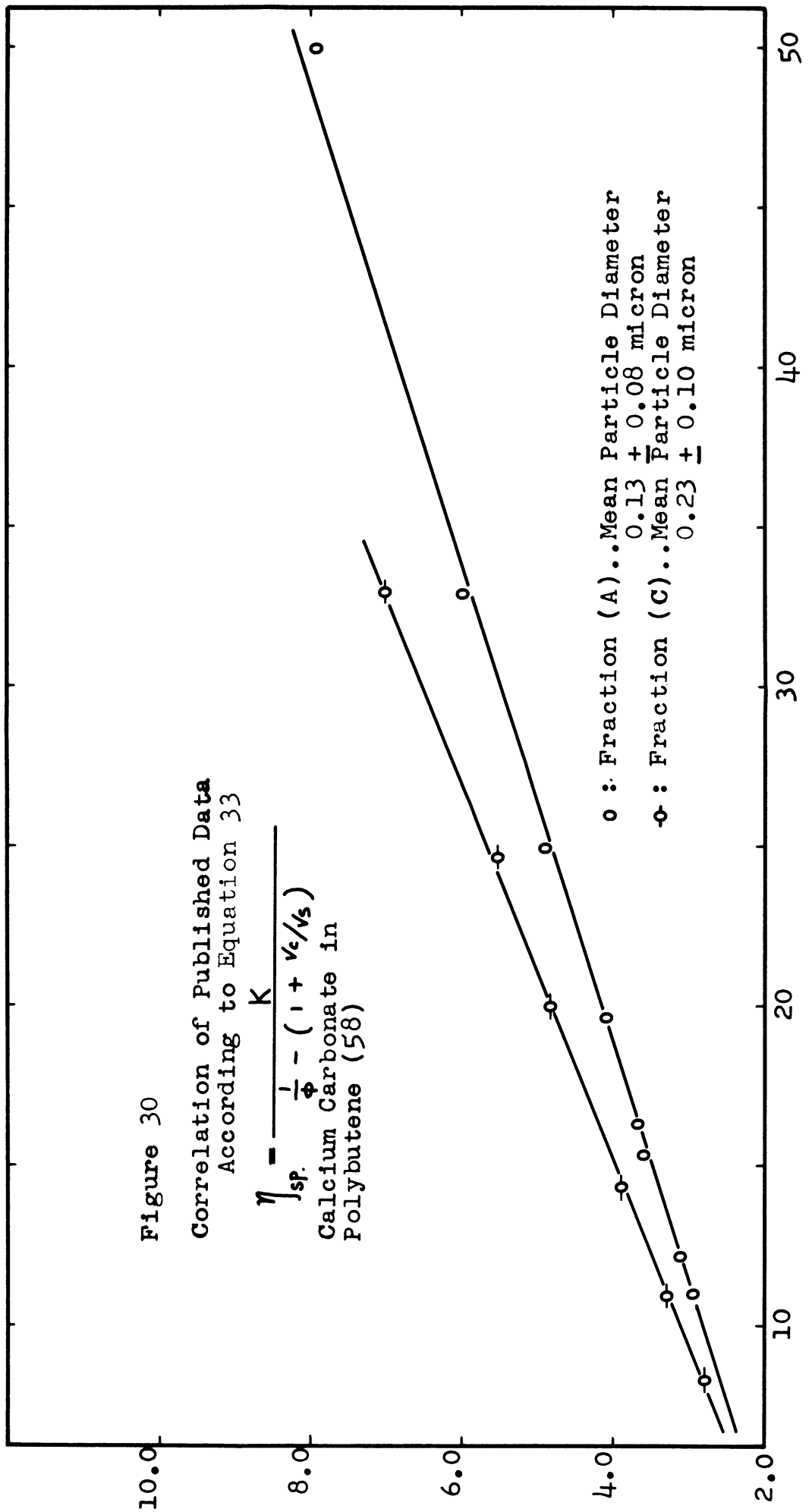

Figure 30

Correlation of Published Data According to Equation 33

$$\eta_{sp.} = \frac{K}{\frac{1}{\phi} - (1 + v_c/v_s)}$$

Calcium Carbonate in Polybutene (58)

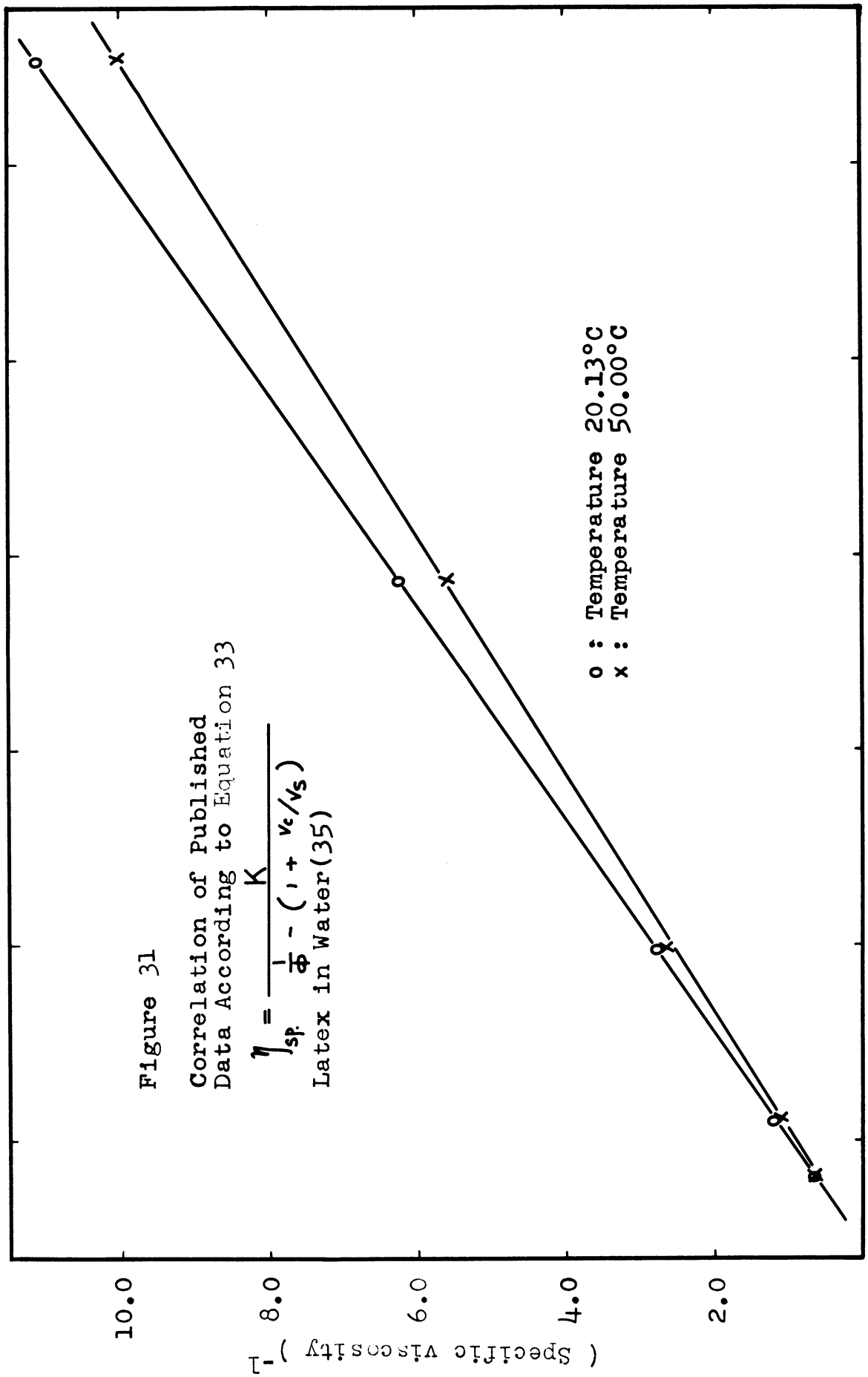

Figure 31

Correlation of Published Data According to Equation 33

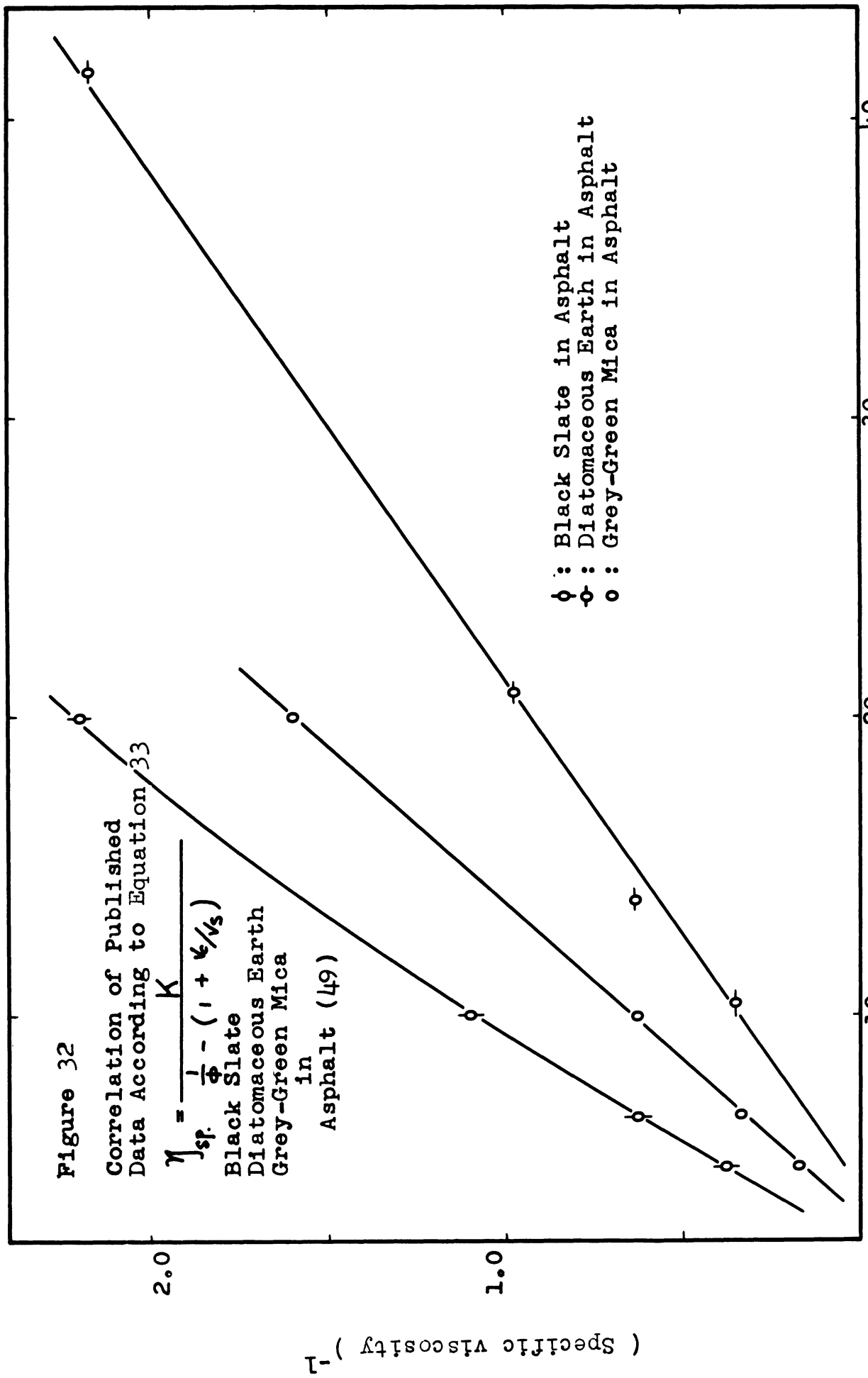
Figure 32
Correlation of Published Data According to Equation 33
$\eta_{sp.} = \frac{K}{\frac{1}{\phi} - (1 + \psi/\psi_s)}$
Black Slate
Diatomaceous Earth
Grey-Green Mica
in
Asphalt (49)
ϕ : Black Slate in Asphalt
ϕ : Diatomaceous Earth in Asphalt
o : Grey-Green Mica in Asphalt
(Specific viscosity)$^{-1}$
(Volume fraction)$^{-1}$
2.0
1.0
10
20
30
40

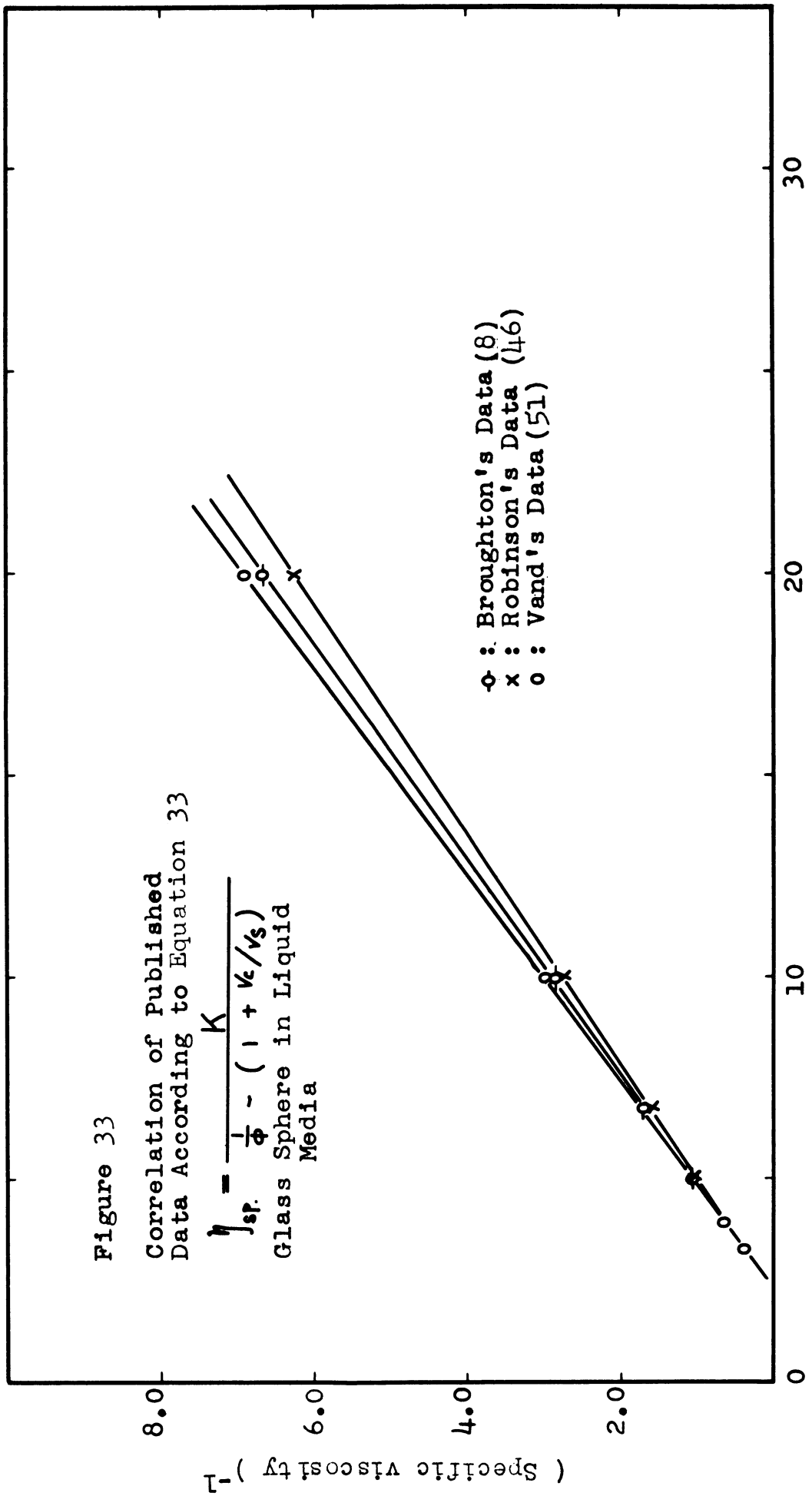

Figure 33

Correlation of Published Data According to Equation 33

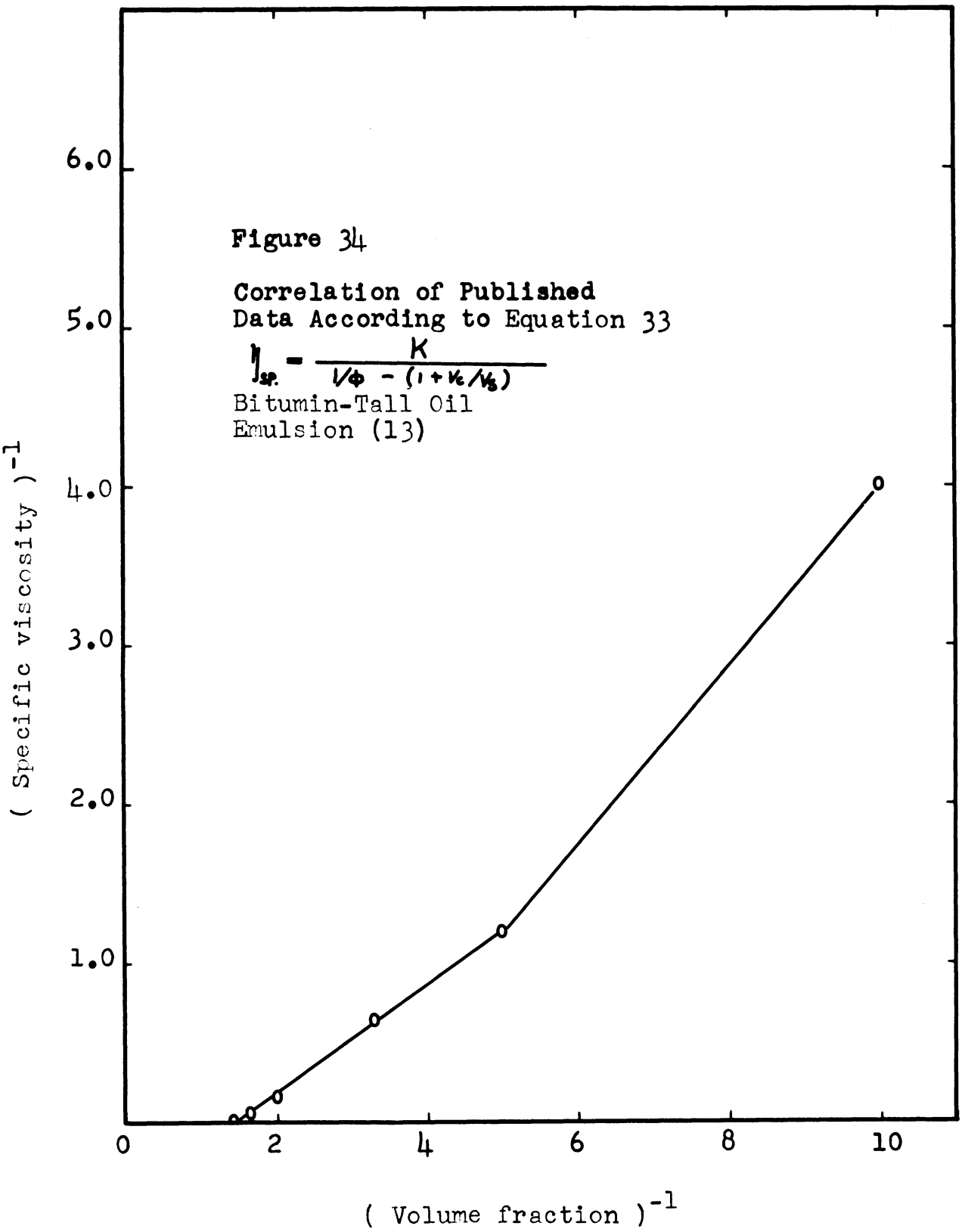

Figure 34

Correlation of Published Data According to Equation 33

$$\eta_{sp.} = \frac{K}{1/\phi - (1 + k_c/k_s)}$$

Bitumin-Tall Oil Emulsion (13)

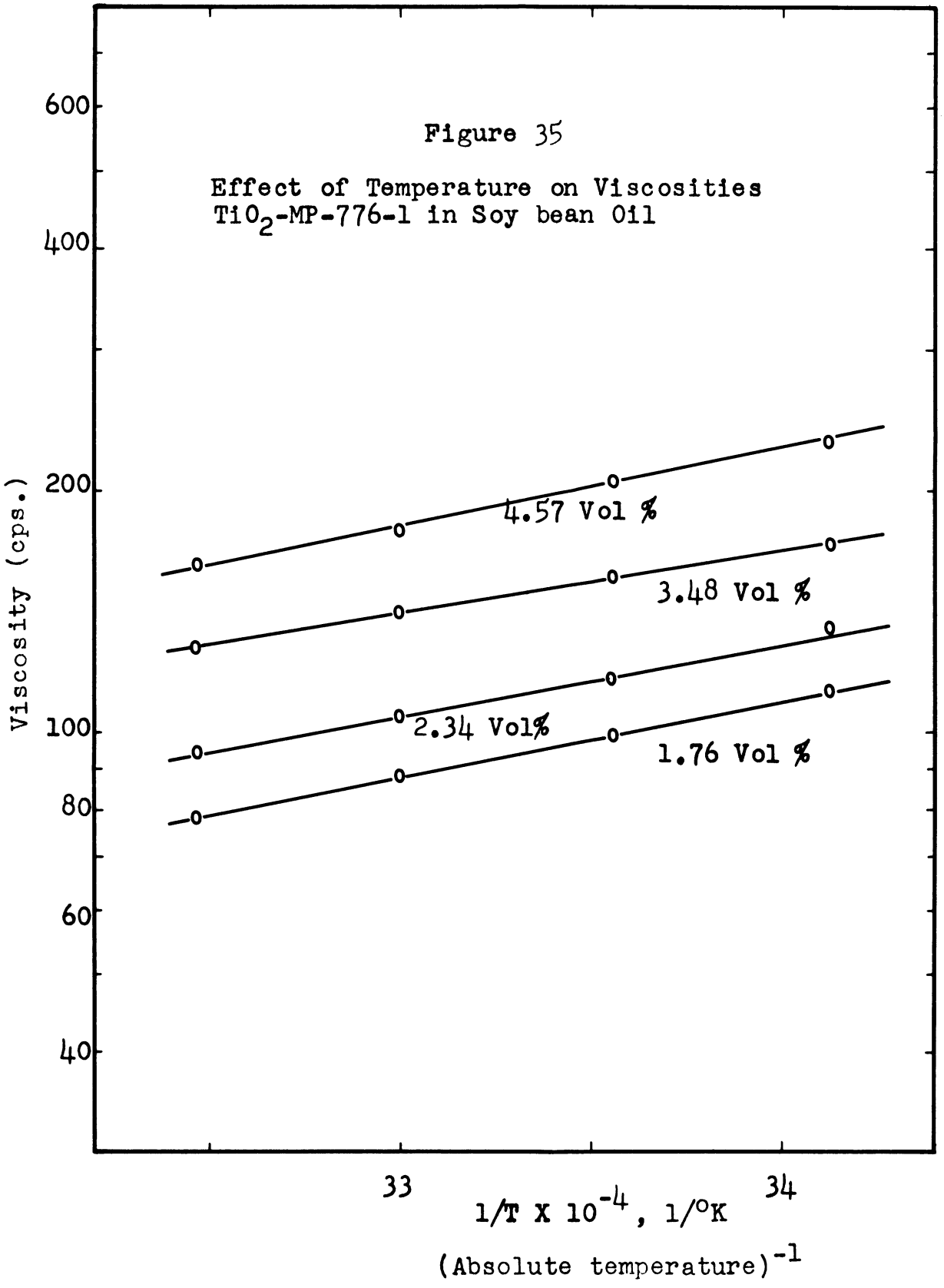

Figure 35

Effect of Temperature on Viscosities
TiO_2-MP-776-1 in Soy bean Oil

Figure 36

Effect of Temperature on Viscosities
TiO_2-MP-776-3 in Soy bean Oil

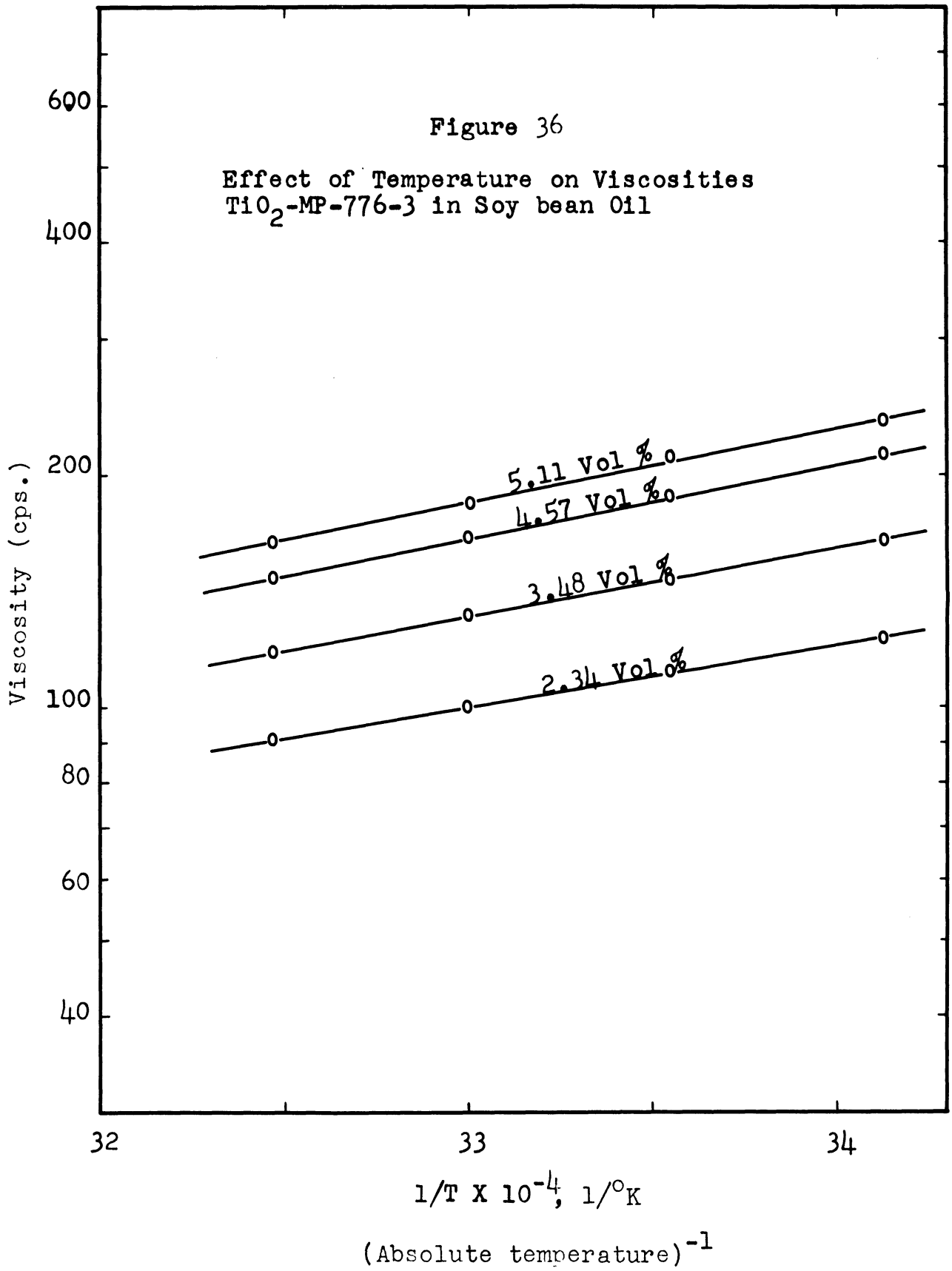

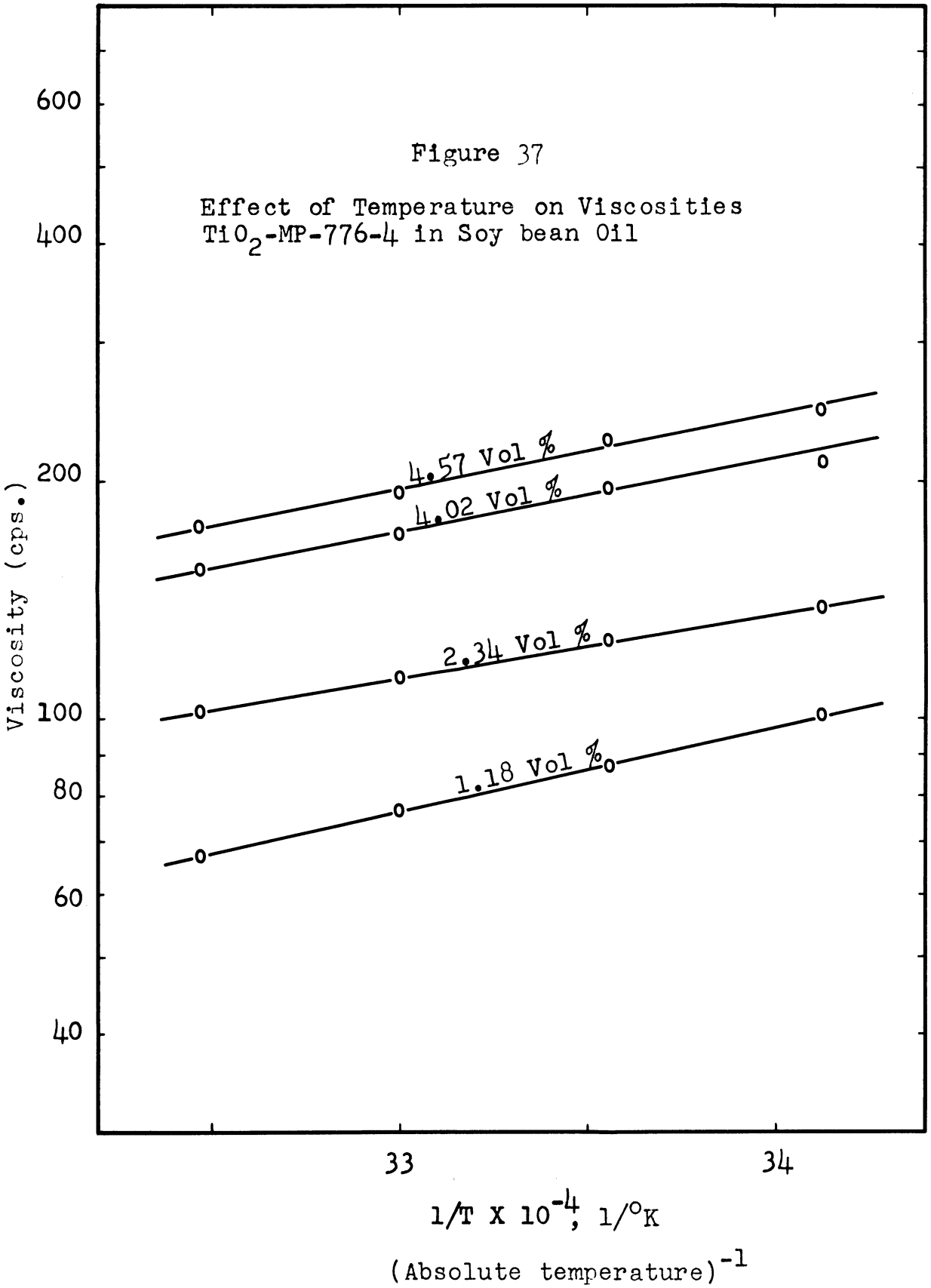

Figure 37

Effect of Temperature on Viscosities
TiO_2-MP-776-4 in Soy bean Oil

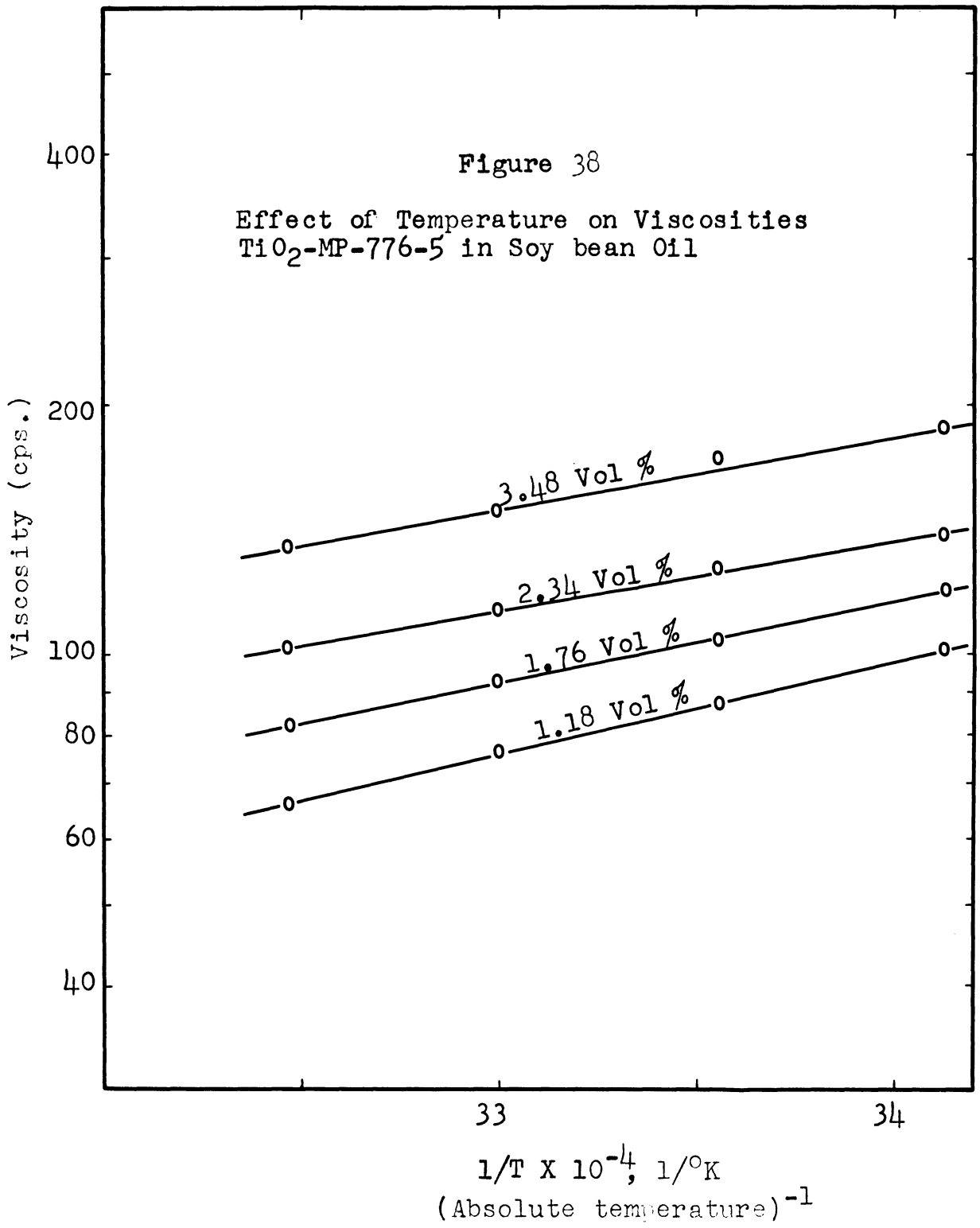

Figure 38

Effect of Temperature on Viscosities
TiO_2-MP-776-5 in Soy bean Oil

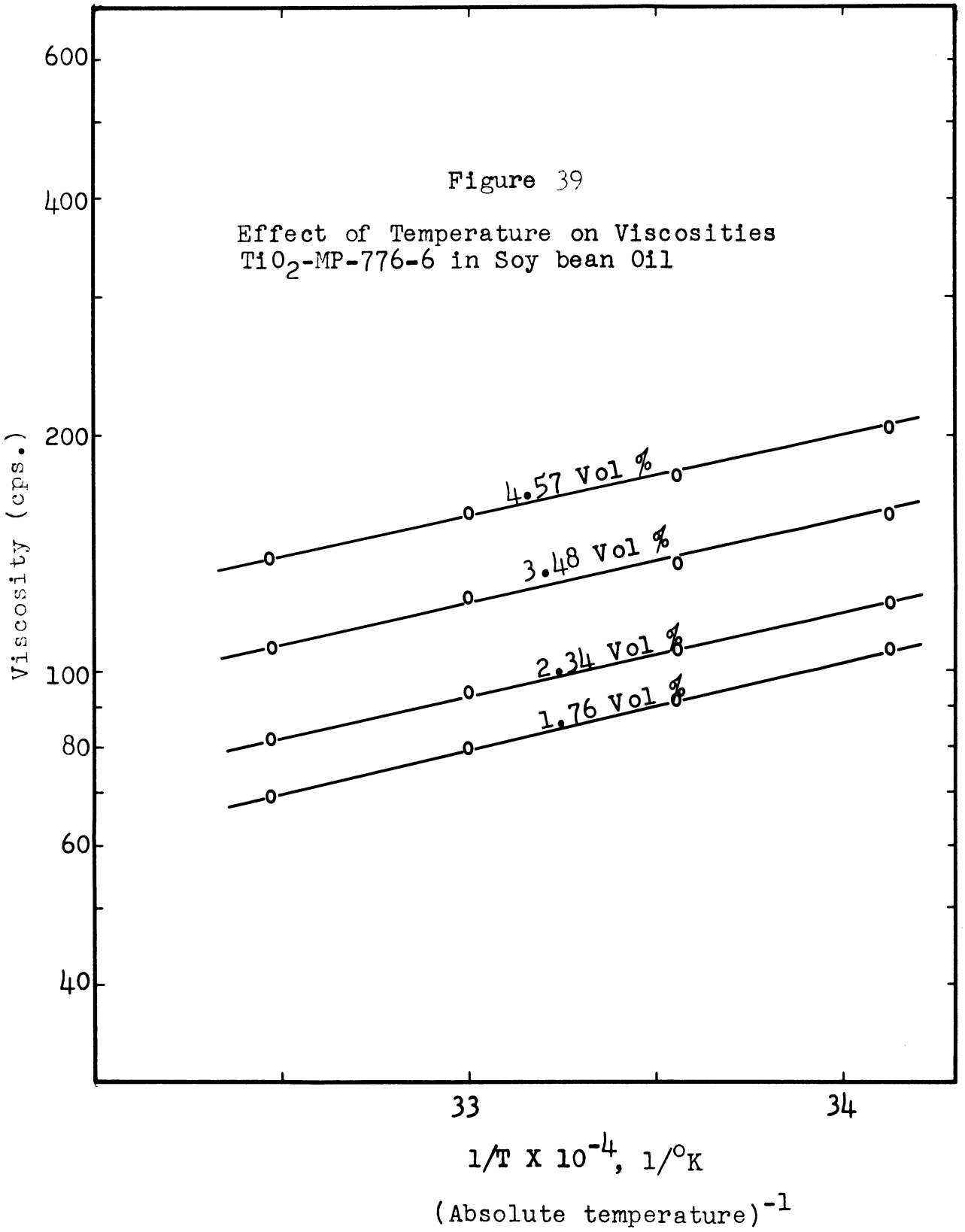

Figure 39

Effect of Temperature on Viscosities
TiO_2-MP-776-6 in Soy bean Oil

TABLE XIV

EFFECT OF MILLING TIME ON THE VISCOSITIES OF THE SUSPENSIONS

Pigment: TiO_2-MP-776-5. Temperature: 25 ± o.1 °C.

Vol. % of Pigment :	3.48						
Milling time (hrs.):	5	10	20	40	60	80	96
Viscosity (cps.):	168.3	176.1	177.9	175.3	173.0	172.0	172.5
Vol. % of Pigment :	2.34						
Milling time (hrs.):	5	10	20	40	60	80	96
Viscosity (cps.):	120.6	131.0	129.2	128.6	126.0	126.0	125.9
Vol. % of Pigment :	1.76						
Milling time (hrs.):	5	10	20	40	60	80	96
Viscosity (cps.):	100.3	106.3	105.6	105.0	103.9	105.0	104.8

Figure 40

Effect of Milling Time on The Viscosities of Suspensions ... TiO_2-MP-776-5 Pigment in Soy bean Oil

Temperature : 25 ± 0.1°C

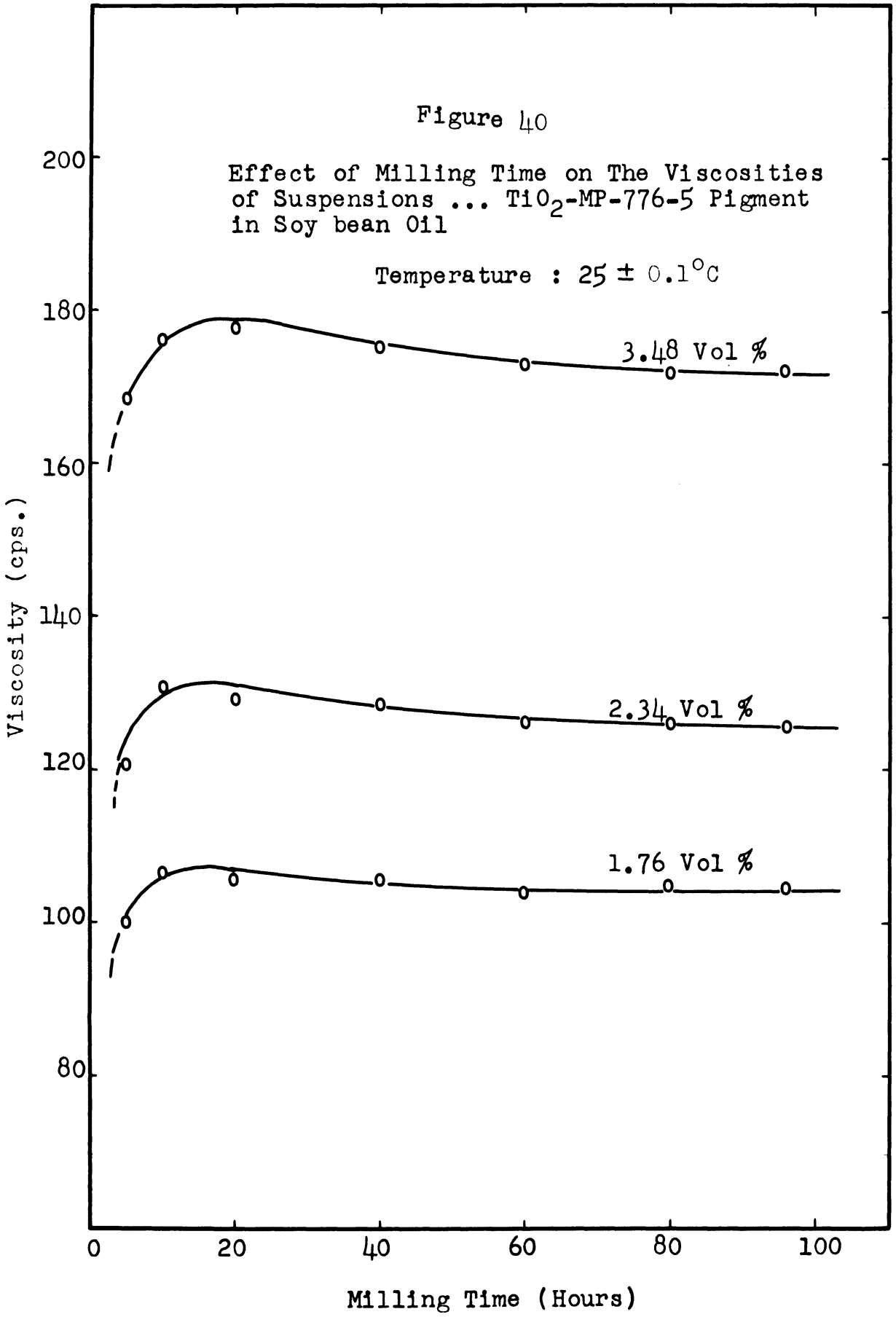

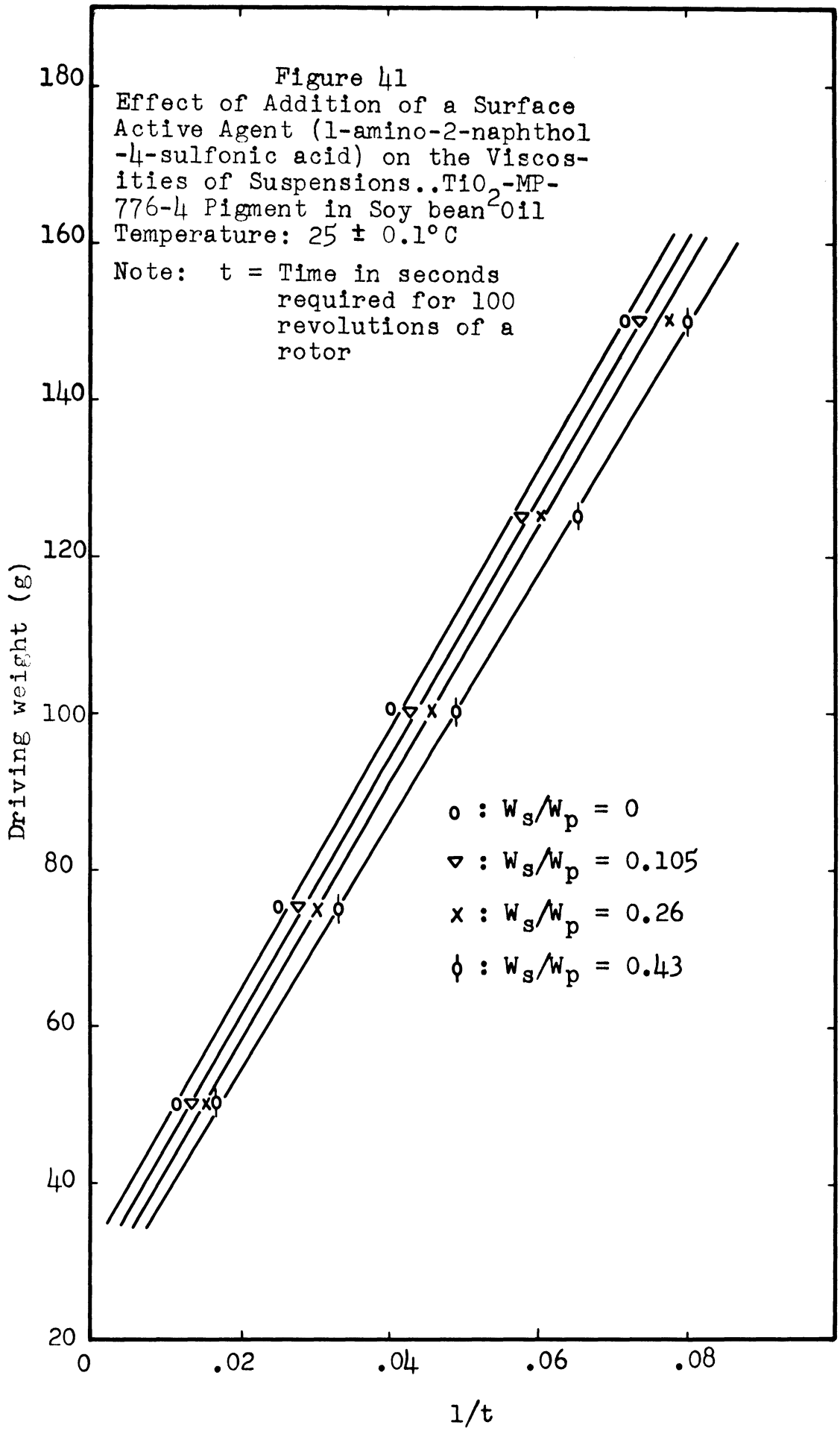
Figure 41
Effect of Addition of a Surface Active Agent (1-amino-2-naphthol -4-sulfonic acid) on the Viscosities of Suspensions..TiO2-MP-776-4 Pigment in Soy bean Oil
Temperature: 25 ± 0.1°C
Note: t = Time in seconds required for 100 revolutions of a rotor
o : Ws/Wp = 0
▽ : Ws/Wp = 0.105
x : Ws/Wp = 0.26
ϕ : Ws/Wp = 0.43
Driving weight (g)
180
160
140
120
100
80
60
40
20
0
.02
.04
.06
.08
1/t

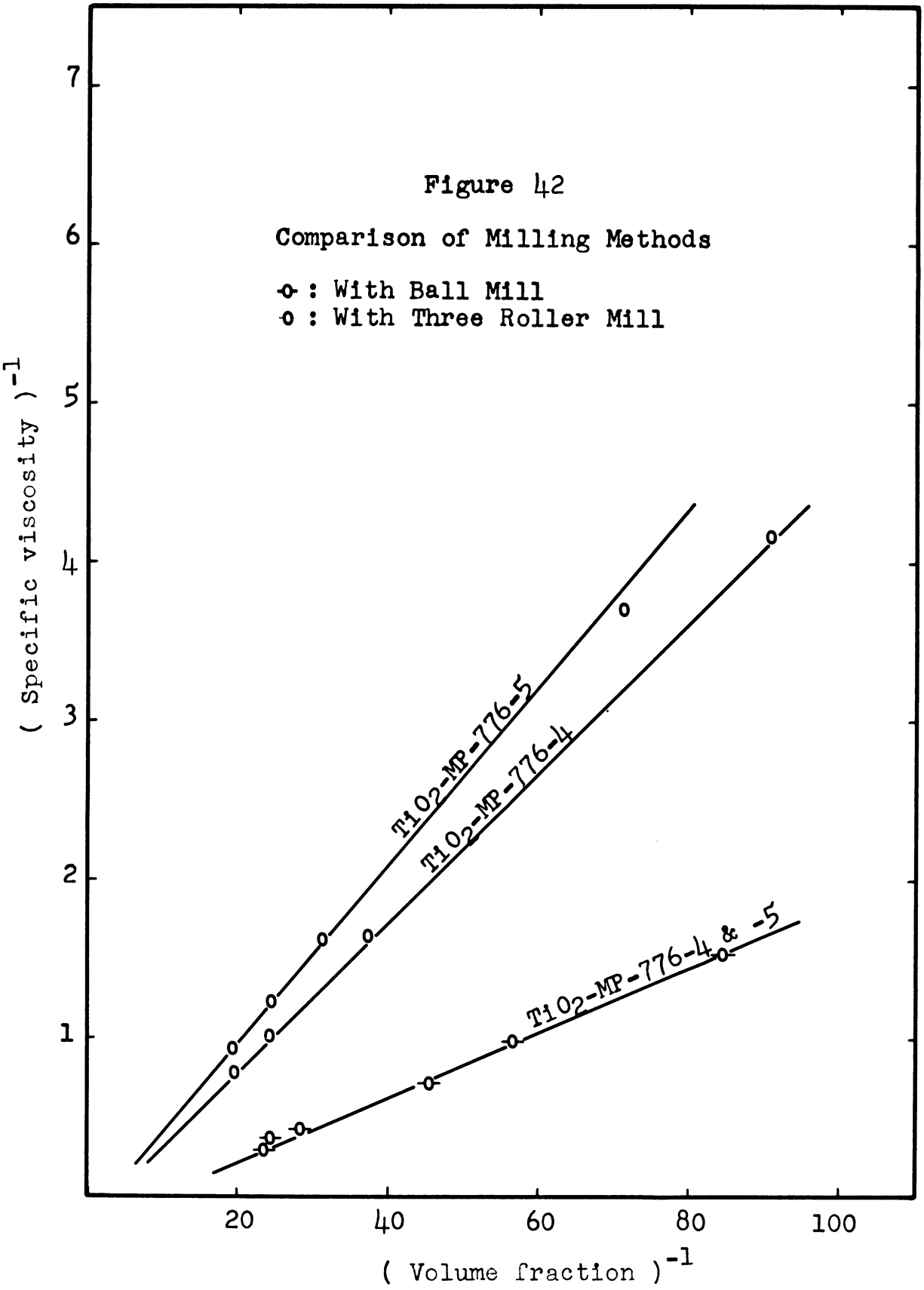
Figure 42
Comparison of Milling Methods
-o- : With Ball Mill
o : With Three Roller Mill
TiO2-MP-776-5
TiO2-MP-776-4
TiO2-MP-776-4 & -5
(Specific viscosity)-1
(Volume fraction)-1
1
2
3
4
5
6
7
20
40
60
80
100

APPENDIX E

COMPARISON OF STORMER VISCOMETER AND BROOKFIELD VISCOMETER

To confirm the experimental method, the viscosity of a suspension was measured by both a Stormer viscometer and a Brookfield viscometer.

For this purpose, the sample suspension was prepared by diluting a paste to 14.00 volume per cent with soy bean oil. This paste was prepared by milling a definite amount of TiO_2-MP-1250 and soy bean oil on a three-roller mill.

The principle of Brookfield viscometer is analogous to that of Stormer viscometer. With a Brookfield viscometer, the viscosity was obtained from the resistance of the fluid to the motion of a rotating spindle. The torque required to rotate the spindle was registered on the viscometer dial. The viscosity of a suspension was, therefore, calculated by (Dial reading at certain rotational speed - Dial reading at zero rotational speed) X (calibration coefficient)/(rotational speed).

A spindle calibration coefficient was determined by measuring the viscosities of the Standard liquids obtained from the Bureau of Standards. (See Appendix F, a calibration coefficient was 100.0).

During the measurement the temperature was kept at 25 $\pm$ 0.1°C.

The experimental data are tabulated in Tables XV-A and XV-B, and are plotted in Figure 43.

TABLE XV-A

COMPARISON OF STORMER VISCOMETER AND BROOKFIELD VISCOMETER

Suspension of TiO_2-MP-1250 Pigment in Soy Bean Oil

Temperature 25 ± 0.1°C. Volume concentration: 14.0%

Stormer Viscometer

Driving weight (g)	200	250	300	350	400
1/t*	0.006	0.0141	0.0243	0.037	0.0514

Brookfield Viscometer

Dial reading	38.10	38.60	40.10	42.23
Rotational speed (r.p.s.)	0.1	0.2	0.5	1.0

TABLE XV-B

COMPARISON OF VISCOSITIES OBTAINED BY DIFFERENT VISCOMETERS

Suspension of TiO_2-MP-1250 Pigment in Soy Bean Oil

Temperature 25 ± 0.1°C. Volume concentration: 14.0%

Rotational Speed (r.p.s.)	Stormer Viscometer η(cps.)	Brookfield Viscometer η(cps.)
0.1	597	600
0.2	553	550
0.5	521	520
1.0	476	473

NOTE: * t is the time in seconds required for 100 revolutions of the bob-type rotor.

This study indicates that the correlation of the viscosity measurements by the Stormer viscometer and Brookfield viscometer is satisfactory, as the variations in viscosity η are small, less than 0.6%.

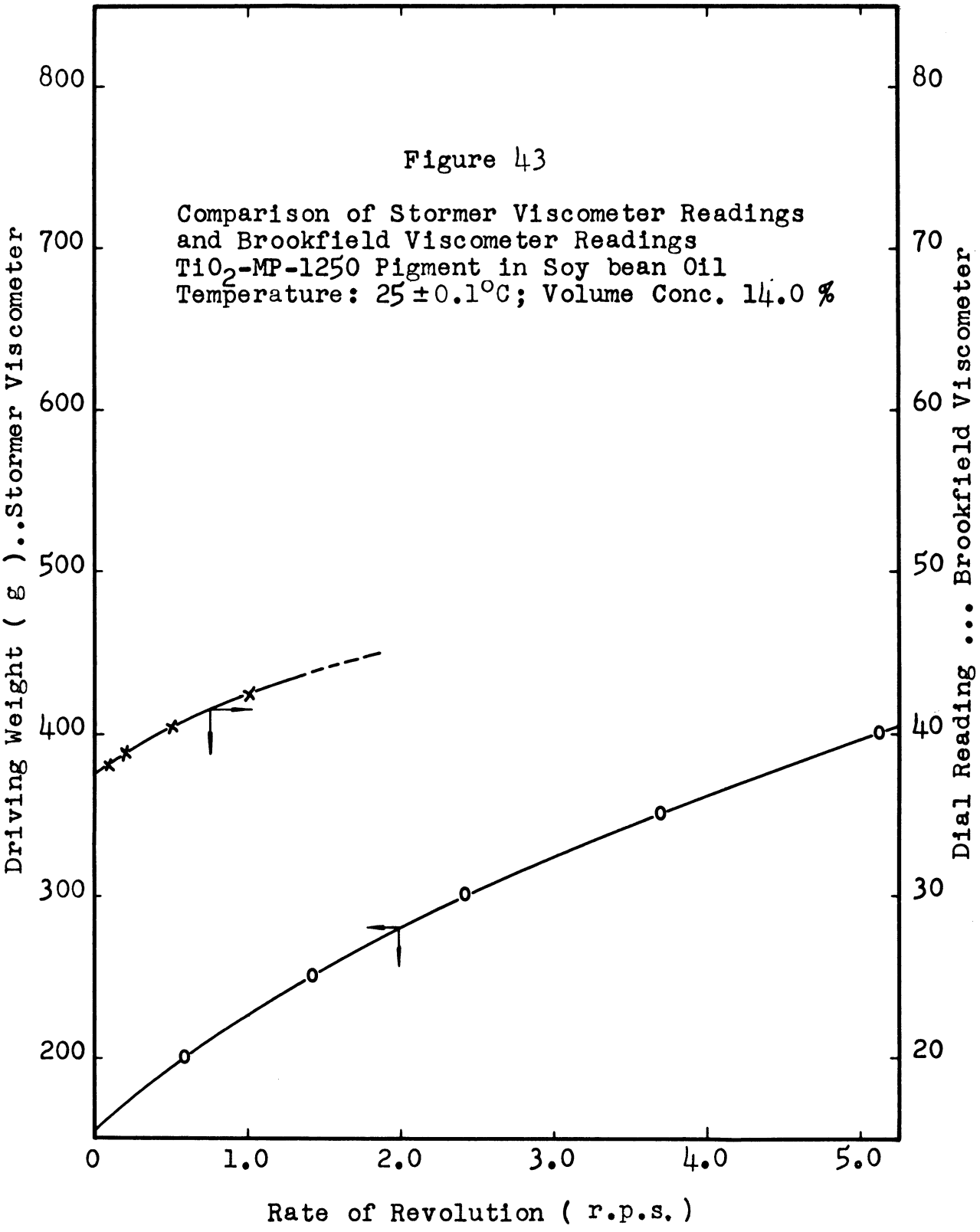

Figure 43

Comparison of Stormer Viscometer Readings and Brookfield Viscometer Readings
TiO_2-MP-1250 Pigment in Soy bean Oil
Temperature: 25 ± 0.1°C; Volume Conc. 14.0 %

APPENDIX F

VISCOMETER CALIBRATION

Viscometers

Stormer viscometer with paddle-type rotor, Stormer viscometer with bob-type rotor and Brookfield viscometer were calibrated against Standard liquids, labeled as J-7, L-20, M-21 and N-19 obtained from Bureau of Standards.

Calibration data are shown in Tables XVI, XVII and XVIII, and are plotted in Figures 44 to 46.

Specification of the standard liquids is as follows:

At Temperature 25°C.

Liquid	:	J-7	L-20	M-21	N-19
Viscosity (cps.)	:	17.43	74.13	201.5	902.3

TABLE XVI

CALIBRATION DATA FOR STORMER VISCOMETER WITH PADDLE-TYPE ROTOR

Liquid...J-7							
Driving wt. (g)	:	20	50	75	100	125	150
* t	:	46.1	27.0	21.3	18.0	15.8	14.2
Liquid...L-20							
Driving wt. (g)	:	50	75	100	125	150	200
t	:	32.9	25.9	21.7	19.1	17.3	14.7
Liquid...M-21							
Driving wt. (g)	:	50	75	100	150	200	300
t	:	44.3	32.8	27.0	20.6	17.1	13.5

* t is the time in seconds required for 100 revolutions of the rotor.

Figure 44 was employed directly to convert experimental readings into viscosity.

TABLE XVII

CALIBRATION DATA FOR STORMER VISCOMETER WITH BOB-TYPE ROTOR

Liquid...L-20							
Driving wt. (g) :	30	40	50	75			
* 1/t :	.028	.037	.047	.070			
Liquid...M-21							
Driving wt. (g) :	50	75	100	150	200		
1/t :	.017	.026	.034	.052	.069		
Liquid...N-19							
Driving wt. (g) :	100	150	200	250	300	350	400
1/t :	.008	.012	.0153	.019	.023	.027	.031

* t is the time in seconds required for 100 revolutions of the rotor.

Calibration coefficient was 6.94×10^{-2} calculated from the slope of Driving weight vs. 1/t curves. (Figure 45).

TABLE XVIII

CALIBRATION DATA FOR BROOKFIELD VISCOMETER

Liquid...M-21				
Dial Reading :	.20	.41	1.01	2.02
Rotational Speed (r.p.s.) :	0.1	0.2	0.5	1.0
Liquid...N-19				
Dial Reading :	.90	1.85	4.51	9.03
Rotational Speed (r.p.s.) :	0.1	0.2	0.5	1.0

Note: r.p.s. stands for revolutions per second.

Calibration coefficient was 100.0 calculated from the slope of Dial Reading vs. r.p.s. curves. (Figure 46)

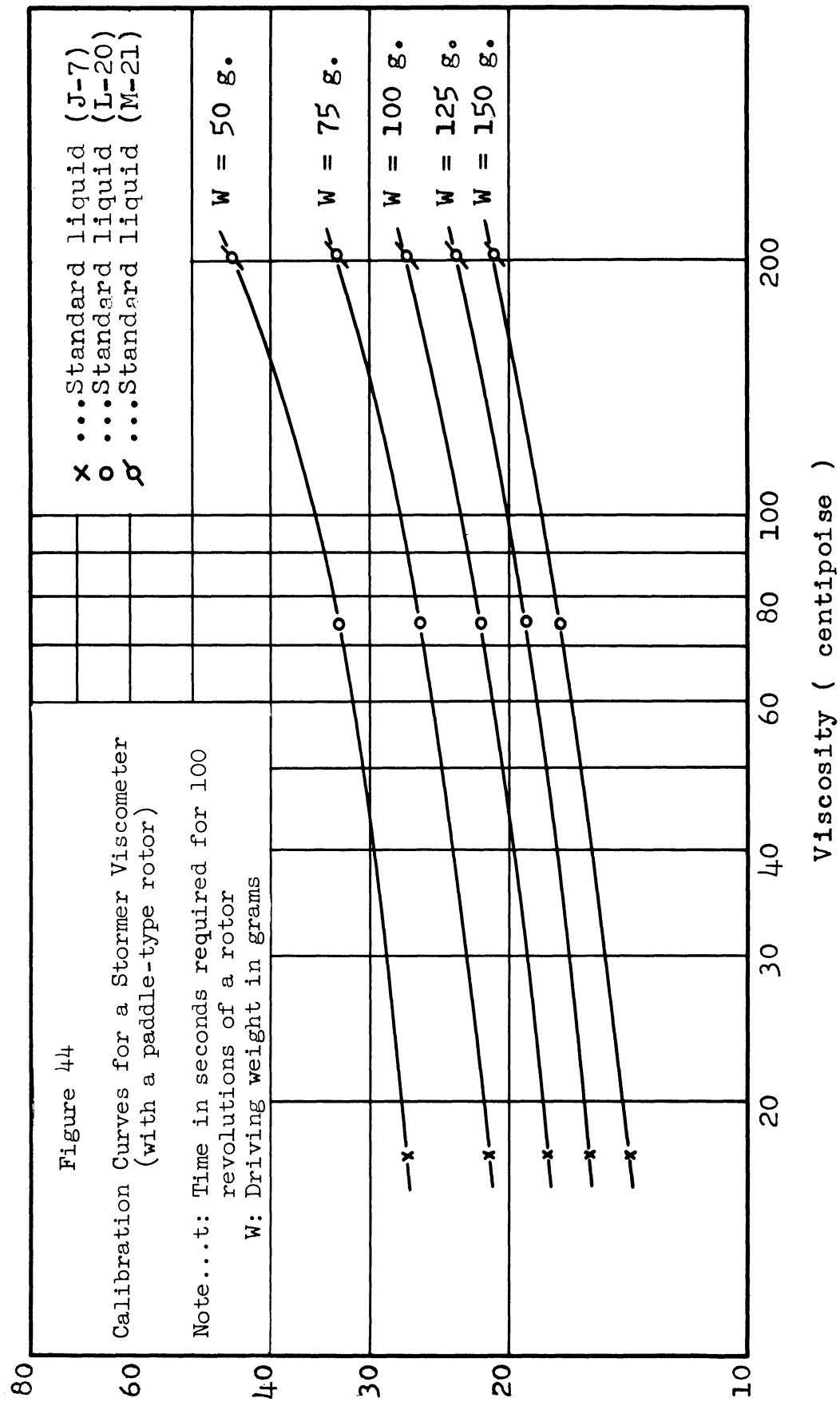

Figure 44

Calibration Curves for a Stormer Viscometer (with a paddle-type rotor)

Note...t: Time in seconds required for 100 revolutions of a rotor
W: Driving weight in grams

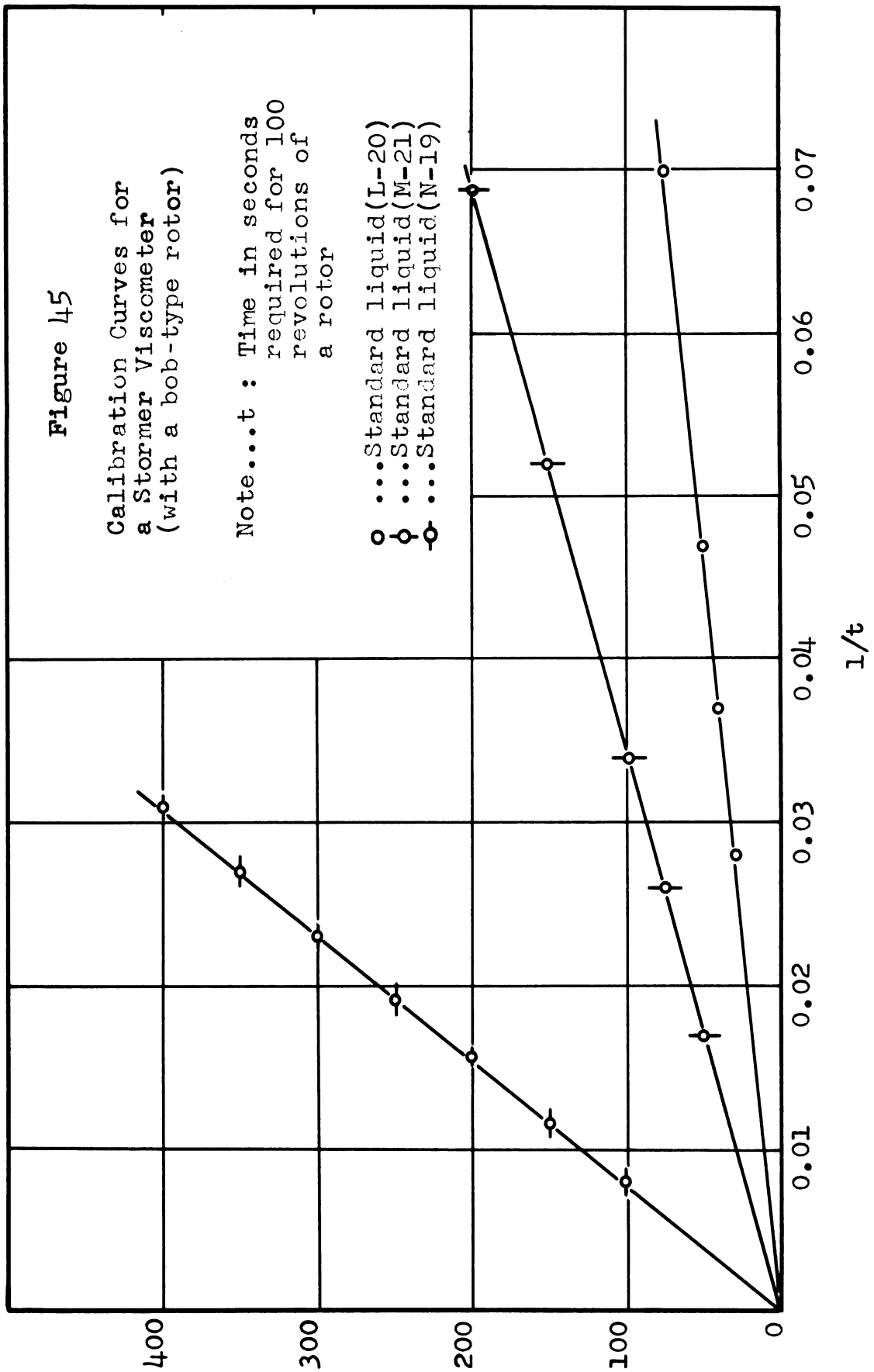
Figure 45
Calibration Curves for
a Stormer Viscometer
(with a bob-type rotor)
Note...t : Time in seconds
required for 100
revolutions of
a rotor
...Standard liquid(L-20)
...Standard liquid(M-21)
...Standard liquid(N-19)
Driving Weight (g)
400
300
200
100
0
0.01
0.02
0.03
0.04
0.05
0.06
0.07
1/t

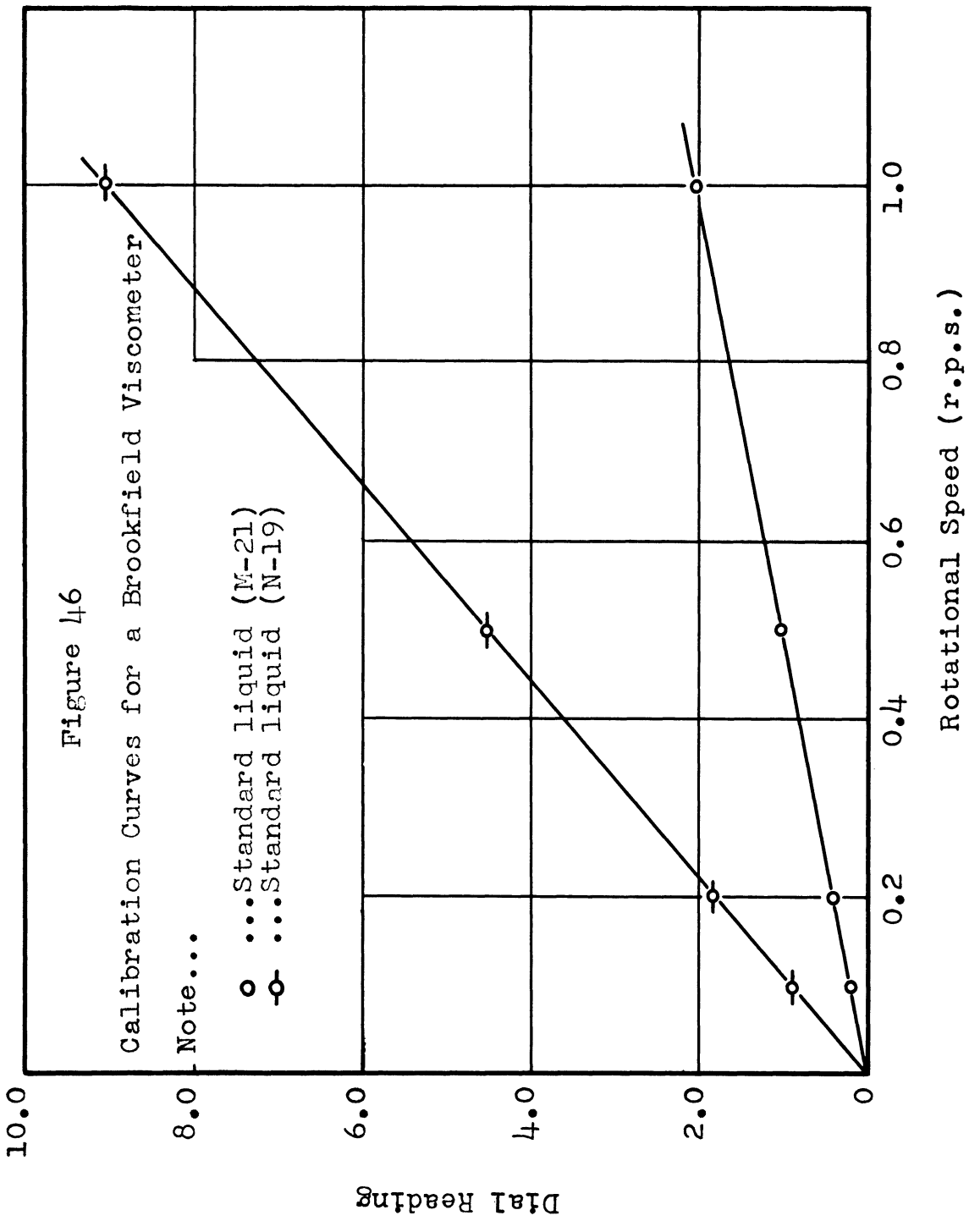
Figure 46
Calibration Curves for a Brookfield Viscometer
Note...
o ...Standard liquid (M-21)
o ...Standard liquid (N-19)
Dial Reading
10.0
8.0
6.0
4.0
2.0
0
0.2
0.4
0.6
0.8
1.0
Rotational Speed (r.p.s.)

APPENDIX G

Examples of Numerical Calculation

(1) Calculation of calibration coefficient, K', for the Stormer Viscometer (with bob-type rotor).

According to the least square mean principle (H. Cramer: "Mathematical Methods of Statistics" Princeton University Press 1951), following equation was derived for the calculation:

$$K' = \eta_o \frac{\Sigma\ (1/t) \cdot (W)}{\Sigma\ (W)^2}$$

Here t is the time in seconds required for 100 revolutions of a rotor, W is the driving weight in grams and η_o is the viscosity of the Standard liquid.

(a) Standard liquid L-20: (viscosity η_o = 74.13 cps. at 25°C)

1/t	W	(1/t)X(W)	$(W)^2$
0.028	30	0.84	900
0.037	40	1.48	1,600
0.047	50	2.35	2,500
0.070	75	5.25	5,625
		9.92	10,625

$$\text{Therefore } K' = \frac{9.92 \times 74.13}{10,625} = 6.92 \times 10^{-2}$$

(b) Standard liquid M-21: (viscosity η_o = 201.5 cps. at 25°C)

1/t	W	(1/t)X(W)	$(W)^2$
0.017	50	0.85	2,500
0.026	75	1.95	5,625
0.034	100	3.40	10,000
0.052	150	7.80	22,500
0.069	200	13.80	40,000
		27.80	80,625

$$\text{Therefore } K' = \frac{27.80 \times 201.5}{80,625} = 6.95 \times 10^{-2}$$

(c) Standard liquid N-19: (viscosity η_o = 902.3 cps. at 25°C)

1/t	W	(1/t)X(W)	$(W)^2$
0.008	100	0.80	10,000
0.012	150	1.80	22,500
0.0154	200	3.08	40,000
0.019	250	4.75	62,500
0.023	300	6.90	90,000
0.027	350	9.45	122,500
0.031	400	12.40	160,000
		39.18	507,500

$$\text{Therefore } K' = \frac{39.18 \times 902.3}{507,500} = 6.96 \times 10^{-2}$$

(d) Average value of the calibration coefficient K' for Stormer viscometer

$$\text{is } \frac{(6.92 + 6.95 + 6.96) \times 10^{-2}}{3} = 6.94 \times 10^{-2}$$

(2) Calculation of calibration coefficient K' for the Brookfield viscometer.

According to the least square mean principle (H. Cramer : " Mathematical Methods of Statistics" Princeton University Press 1955), following equation was derived for the calculation:

$$K' = \eta_o \frac{\Sigma(\text{Dial Reading}) \times (\text{r.p.s.})}{\Sigma(\text{r.p.s.})^2}$$

Here (r.p.s.) stands for revolutions per second and η_o is a viscosity of Standard liquid.

(a) Standard liquid M-21 : (viscosity η_o = 201.5 cps. at 25°C)

(r.p.s.)	(Dial Reading)	(Dial Reading)X(r.p.s.)	$(\text{r.p.s.})^2$
0.1	0.21	0.021	0.04
0.2	0.40	0.080	0.16
0.5	1.01	0.505	1.02
1.0	2.01	2.01	4.04
		2.607	5.26

$$\text{Therefore } K' = \frac{2.607 \times 201.5}{5.26} = 99.87$$

(b) Standard liquid N-19: (viscosity η_0 = 902.3 cps. at 25°C)

(r.p.s.)	(Dial Reading)	(Dial Reading) x (r.p.s.)	$(r.p.s.)^2$
0.1	0.90	0.09	0.81
0.2	1.80	0.36	3.24
0.5	4.51	2.255	20.34
1.0	9.01	9.01	81.18
		11.715	105.57

$$\text{Therefore } K' = \frac{11.715 \times 902.3}{105.57} = 100.13$$

(c) Average value of the calibration coefficient K' for Brookfield viscometer is $\frac{99.87 + 100.13}{2} = 100.0$

(3) Example calculation of viscosity η of TiO_2-MP-1250 - soy bean oil suspension (14.0% concentration by volume) at 25°C and rate of shear 0.5 revolutions per second. (Table XV-B or Figure 43).

(a) When the measurements were made by a Stormer viscometer:

1/t = 0.005, Driving weight = 194.5 grams, yield value = 157.0 grams and calibration coefficient for the Stormer viscometer = 6.94×10^{-2}.

Therefore, the viscosity of the suspension is:

$$\eta = \frac{(194.5 - 157.0) \times 6.94 \times 10^{-2}}{0.005} = 521 \text{ cps.}$$

(b) When Brookfield viscometer was employed:

Revolutions per second = 0.5 r.p.s., dial reading = 40.10
Intersection with dial reading axis (see Fig.43) = 37.5

Calibration coefficient for Brookfield viscometer = 100.0

Therefore, the viscosity of the suspension is:

$$\eta = \frac{(40.10 - 37.5) \times 100.0}{0.5} = 520 \text{ cps.}$$

(4) Example calculation of specific viscosity of TiO_2-MP-776-3-soy bean oil suspension (3.5 % of solid particles by volume) at 25°C employing equation 33 :

$$\eta_{sp} = \frac{K}{\frac{1}{\phi} - \left(1 + \frac{V_c}{V_s} \right)} \qquad 33$$

From Table V, the characteristic constants , V_c/V_s and K , for this suspension are $V_c/V_s = 4.5$ and $K = 41.4$. $1/\phi = 1/0.035 = 28.57$

The specific viscosity of the suspension is calculated from the equation 33 shown above:

$$\eta_{sp} = \frac{K}{\frac{1}{\phi} - \left(1 + \frac{V_c}{V_s} \right)}$$

$$= \frac{41.4}{28.57 - (1 + 4.5)} = 41.4/23.07$$

$$= 1.79$$

Reading from Figure 21 gives

$$1/\eta_{sp} = 0.555 \quad \text{or} \quad \eta_{sp} = 1.80$$

BIBLIOGRAPHY

1. Andrade, E. N. da C., "Viscosity and Plasticity", p. 82, Chemical Publishing Co., Inc. New York (1951).

2. Arrhenius, S., "The Internal Friction of Dilute Water Solutions," Z. Phys. Chem., 1 . 285-98 (1887).

3. Bancelin, M., "The Viscosity of Suspensions and the Determination of Avogadro's Number," Kolloid Z., 9 , 154-6 (1911).

4. Bingham, E. C., "An Investigation of the Laws of Plastic Flow," National Bureau of Standards Science Papers 278 (1916).

5. Bingham, E. C., and Green, H., "Paint, A Plastic Material and not a Viscous Liquid: The Measurements of Its Mobility and Yield Value," Proc. ASTM, 19, Part II (1919).

6. Bingham, E., "Fluidity and Plasticity," McGraw-Hill Co., (1922).

7. Blow, C. M. "Viscosity of Rubber Solution," Trans. Faraday Soc., 25, 458 (1929).

8. Broughton, G. and Windebank, C. S., "Agglomeration and Viscosity in Dilute Suspensions," Ind. Eng. Chem., 30, 407 -9 (1938).

9. Bruggeman, D. A. G., "Studies of Physical Constants of Heterogeneous Substances, I-Dielectric Constant of Mixtures of Isotropic Substances," Ann. Physik, 24, 636-79 (1935).

10. de Wael, A., and Lewis, G. L., "The Rheological Diagram," Kolloid Z., 133, 86 (1953).

11. Donnet, J. B., "Viscosity of a Dilute Suspension of Rigid Spheres," J. Chim. Phys., 48, 563 - 8 (1951).

12. Duclaus, J. et. al., "The Viscosity of Suspensions," J. Chim. Phys., 28, 511-6 (1931).

13. Eilers, H., "The Viscosity of the Emulsions of High Viscosity Material as the Function of Concentration," Kolloid Z., 97, 313 (1941).

BIBLIOGRAPHY (Cont'd)

14. Einstein, A., " A New Determination of Molecular Dimensions," Ann. Physik, 19, 289-306 (1906).

15. Eirich, F., et. a., "The Viscosity of Suspensions and Solutions of Spheres, "Kolloid Z., 74, 276-85 (1936).

16. Geddes, J. A., "Calculation of Viscosity from Stormer Viscometer Data", Ind. Eng. Chem., 34, 163 (1942)

17. Green, H., "Factors Governing Paint Consistency", Ind. Eng. Chem., 15, 122 (1923).

18. Guth, E. and Simha, R., "The Viscosity of Suspensions and Solutions. III The Viscosity of Sphere Suspensions," Kolloid Z., 74, 266-75 (1936).

19. Guth, E. and Gold, O., "Hydrodynamic Theory of The Viscosity of Suspensions", Phys. Rev., 52, 322 (1937).

20. Harper, R. C., "Interpretation of Plastic Viscosities in Terms of Newtonian Viscosities", J. Colloid, Sci., 9, 81 (1954).

21. Harrison, W., "Some Properties of Starch Relating to Its Stiffening Power", J. Soc. Dyers and Colourists, 27, 84-8 (1911).

22. Harvey, E. N. Jr., "Effect of Magnetic Fields on the Rheology of Ferromagnetic Dispersions", J. Colloid Sci., 8, 543 (1953).

23. Hatschek, E., "The Viscosity of Dispersed Systems", Kolloid Z., 7, 301-4 (1911).

24. Hatschek, E., "The Existence and Probable Thickness of Absorption Layers on Suspensoid Particles", Kolloid Z., 11, 280-4 (1912).

25. Hatschek, E., and Jane, R. S., "Viscosity of Suspensions of Rigid Particles and Their Dependence on Shear Gradient", Kolloid Z., 40 , 53-8 (1926).

26. Heim, G. A. M. and Roder, H. L., "The Adhesion of Two Surfaces Produced by a Liquid", Chem. Weekblad, 39, 538-42 (1942).

27. Hess, W. R., "Theory of the Viscosity of Heterogeneous Systems", Kolloid Z., 27, 1-11 (1920).

BIBLIOGRAPHY (Cont'd)

28. Hoback, W. H., "Practical Aspects of Pigment Dispersion", Official Digest, 316, 255 (1951)

29. Lawrence, A. S. C., "The Anomalous Flow of Colloidal Systems", Proc. Roy. Soc. (London) A, 148, 59-87 (1935).

30. Loeb. J., "Proteins and the Theory of Colloidal Behavior", p. 202, McGraw-Hill Book Co., New York (1922).

31. Mardles, E. W. J., "Viscosity of Suspension in Non-aqueous Liquids", Trans, Faraday Soc., 36, 1007-17 (1940).

32. Mardles, E. W. J., "Specific Viscosity of Suspensions and Solutions", Trans, Faraday Soc., 38, 47-54 (1942).

33. Mardles, E. W. J., "Notes on the Rheology of Paints", J. Oil Colour Chem. Assoc., 25, 194-210 (1942).

34. Mardles, E. W. J., "Sediment Volume and Specific Viscosities of Suspensions and Solutions in Mixed Liquids", Trans. Faraday Soc., 38, 222-7 (1942).

35. Maron, S. H., "Rheology of Synthetic Latex. II. Concentration Dependence of Flow in Type V GR-S Latex" J. Colloid Sci., 6, 584 (1951).

36. Maron, S. H., "Application of Ree-Eyring Generalized Flow Theory to Suspension of Spherical Particles", J. Colloid Sci., 11, 80-95 (1956).

37. Matiello, J.J., "Protective and Decorative Coatings", Vol. IV, p. 132, John Wiley and Sons, Inc., (1944).

38. McDowell, C. W., et. al., "Viscosity and Rigidity in Suspensions of Fine Particles. II. Non-aqueous Suspensions", Proc. Roy Soc. (London) A, 131, 564-76 (1931).

39. Mooney, M ., "The Viscosity of a Concentrated Suspensions of Spherical Particles", J. Colloid Sci., 6, 162 (1951).

40. Oden, S., "Physico-Chemical Properties of Sulfur Hydrosole", Z. Physik. Che., 80, 709-46 (1912).

41. Orr, C. Jr., "The Viscosity of Suspensions of Spheres", J. Colloid Sci., 6, 162 (1951)

BIBLIOGRAPHY (Cont'd)

42. Pryce-Jones, J., "Studies on Thixotropy", Kolloid Z., 129, 96 (1952).

43. Ree, T. and Eyring H., "Theory of Non-Newtonian Flow. I. Solid Plastic System". J. Appl. Physics, 26, 793 (1955).

44. Richardson, C., "(1) The Modern Asphalt Pavement; (2) The Colloidal State of Matter in its Relation to the Asphalt Industry", Dept. Sci. Ind. Research, Brit. Assoc. Adv. Sci., 3rd Report on Colloidal Chem., (1920).

45. Robinson, J. V. "Studies in the Viscosity of Colloids", Proc. Roy. Soc., 170A, 519 (1939)

46. Robinson J. V., "Viscosity of Suspensions", J. Phys. and Colloid Chem., 53, 1042-56 (1949).

47. Robinson, J. V., "The Viscosity of Suspensions of Spheres. II. The Effect of Sphere Diameter", J. Phys. and Colloid Chem., 55, 455-64 (1951).

48. Street, N., "The Rheology of Paint System", J. Color and Chemist Assoc., 39, 391-398 (1956).

49 Traxler, R. N., et. al., "Viscosities of Liquid-Solid Systems. Influence of Dispersed Particles", Ind. Eng. Chem., 29, 489-92 (1937).

50. Vand, V., "Theory of Viscosity of Concentrated Suspensions", Nature. 155, 364-5 (1945).

51. Vand, V., "Viscosity of Solution and Suspensions. I. Theory", J. Phys. and Colloid Chem., 52, 277-99 (1948).

52. Vand, V., "Viscosity of Solution and Suspensions. II. Experimental Determination of the Viscosity-Concentration Function of Spherical Suspensions", J. Phys. and Colloid Chem., 52, 300-14 (1948).

53. Vand der Walt, P. J., "The Calibration of a Stormer Viscometer Modified for Testing Suspensions", J. S. African Chem. Inst., 7, 61-78 (1954).

54. Voet, A., "Dielectrics and Rheology of Non-aqueous Dispersions", J. Phys. and Colloid Chem., 51, 1037 (1947).

55. Weltmann, R. N. and Green, H., "Rheological Properties of Colloidal Suspensions, Pigment Suspensions and Oil Mixtures," J. App. Physics, 14, 569 (1943).

BIBLIOGRAPHY (Cont'd)

56. Weltmann, R. N. and Kuhns, P. W., "An Automatic Viscometer for Non-Newtonian Materials", National Advisory Committee for Aeronautics Technical Note 3510, August (1955).

57. Williams, P. S., "Flow of Concentrated Suspensions", J. App. Chem., 3, 120 (1953).

58. Zettlemoyer, A. C., et. al,, "The Rheology of Printing Inks", J. Colloid Sci., 10, 29-49 (1955).